Discontinuous Galerkin Methods for Computational Fluid Dynamics

B. Cockburn

University of Minnesota, MN, USA

ABSTRACT

The discontinuous Galerkin methods are locally conservative, high-order accurate, robust methods which can easily handle elements of arbitrary shapes, irregular meshes with hanging nodes, and polynomial approximations of different degrees in different elements. These properties, which render them ideal for *hp*-adaptivity in domains of complex geometry, have brought them to the main stream of computational fluid dynamics. We study the properties of the DG methods as applied to a wide variety of problems arising in fluid dynamics with a special emphasis on linear, symmetric positive hyperbolic systems, the Euler equations of gas dynamics, purely elliptic problems, and the incompressible and compressible Navier-Stokes equations. In each instance, we discuss the main properties of the methods, display the mechanisms that make them work so well, and present numerical experiments showing their performance.

KEY WORDS: computational fluid dynamics, discontinuous finite elements

1. Introduction

This is a short, introductory essay to the study of the so-called Discontinuous Galerkin (DG) methods for fluid dynamics. The DG methods provide *discontinuous* approximations defined by using a Galerkin method *element by element*, the connection between the values of the approximation in different elements being established by the so-called *numerical traces*. Since the methods use discontinuous approximations, they can easily handle elements of arbitrary shapes, irregular meshes with hanging nodes, and polynomial approximations of different degrees in different elements. The methods are thus ideally suited for *hp*-adaptivity in domains of complex geometry. Moreover, since they use a Galerkin method on each element, they can easily achieve high-order accuracy when the exact solution is smooth and high resolution when

Encyclopedia of Computational Mechanics. Edited by Erwin Stein, René de Borst and Thomas J.R. Hughes.
 ISBN: 0-470-84699-2

it is not. Finally, when their numerical traces are properly chosen, they achieve a high degree of locality (and hence a high degree of parallelizability for time-dependent hyperbolic problems), they become locally conservative (a highly valued property in computational fluid dynamics), easy to solve and, last but not least, very stable even in the presence of discontinuities or strong gradients.

The first DG method was introduced by Reed and Hill (1973 for numerically solving the neutron transport equation, a linear hyperbolic equation for a scalar-valued unknown. Lesaint and Raviart (1974 recognized the relevance of the method and carried out its first theoretical analysis. Since then, the method has been slowly evolving as it was applied to different problems. In the 1990s, the method was successfully extended to nonlinear time-dependent hyperbolic systems by Cockburn and Shu (see the review by Cockburn and Shu (2001) and since then the method has known a remarkably vigorous development, as suggested in Figure 1, where we display the number of papers (in the American Mathematical Society database MathSciNet) whose title contains the words *discontinuous Galerkin*. In this paper, we describe the method, discuss its main properties, uncover the mechanisms that make it work so well, and show its performance in a variety of problems in fluid dynamics.

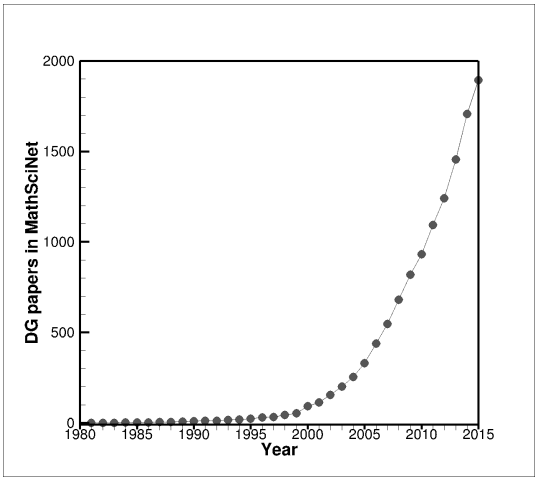

Figure 1. Cumulative number of papers, in MathSciNet, containing the words *discontinuous Galerkin* in their title.

The paper is organized as follows. Since the main properties of *all* DG methods are already displayed in the very first DG method, we begin, in Section 2, by considering the original DG method for the neutron transport equation. In Section 3, we extend the DG method to linear, symmetric positive hyperbolic systems, and, In Section 4, to nonlinear hyperbolic conservation laws. This key extension, which takes advantage of the relation between the so-called finite-volume monotone schemes and the DG methods, is what made these methods relevant in computational fluid dynamics. In Section 5, we consider DG methods for steady-state diffusion problems. We argue that the DG methods can be considered to lie *in between* the well known continuous Galerkin and the mixed methods for second-order elliptic problems.

Encyclopedia of Computational Mechanics. Edited by Erwin Stein, René de Borst and Thomas J.R. Hughes.
 ISBN: 0-470-84699-2

In Section 6, we extend theses methods to the Stokes equations of incompressible flow. In Section 7, we consider convection-dominated flows including convection-diffusion, the Oseen and the compressible Navier-Stokes equations. In these last three sections, special attention will be devoted to the so-called hybridizable DG (HDG) methods, which constitute a subclass of DG methods amenable to *static condensation*. Finally, we end in Section 8 with some concluding remarks and bibliographical notes.

2. The neutron transport equation

In this section, we consider the original DG method for numerically solving the neutron transport equation. It is in this framework that the idea of combining a Galerkin method on *each* element together with a suitably defined *numerical trace* linking the different elements was introduced. We discuss the properties of local conservativity and local solvability of the method and show that the jumps of the approximate solution across interelement boundaries *enhance* the stability of the method. We also show that these jumps are related to the *local residuals* in a linear fashion. This establishes that the original DG method is what we nowadays call a *residual-stabilized* method.

2.1. The original DG method

We begin by considering the original DG method of Reed and Hill (1973 which was devised to numerically solve the neutron transport equation,

$$\begin{aligned} \sigma\, u + \nabla \cdot (\boldsymbol{a}\, u) &= f \quad \text{in } \Omega \\ u &= u_D \quad \text{on } \partial\Omega_- \end{aligned}$$

where σ is a positive number, $\boldsymbol{a}$ a constant vector and $\partial\Omega_-$ the *inflow* boundary of Ω, that is,

$$\partial\Omega_- = \{\boldsymbol{x} \in \partial\Omega : \boldsymbol{a} \cdot \boldsymbol{n}(\boldsymbol{x}) < 0\}$$

Here $\boldsymbol{n}(\boldsymbol{x})$ is the outward unit normal at $\boldsymbol{x}$.

2.2. Definition

To define the method, we proceed as follows. First, we find the weak formulation that the Galerkin procedure will be based upon. For each element K of the mesh $\mathcal{T}_h$ of the domain Ω, we multiply the neutron transport equation by a test function v and integrate over K to get

$$\sigma\,(u,v)_K - (u, \boldsymbol{a}\cdot\nabla v)_K + \langle \boldsymbol{a}\cdot\boldsymbol{n}_K\, u, v\rangle_{\partial K} = (f,v)_K \tag{1}$$

where $\boldsymbol{n}_K$ is the outward unit normal to K,

$$(u,v)_K = \int_K u\, v \mathtt{d}x, \quad \text{and} \quad \langle w, v\rangle_{\partial K} = \int_{\partial K} w\, v \mathtt{d}s$$

Encyclopedia of Computational Mechanics. Edited by Erwin Stein, René de Borst and Thomas J.R. Hughes.
 ISBN: 0-470-84699-2

This is the weak formulation with which we define the approximation to u, u_h. Thus, for each element $K \in \mathcal{T}_h$, we take $u_h|_K$ in the space of polynomials of degree k, $\mathbb{P}_k(K)$, and define it by requiring that

$$\sigma\,(u_h, v)_K - (u_h, \boldsymbol{a}\cdot\nabla v)_K + \langle \boldsymbol{a}\cdot\boldsymbol{n}_K\,\widehat{u}_h, v\rangle_{\partial K} = (f, v)_K \tag{2}$$

for all $v \in \mathbb{P}_k(K)$. Here, the numerical trace $\widehat{u}_h$ is given by

$$\widehat{u}_h(\boldsymbol{x}) = \begin{cases} u_D(\boldsymbol{x}) & \text{for } \ \boldsymbol{x} \in \partial\Omega_- \\ \lim_{\epsilon\downarrow 0} u_h(\boldsymbol{x} - \epsilon\boldsymbol{a}) & \text{otherwise.} \end{cases} \tag{3}$$

Note that if the vector $\boldsymbol{a}$ is perpendicular to the normal $\boldsymbol{n}_K$, the above numerical trace is not well defined. However, the numerical trace of the flux $\boldsymbol{a}\cdot\boldsymbol{n}_K\,\widehat{u}_h$, usually called the *numerical flux*, is actually well defined and is called the *upwinding* numerical flux. This completes the definition of the DG method.

2.3. The numerical trace of the flux

Now, let us discuss some of the properties of this method. Let us begin by noting that the numerical trace of the flux, $\boldsymbol{a}\cdot\boldsymbol{n}_K\,\widehat{u}_h$, is a linear function of the trace of u_h which is consistent and single valued. The numerical trace is easy of evaluate and its form ensures a great degree of locality of the method. The fact that it is consistent, namely, that

$$\boldsymbol{a}\cdot\boldsymbol{n}_K\,\widehat{u} = \boldsymbol{a}\cdot\boldsymbol{n}_K\,u,$$

where u is the exact solution, ensures that we are approximating the correct exact solution. The fact that it is single valued implies that the DG method is a locally conservative method. Indeed, since on any face $F := \partial K_1 \cap \partial K_2$, we have

$$\boldsymbol{a}\cdot\boldsymbol{n}_{K_2}\,\widehat{u}_h + \boldsymbol{a}\cdot\boldsymbol{n}_{K_1}\,\widehat{u}_h = 0,$$

for any set S which is the union of elements $K \in \mathcal{T}_h$, we have

$$\sigma\int_S u_h \mathtt{d}x + \int_{\partial S} \boldsymbol{a}\cdot\boldsymbol{n}_S\,\widehat{u}_h \mathtt{d}s = \int_S f\,\mathtt{d}x$$

This equation is obtained by simply taking $v := 1$ in the weak formulation (2) for each K in S and then adding the equations.

2.4. A local energy identity and the elementwise solvability of the method

Next, note that, thanks for the definition of the numerical trace of the flux, the method satisfies a local *energy identity* we deduce next. Setting $v := u_h$ in the weak formulation (2), we get that

$$\sigma\,\|u_h\|_K^2 + \tfrac{1}{2}\langle 1, \boldsymbol{a}\cdot\boldsymbol{n}_K\,\widehat{u}_h^2\rangle_{\partial K} + \Theta_K(u_h) = (f, u_h)_K$$

where $\|\zeta\|_K := (\zeta,\zeta)_K^{1/2}$ and

$$\Theta_K(u_h) := -\tfrac{1}{2}\langle 1, \boldsymbol{a}\cdot\boldsymbol{n}_K\,(\widehat{u}_h - u_h)^2\rangle_{\partial K} = \tfrac{1}{2}\langle 1, |\boldsymbol{a}\cdot\boldsymbol{n}_K|\,(\widehat{u}_h - u_h)^2\rangle_{\partial K_-}$$

Encyclopedia of Computational Mechanics. Edited by Erwin Stein, René de Borst and Thomas J.R. Hughes.
 ISBN: 0-470-84699-2

by the definition of the numerical trace of the flux. Completing squares, we get that

$$\tfrac{1}{2}\sigma\,\|u_h\|_K^2 + \tfrac{1}{2}\sigma\|u_h - f/\sigma\|_K^2 + \tfrac{1}{2}\langle 1, \boldsymbol{a}\cdot\boldsymbol{n}_K\,\widehat{u}_h^2\rangle_{\partial K} + \Theta_K(u_h) = \tfrac{1}{2\sigma}\|f\|_K^2,$$

and finally,

$$\tfrac{1}{2}\sigma\,\|u_h\|_K^2 + \tfrac{1}{2}\sigma\|u_h - f/\sigma\|_K^2 + \tfrac{1}{2}\langle 1, |\boldsymbol{a}\cdot\boldsymbol{n}_K|\,\widehat{u}_h^2\rangle_{\partial K_+} + \Theta_K(u_h) = \tfrac{1}{2\sigma}\|f\|_K^2 + \tfrac{1}{2}\langle 1, |\boldsymbol{a}\cdot\boldsymbol{n}_K|\,\widehat{u}_h^2\rangle_{\partial K_-},$$

where $\partial K_+ = \partial K \backslash \partial K_-$.

We claim that an immediate consequence of this local energy identity is the fact that the approximate solution can be efficiently computed in an element-by-element fashion. Indeed, from the weak formulation (2) and the definition of the numerical trace (3), we have

$$(\sigma\,u_h, v)_K - (u_h, \boldsymbol{a}\cdot\nabla v)_K + \langle \boldsymbol{a}\cdot\boldsymbol{n}_K\,u_h, v\rangle_{\partial K_+} = (f, v)_K - \langle \boldsymbol{a}\cdot\boldsymbol{n}_K\,\widehat{u}_h, v\rangle_{\partial K_-},$$

for all $v \in \mathbb{P}_k(K)$, since, on ∂K_+, $\boldsymbol{a}\cdot\boldsymbol{n}_K\,\widehat{u}_h = \boldsymbol{a}\cdot\boldsymbol{n}_K\,u_h|_K$. Since the above formulation defines a square system, the existence and uniqueness of the approximation u_h on K holds if and only if, when we set the data $f|_K$ and $\widehat{u}_h|_{\partial K_-}$ to zero, the only solution is $u_h = 0$. But, in this case, the above energy identity reads

$$\sigma\|u_h\|_K^2 + \tfrac{1}{2}\langle 1, |\boldsymbol{a}\cdot\boldsymbol{n}_K|\,u_h^2\rangle_{\partial K} = 0,$$

which immediately implies that $u_h = 0$.This proves the claim.

In Figure 2.4, the approximate solution u_h on the elements of number i can only be computed after the approximate solution on the neighboring elements of number $j < i$ were obtained. The approximate solution u_h on the elements with equal number can be computed simultaneously.

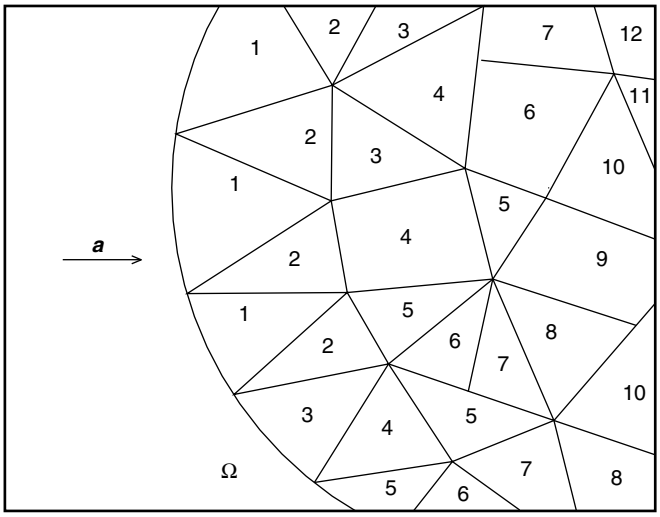

Figure 2. Solving the neutron transport equation with the DG method.

Encyclopedia of Computational Mechanics. Edited by Erwin Stein, René de Borst and Thomas J.R. Hughes.
 ISBN: 0-470-84699-2

2.5. A global energy identity and stabilization by the jumps

Another consequence of the above local energy identity is a global energy identity obtained by simply adding the identities for all the elements $K \in \mathcal{T}_h$, that is,

$$\tfrac{1}{2}\sigma\,\|u_h\|^2_\Omega + \tfrac{1}{2\sigma}\|\sigma\,u_h - f\|^2_\Omega + \tfrac{1}{2}\langle 1, |\boldsymbol{a}\cdot\boldsymbol{n}|\,u_h^2\rangle_{\partial\Omega_+} + \Theta_h(u_h) = \tfrac{1}{2\sigma}\|f\|^2_\Omega + \tfrac{1}{2}\langle 1, |\boldsymbol{a}\cdot\boldsymbol{n}|\,u_D^2\rangle_{\partial\Omega_-},$$

where

$$\Theta_h(u_h) := \frac{1}{2}\sum_{K\in\mathcal{T}_h}\Theta_K(u_h) = \frac{1}{2}\sum_{K\in\mathcal{T}_h}\langle 1, |\,\boldsymbol{a}\cdot\boldsymbol{n}_K\,|\,(\widehat{u}_h - u_h)^2\rangle_{\partial K_-}.$$

Of course, $\|\zeta\|^2_\Omega := \sum_{K\in\mathcal{T}_h}\|\zeta\|^2_K$.

Note that the left-hand side of the above identity can be considered to be a discrete energy. As a consequence, the term $\Theta_h(u_h)$ can be interpreted as the energy associated to the inter-element jumps. This is why we say that the method is *stabilized* by the jumps. Moreover, we see that the energy of the inter-element jumps is uniformly bounded regardless of the mesh $\mathcal{T}_h$ and of the approximating spaces $\mathbb{P}_k(K), K \in \mathcal{T}_h$. Thus, the method exerts an automatic control on the size of the jumps.

2.6. Control of the residuals by the inter-element jumps

Next, we argue that the size of the jumps is related to the ability of the method to solve the partial differential equation *inside* the element. To see this, let us first note that the size of the *local residuals*,

$$R_K := \sigma\,u_h + \nabla\cdot(\,\boldsymbol{a}\,u_h) - f \quad \text{and} \quad r_{\partial K} := \boldsymbol{a}\cdot\boldsymbol{n}_K\,(\widehat{u}_h - u_h),$$

control the quality of the approximation since only when they are zero, we have that u_h coincides with the exact solution u. Now, let us show that these two residuals are related by the very definition of the method. Indeed, a simple integration by parts in the weak formulation (2), reveals that

$$(R_K, v)_K = \langle r_{\partial K}, v\rangle_{\partial K},$$

for all $v \in \mathbb{P}_k(K)$. Taking $v := \mathsf{P}_k R_K$, where P_k denotes the $L^2(K)-$projection into $\mathbb{P}_k(K)$, we immediately obtain that

$$\|\mathsf{P}_k R_K\|_K \le C\,h_K^{-1/2}\,\|r_{\partial K}\|_{\partial K}$$

This implies that only the size of the jumps $\boldsymbol{a}\cdot\boldsymbol{n}_K\,(\widehat{u}_h - u_h)$, and the size of $f - \mathsf{P}_k f$, control the quality of the approximation. Thus, if the size of the jumps is very small, then the projection of the residual $\mathsf{P}_k R_K$ is also very small. If $f|_K$ is very smooth, then the residual R_K is also very small. As a consequence, the quality of the approximation on K is very good.

On the other hand, if the quality of the approximation in the element K is very poor, as we expect it would be, for example, in the presence of discontinuities, then the projection of the residual $\mathsf{P}_k R_K$, and hence the jumps $\boldsymbol{a}\cdot\boldsymbol{n}_K\,(\widehat{u}_h - u_h)$ across the inflow boundary of K, would

Encyclopedia of Computational Mechanics. Edited by Erwin Stein, René de Borst and Thomas J.R. Hughes.
 ISBN: 0-470-84699-2

be huge. Fortunately, this faux pas of the method is automatically compensated by an increase in the dissipative term $\Theta_K(u_h)$, see the above energy identities, which in practice results in the damping of the typical spurious oscillations that appear around the discontinuities.

2.7. Convergence properties

For very smooth solutions and general meshes, we have the following simple a priori error estimate.

Theorem 1. (Error estimates for the original DG method) *Consider the original DG method for the neutron transport equation given by* (2) *and* (3)*. Then, for regular meshes $\mathcal{T}_h$ made of arbitrarily shaped elements, we have that*

$$\sigma^{1/2}\| u - u_h \|_\Omega + \langle 1, |\boldsymbol{a}\cdot\mathbf{n}|(u-u_h)^2\rangle_{\partial\Omega^+} + \Theta_h^{1/2}(u_h) \leq C|\, u\,|_{H^{k+1}(\mathcal{T}_h)}\, h^{k+1/2}$$

where C is independent of u and h is the maximum of the diameters h_K of the elements $K \in \mathcal{T}_h$.

This elementary result was improved by Johnson and Pitkäranta (1986 who proved, among other things, the same order of convergence of $k+1/2$ for $\| u-u_h \|_\Omega$ independently of σ. This order of convergence was shown to be sharp by Peterson (1991 and then by Richter (2008. However, in some instances, the order of convergence of $k+1$ can be obtained. This happens for Cartesian meshes and tensor- product polynomials of degree k (see Lesaint and Raviart (1974), for some structured meshes of triangles and spaces of polynomials of degree k (see Richter (1988), and for some unstructured meshes which are, roughly speaking, aligned with the transport velocity $\boldsymbol{a}$ (see Cockburn et al. (2008a; Cockburn et al. (2010a.

An early a posteriori error estimate and superconvergence results can be found in Adjerid and Massey (2002. For finer results, see the work by Adjerid and Mechai (2014 and the references therein.

For early work on adaptivity on linear, steady state hyperbolic problems, see the paper by Bey (1994, Bey and Oden (1996, and then to the papers Houston et al. (2000; Houston et al. (2001; Houston et al. (2002, Houston and Süli (2001, and Süli and Houston (2002.

2.8. Devising DG methods for general partial differential equations

Let us end by pointing out that, by rewriting a partial differential equation as first-order system, the same approach used to define the original DG method can be readily applied. As we are going to see, *all* the resulting DG methods share with the original DG method several important, distinctive properties. First is the use of approximations of the variables *inside* the elements as well as on their *boundary*. Since no interelement continuity is required for the approximations, the DG methods can handle arbitrarily-shaped elements and general basis functions. Because of this, the DG methods are ideally suited for *hp*-adaptivity and for

Encyclopedia of Computational Mechanics. Edited by Erwin Stein, René de Borst and Thomas J.R. Hughes.
 ISBN: 0-470-84699-2

capturing special features of the exact solution by using special basis functions. Second is the enforcement of the equations by means of an elementwise Galerkin method. This results in locally conservative numerical methods and automatically implies the control of the residuals inside the elements by the residuals at the boundaries (which depend on the jumps of the variables). Finally, by suitably defining their numerical traces, a stabilization mechanism is introduced which depends on the interelement jumps of the variables. It renders the methods robust and can even improve their convergence properties.

3. Linear, symmetric positive hyperbolic systems

In this section, we exploit the hyperbolic nature of the neutron transport problem to extend the original DG method to linear, symmetric positive hyperbolic systems like the wave equation or the Maxwell equations. To show how to do that, we consider the model problem

$$\begin{aligned} \boldsymbol{u}_t + \sum_{i=1}^{N} A^i\, \boldsymbol{u}_{x_i} + B\boldsymbol{u} &= \boldsymbol{f} \quad \text{in } \Omega \times (0,T) \\ (A_{\boldsymbol{n}} - M)\,(\boldsymbol{u} - \boldsymbol{u}_D) &= \boldsymbol{0} \quad \text{on } \partial\Omega \times [0,T] \\ \boldsymbol{u}(t=0) &= \boldsymbol{u}_0 \quad \text{on } \Omega \end{aligned}$$

where $\boldsymbol{u}$ is an $\mathbb{R}^m$-valued function and A^i is a symmetric matrix for $i = 1, \ldots, N$. Here $A_{\boldsymbol{n}}$ denotes the matrix $\sum_{i=1}^{N} n_i\, A^i$ where $\boldsymbol{n} = (n_1, \ldots, n_N)$ is the unit outward normal at the boundary of Ω. Friedrichs (1958 has shown that this problem has a unique solution under some smoothness conditions on the data, under the positivity property

$$B + B^* - \sum_{i=1}^{N} A^i_{x_i} \geq \beta I, \quad \beta > 0$$

and under the following properties on the *boundary condition* matrix M:

$$\begin{gathered} M + M^* \geq 0 \\ \ker(A_{\boldsymbol{n}} - M) + \ker(A_{\boldsymbol{n}} + M) = \mathbb{R}^m \quad \text{on } \partial\Omega \times [0,T]. \end{gathered}$$

We can easily verify that the neutron transport equation is a particular case of the above problem. Indeed, in that case, we have that $m = 1$ and so the matrices A^i are real numbers; moreover, we have that $\boldsymbol{a} = (A^1, \ldots, A^N)$ and that $A_{\boldsymbol{n}} = \boldsymbol{a} \cdot \boldsymbol{n}$. The boundary condition matrix M is simply $|\, \boldsymbol{a} \cdot \boldsymbol{n}\,|$, so that the boundary condition reads

$$(\boldsymbol{a} \cdot \boldsymbol{n} - |\, \boldsymbol{a} \cdot \boldsymbol{n}\,|)(u - u_D) = 0 \quad \text{on } \partial\Omega \times [0,T]$$

that is,

$$u = u_D \quad \text{on } \partial\Omega_- \times [0,T]$$

Encyclopedia of Computational Mechanics. Edited by Erwin Stein, René de Borst and Thomas J.R. Hughes.
 ISBN: 0-470-84699-2

3.1. Definition

To define a DG method, we proceed as follows. First, we obtain a mesh $\mathcal{T}_h$ of the space-time domain $\Omega \times (0,T)$. Then, for each element $K \in \mathcal{T}_h$, we take $\boldsymbol{u}_h|_K$ to be in the finite dimensional space $V(K)$ and define it by requiring that

$$-(\boldsymbol{u}_h, \boldsymbol{v}_t)_K - \sum_{i=1}^{N} (A^i\, \boldsymbol{u}_h, \boldsymbol{v}_{x_i})_K + \langle \widehat{\mathbb{A}_{\boldsymbol{n}_K}\, \boldsymbol{u}_h}, \boldsymbol{v} \rangle_{\partial K} + ((B - \sum_{i=1}^{N} A^i_{x_i})\boldsymbol{u}_h, \boldsymbol{v})_K = (\boldsymbol{f}, \boldsymbol{v})_K$$

for all $\boldsymbol{v} \in V(K)$. Here we have taken $\mathbb{A}_{\boldsymbol{n}_K} = A_{\boldsymbol{n}} + n_t\, Id$, where $\boldsymbol{n}_K = (\boldsymbol{n}, n_t)$. Next, let us define the numerical flux $\widehat{\mathbb{A}_{\boldsymbol{n}_K}\, \boldsymbol{u}}$.

On the boundary of the space-time domain, we take

$$\widehat{\mathbb{A}_{\boldsymbol{n}_K}\, \boldsymbol{u}_h} = \begin{cases} \boldsymbol{u}_0 & \text{on } \Omega \times \{t = 0\} \\ \boldsymbol{u}_h & \text{on } \Omega \times \{t = T\} \\ \frac{1}{2}\, A_{\boldsymbol{n}}(\boldsymbol{u}_h + \boldsymbol{u}_D) & \\ \quad + \frac{1}{2}\, M(\boldsymbol{u}_h - \boldsymbol{u}_D) & \text{on } \partial\Omega \times (0,T) \end{cases}$$

and on the interelement boundaries,

$$\widehat{\mathbb{A}_{\boldsymbol{n}_K}\, \boldsymbol{u}_h} = \mathbb{A}_{\boldsymbol{n}_K} \{\boldsymbol{u}_h\} + \tfrac{1}{2}\, \mathbb{M}\, [\![\boldsymbol{u}_h]\!]_{\boldsymbol{n}_K}$$

where $\{\boldsymbol{u}_h\} = \frac{1}{2}(\boldsymbol{u}_h^- + \boldsymbol{u}_h^+)$, $[\![\boldsymbol{u}_h]\!]_{\boldsymbol{n}_K} = \boldsymbol{u}_h^- - \boldsymbol{u}_h^+$ and $\boldsymbol{u}_h^{\pm}(\boldsymbol{x}) = \lim_{\epsilon \downarrow 0} \boldsymbol{u}_h(\boldsymbol{x} \pm \epsilon\, \boldsymbol{n}_K)$.

It only remains to define the matrices $\mathbb{M}$. The two main choices are $\mathbb{M} = |\, \mathbb{A}_{\boldsymbol{n}_K}\, |$, which gives rise to the so-called upwinding numerical flux, and $\mathbb{M} = \varrho(\mathbb{A}_{\boldsymbol{n}_K})\, Id$, where $\varrho(E)$ is the spectral radius of the matrix E, which gives rise to the so-called Lax-Friedrichs numerical flux. This completes the definition of the DG method.

3.2. The numerical trace of the flux

Note how the numerical trace of the flux, $\widehat{\mathbb{A}_{\boldsymbol{n}_K}\, \boldsymbol{u}_h}$, is a linear function of the traces of $\boldsymbol{u}_h$ which is consistent and single valued. As in the case of neutron transport, the form the numerical race of the flux is easy to evaluate and ensures a high degree of locality of the method. The property of consistency ensures that we are approximating the correct exact solution. It is satisfied if

$$\widehat{\mathbb{A}_{\boldsymbol{n}_K}\, \boldsymbol{u}} = \mathbb{A}_{\boldsymbol{n}_K}\, \boldsymbol{u}$$

where $\boldsymbol{u}$ is the exact solution. Since $[\![\boldsymbol{u}]\!]_{\boldsymbol{n}_K} = \boldsymbol{0}$, we do have that the numerical flux is consistent in the interelement boundaries. It is trivial to see it is consistent on $\Omega \times \{t = 0\}$ and on $\Omega \times \{t = T\}$. It remains to see what happens on $\partial\Omega \times (0,T)$. But there we have

$$\begin{aligned} \widehat{\mathbb{A}_{\boldsymbol{n}_K}\, \boldsymbol{u}} &= \tfrac{1}{2}\, A_{\boldsymbol{n}}(\boldsymbol{u} + \boldsymbol{u}_D) + \tfrac{1}{2}\, M(\boldsymbol{u} - \boldsymbol{u}_D) \\ &= A_{\boldsymbol{n}}\boldsymbol{u} + \tfrac{1}{2}\, (M - A_{\boldsymbol{n}})(\boldsymbol{u} - \boldsymbol{u}_D) = A_{\boldsymbol{n}}\boldsymbol{u} \end{aligned}$$

Encyclopedia of Computational Mechanics. Edited by Erwin Stein, René de Borst and Thomas J.R. Hughes.
 ISBN: 0-470-84699-2

since the exact solution satisfies the boundary condition $(M - A_{\boldsymbol{n}})(\boldsymbol{u} - \boldsymbol{u}_D) = 0$. The numerical trace of the flux is thus consistent.

Finally, the fact that it is single valued, that is , that on the face $F := \partial K_1 \cap \partial K_2$,

$$\widehat{\mathbb{A}_{\boldsymbol{n}_{K_1}} \boldsymbol{u}_h} + \widehat{\mathbb{A}_{\boldsymbol{n}_{K_2}} \boldsymbol{u}_h} = \boldsymbol{0}$$

ensures the highly valued property of local conservatively which states that for any set S, which is the union of elements $K \in \mathcal{T}_h$, we have

$$\int_S (B - \sum_{i=1}^{N} A^i_{x_i}) \boldsymbol{u}_h \mathrm{d}x + \int_{\partial S} \widehat{\mathbb{A}_{\boldsymbol{n}_S} \boldsymbol{u}_h} \mathrm{d}s = \int_S \boldsymbol{f} \mathrm{d}x.$$

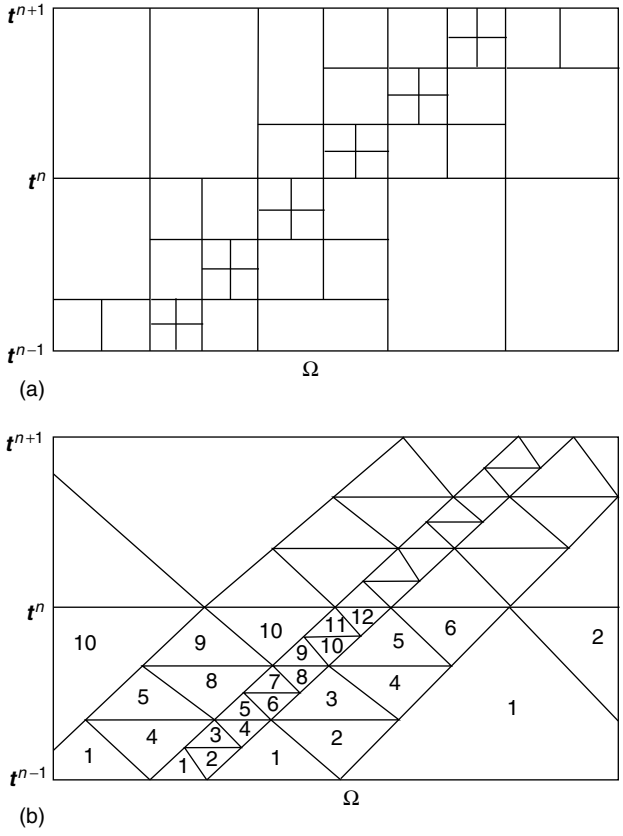

Figure 3. Space-time meshes for the DG method. On each time slab $\Omega \times (t^n, t^{n+1})$, the resolution can be globally implicit (a) or implicit only on each element (b).

Encyclopedia of Computational Mechanics. Edited by Erwin Stein, René de Borst and Thomas J.R. Hughes.
 ISBN: 0-470-84699-2

3.3. A local energy identity and the elementwise solvability of the method

To obtain the local energy identity, we consider the case in which $M = \mathbb{M} = |\mathbb{A}_{\boldsymbol{n}_K}|$ in order to emphasize the closeness of this case with that of the neutron transport problem. In this case, the resulting numerical flux is called the *unwinding* flux:

$$\widehat{\mathbb{A}_{\boldsymbol{n}_K}\boldsymbol{u}_h} = \mathbb{A}_{\boldsymbol{n}_K}\{\boldsymbol{u}_h\} + \tfrac{1}{2}\,|\mathbb{A}_{\boldsymbol{n}_K}|\,[\![\boldsymbol{u}_h]\!]_{\boldsymbol{n}_K} = \mathbb{A}^+_{\boldsymbol{n}_K}\boldsymbol{u}^-_h + \mathbb{A}^-_{\boldsymbol{n}_K}\boldsymbol{u}^+_h,$$

where $\mathbb{A}^-_{\boldsymbol{n}_K} := (\mathbb{A}_{\boldsymbol{n}_K} - |\mathbb{A}_{\boldsymbol{n}_K}|)/2$ and $\mathbb{A}^+_{\boldsymbol{n}_K} := (\mathbb{A}_{\boldsymbol{n}_K} + |\mathbb{A}_{\boldsymbol{n}_K}|)/2$. We can now proceed exactly as in the neutron transport problem to obtain the following local energy identity:

$$\tfrac{1}{2}\|\boldsymbol{u}_h\|^2_{K,\Sigma} + \tfrac{1}{2}\|\Sigma\boldsymbol{u}_h - \boldsymbol{f}\|^2_{K,\Sigma^{-1}} + \tfrac{1}{2}\langle\mathbb{A}^+_{\boldsymbol{n}_K}\boldsymbol{u}^-_h, \boldsymbol{u}^-_h\rangle_{\partial K} + \Theta_K(u_h) = \tfrac{1}{2}\|f\|^2_{K,\Sigma^{-1}} - \tfrac{1}{2}\langle\mathbb{A}^-_{\boldsymbol{n}_K}\boldsymbol{u}^+_h, \boldsymbol{u}^+_h\rangle_{\partial K},$$

where

$$\Theta_K(\boldsymbol{u}_h) := -\tfrac{1}{2}\langle\mathbb{A}^-_{\boldsymbol{n}_K}[\![\boldsymbol{u}_h]\!], [\![\boldsymbol{u}_h]\!]\rangle_{\partial K}.$$

Here, we are using the notation $\|\boldsymbol{z}\|^2_{K,C} := (C\boldsymbol{z}, \boldsymbol{z})_K$ and $\Sigma := \frac{1}{2}(B + B^* - \sum_{i=1}^N A^i_{x_i})$.

This identity implies that the approximate solution on each element is well defined provided appropriate data is provided. Indeed, on the element $K \in \mathcal{T}_h$, we have that $\boldsymbol{u}_h$ is the element of $V(K)$ that solves

$$-(\boldsymbol{u}_h, \boldsymbol{v}_t)_K - \sum_{i=1}^N (A^i\,\boldsymbol{u}_h, \boldsymbol{v}_{x_i})_K + \langle\mathbb{A}^+_{\boldsymbol{n}_K}\,\boldsymbol{u}^-_h, \boldsymbol{v}\rangle_{\partial K} + ((B - \sum_{i=1}^N A^i_{x_i})\boldsymbol{u}_h, \boldsymbol{v})_K = (\boldsymbol{f}, \boldsymbol{v})_K - \langle\mathbb{A}^-_{\boldsymbol{n}_K}\,\boldsymbol{u}^+_h, \boldsymbol{v}\rangle_{\partial K}$$

for all $\boldsymbol{v} \in V(K)$. Since this defines a square system, to prove the existence and uniqueness of $\boldsymbol{u}_h$, it is enough to set the data $\mathbb{A}^-_{\boldsymbol{n}_K}\boldsymbol{u}^+_h$ and $\boldsymbol{f}$ to zero and show that the only possible solution is the trivial one. But in this case, the above local energy identity gives

$$\|\boldsymbol{u}_h\|^2_{K,\Sigma} + \tfrac{1}{2}\langle|\mathbb{A}_{\boldsymbol{n}_K}|\boldsymbol{u}^-_h, \boldsymbol{u}^-_h\rangle_{\partial K} = 0,$$

which immediately implies that $\boldsymbol{u}_h = \boldsymbol{0}$ in K.

This means that approximate solution $\boldsymbol{u}_h|_K$ can be obtained on the element K once the trace $\boldsymbol{u}^+_h|_{\partial K}$ such that $\mathbb{A}^-_{\boldsymbol{n}_K} = \boldsymbol{0}$ is available. In spite of the possibility of solving in an elementwise manner, sometimes it is possible to solve only on the time slab $\Omega \times [t^n, t^{n+1}]$, as indicated by Johnson et al. (1984. This gives rise to a globally implicit method; see Figure 3(a). This difficulty can be avoided if *suitably* defined meshes are used together with the *upwinding* numerical flux as shown by Lowrie et al. (1995, Lowrie (1996, and Lowrie et al. (1998 in the frame of nonlinear hyperbolic systems, and later by Yin et al. (2000 in the framework of elastodynamics, and by Falk and Richter (1999 in the framework of linear symmetric positive hyperbolic systems. See Figure 3(b).

Encyclopedia of Computational Mechanics. Edited by Erwin Stein, René de Borst and Thomas J.R. Hughes.
 ISBN: 0-470-84699-2

3.4. A global energy identity and stabilization by the jumps

As in the case of the neutron transport problem, we can easily get the following global energy identity:

$$\begin{aligned}\tfrac{1}{2}\|\boldsymbol{u}_h\|^2_{\Omega_T,\Sigma}+\tfrac{1}{2}\|\Sigma\boldsymbol{u}_h-\boldsymbol{f}\|^2_{\Omega_T,\Sigma^{-1}}+\tfrac{1}{2}\langle\mathbb{A}^+_{\boldsymbol{n}}\boldsymbol{u}^-_h,\boldsymbol{u}^-_h\rangle_{\partial\Omega_T}+\Theta_h(u_h)\\ =\tfrac{1}{2}\|f\|^2_{\Omega_T,\Sigma^{-1}}-\tfrac{1}{2}\langle\mathbb{A}^-_{\boldsymbol{n}}\boldsymbol{u}_D,\boldsymbol{u}_D\rangle_{\partial\Omega\times[0,T]}+\tfrac{1}{2}\langle\boldsymbol{u}_0,\boldsymbol{u}_0\rangle_\Omega,\end{aligned}$$

where $\Omega_T:=\Omega\times(0,T)$ and

$$\Theta_h(u_h):=\frac{1}{2}\sum_{K\in\mathcal{T}_h}\Theta_K(u_h)=-\frac{1}{2}\,\langle\,\mathbb{A}^-_{\boldsymbol{n}}[\![\boldsymbol{u}_h]\!],[\![\boldsymbol{u}_h]\!]\rangle_{\partial\Omega_T}+\frac{1}{2}\sum_{F\in\mathcal{F}^i}\langle|\,\mathbb{A}_{\boldsymbol{n}_F}|\,[\![\boldsymbol{u}_h]\!],[\![\boldsymbol{u}_h]\!]\rangle_F.$$

Here, $\boldsymbol{n}_F$ is any unit vector normal to the face F and $\mathcal{F}^i_h$ is the collection of all interior faces of the mesh $\mathcal{T}_h$. Again, we see that the method is *stabilized* by the jumps and that the energy of the inter-element jumps is uniformly bounded regardless of the mesh $\mathcal{T}_h$ and of the approximating spaces $V(K),K\in\mathcal{T}_h$.

3.5. Control of the residuals by the inter-element jumps

Now, consider the residuals

$$\boldsymbol{R}_K:=(\boldsymbol{u}_h)_t+\sum_{i=1}^N A^i\,(\boldsymbol{u}_h)_{x_i}+B\boldsymbol{u}_h-\boldsymbol{f}\quad\text{and}\quad\boldsymbol{r}_{\partial K}:=\widehat{\mathbb{A}_{\boldsymbol{n}_K}\boldsymbol{u}_h}-\mathbb{A}_{\boldsymbol{n}_K}\boldsymbol{u}_h=-\mathbb{A}^-_{\boldsymbol{n}_K}[\![\boldsymbol{u}_h]\!].$$

A simple integration by parts in the weak formulation defining the scheme gives

$$(\boldsymbol{R}_K,\boldsymbol{v})_K=\langle\boldsymbol{r}_{\partial K},\boldsymbol{v}\rangle_{\partial K},$$

for all $v\in V(K)$, and this implies that

$$\|\mathsf{P}_V\boldsymbol{R}_K\|_K\le C\,h_K^{-1/2}\,\|\boldsymbol{r}_{\partial K}\|_{\partial K}$$

where P_V is the $L^2(K)$-projection into the space $V(K)$. If we assume, for simplicity, that the matrices $A^i,i=1,\cdots,N$ and B are constant, this implies that only the size of the jumps $-\mathbb{A}^-_{\boldsymbol{n}_K}[\![\boldsymbol{u}_h]\!]$, and the size of $f-\mathsf{P}_Vf$ control the quality of the approximation.

3.6. Convergence properties

For very smooth solutions and general meshes, we have the following simple a priori error estimate.

Theorem 2. (Error estimates for the DG method) *Consider the DG method for which each component of the space $V(K)$ contains the space of polynomials $\mathbb{P}_k(K)$. Then, for regular meshes $\mathcal{T}_h$ made of arbitrarily shaped elements, we have that*

$$\|\,\mathbf{u}-\mathbf{u}_h\,\|_{\Omega_T,\Sigma}+\langle\mathbb{A}^+_{\mathbf{n}}(\mathbf{u}-\mathbf{u}_h),(\mathbf{u}-\mathbf{u}_h)\rangle^{1/2}_{\partial\Omega}+\Theta^{1/2}_h(\mathbf{u}_h)\le C|\,\mathbf{u}\,|_{H^{k+1}(\mathcal{T}_h)}\,h^{k+1/2}$$

Encyclopedia of Computational Mechanics. Edited by Erwin Stein, René de Borst and Thomas J.R. Hughes.
 ISBN: 0-470-84699-2

where C is independent of $\mathbf{u}$ *and* h *is the maximum of the diameters* h_K *of the elements* $K \in \mathcal{T}_h$.

See the a priori error estimates in Falk and Richter (1999. Asymptotically exact discontinuous Galerkin error estimates for linear symmetric hyperbolic systems have been obtained by Adjerid and Weinhart (2014; see also Adjerid and Weinhart (2011.

3.7. Enhanced accuracy by local postprocessing

The method of lines for these linear systems has been studied by Cockburn et al. (2003 where it was shown that, if uniform meshes are used, a local postprocessing of the approximate solution of the DG method is of order $2\,k+1$ when polynomials of degree k are used.

This remarkable technique, which can be used for all other DG methods, was introduced by Bramble and Schatz (1977 for finite element solutions to elliptic equations. It was explored from a Fourier perspective, and for derivative filtering, by Thomée (1977. Its application to discontinuous Galerkin solutions to linear hyperbolic equations was then done by Cockburn et al. (2003. Applications to the approximation of derivatives were carried by Ryan and Cockburn (2009 and more recently by Li et al. (2016. For applications to convection-diffusion equations see Ji et al. (2012, to variable-coefficient equations see Mirzaee et al. (2011, and to nonlinear hyperbolic equations with smooth solutions see Ji et al. (2013. This filtering technique, later called Smoothness-Increasing Accuracy-Conserving (SIAC) filtering, requires translation-invariant meshes, used originally a symmetric convolution kernel, and cannot be applied up to the boundary. Extensions to smoothly varying mesh sizes-uniform cartesian meshes were carried out by Curtis et al. (0708, and to unstructured triangular meshes by Mirzaee et al. (2013, (applications to structured triangular meshes were done by Mirzaee et al. (2011 and to structured tetrahedral meshes by Mirzaee et al. (2014. The development of one-sided convolution kernels which can be applied up to the boundary, was carried out in the series of papers by Ryan and Shu (2003; van Slingerland et al. (2011; Ryan et al. (2015; see also the $L^\infty-$error estimates by Ji et al. (2014. The application of SIAC filtering to streamline visualization and isosurface extraction was done by Walfisch et al. (2009.

Let us illustrate how powerful is this filtering on the model problem,

$$\begin{aligned} u_t + u_x &= 0, \quad \text{in } (0,2\pi)\times(0,T) \\ u(x,0) &= \sin(x) \quad x \in (0,2\pi) \end{aligned} \tag{4}$$

with periodic boundary conditions. In Table 1, we see that the order of convergence of both the L^2 and L^∞ errors for P^k elements is of $(k+1)$ before postprocessing and of at least $(2k+1)$ after postprocessing, for $k=1,2,3,4$. In Figure 4, we see the absolute errors before and after postprocessing for P^2. The postprocessing of the approximate solution is obtained by convolution with a kernel whose support is the union of a number of elements, which only depends on k; for details, see Cockburn et al. (2003.

Encyclopedia of Computational Mechanics. Edited by Erwin Stein, René de Borst and Thomas J.R. Hughes.
 ISBN: 0-470-84699-2

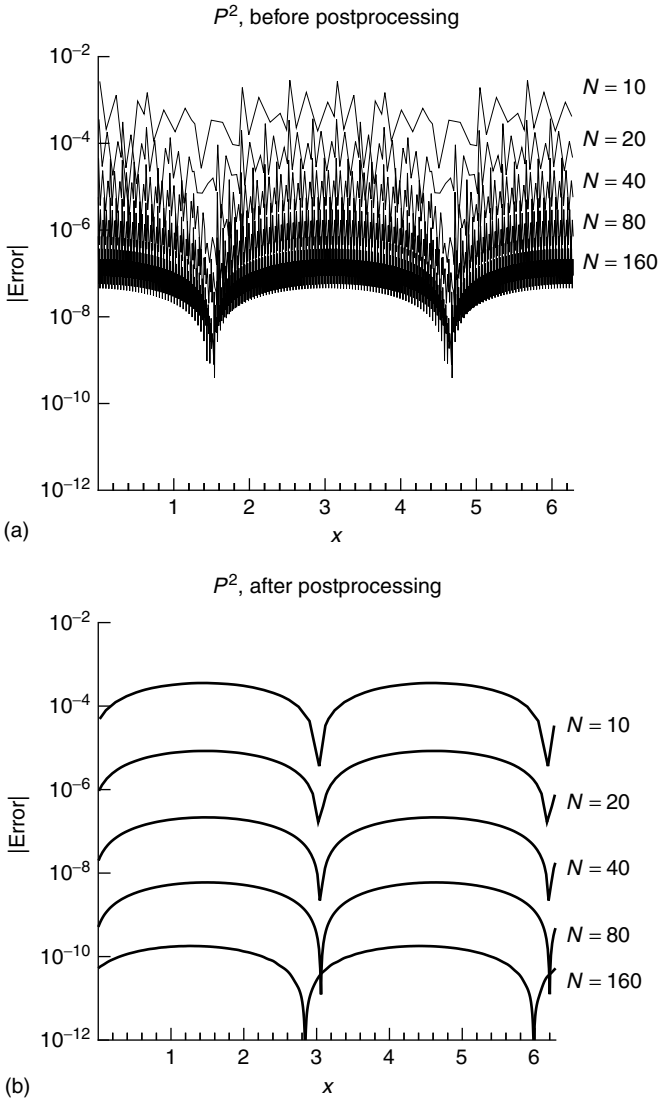

Figure 4. The absolute value of the errors for P^2 with $N = 10$, 20, 40, 40, 80 and 160 elements. Before postprocessing (a) and after postprocessing (b). (From Cockburn B, Luskin M, Shu C-W and Süli E. Enhanced accuracy by post-processing for finite element methods for hyperbolic equations. *Math. Comput.* 2003; **72**:577-606.)

Encyclopedia of Computational Mechanics. Edited by Erwin Stein, René de Borst and Thomas J.R. Hughes.

4. Nonlinear Hyperbolic Problems

In this section, we consider DG methods for nonlinear hyperbolic problems. We begin by showing that to ensure convergence towards the physically relevant solution, usually called the *entropy solution*, the DG methods need to use a numerical flux based on a suitable *approximate Riemann solver* and that they must use either a *shock-capturing* term or a *slope limiter*. We show that the shock-capturing DG methods are strongly related to stabilized methods like the streamline diffusion method, and that slope-limiter DG methods can be considered to be an extension of finite volume methods. We then show computational results for some shock-capturing DG methods and describe and analyze the so-called Runge-Kutta DG (RKDG) method, a slope-limiter DG method. We show how the different ingredients of the method, namely, the DG space discretization, a special Runge-Kutta time discretization, and a *generalized* slope limiter, are put together to ensure its stability. Several numerical experiments showing the performance of the RKDG methods are given. Particular attention is devoted to the Euler equations of gas dynamics. Finally, we discuss, and illustrate, a remarkable technique for enforcing a range-invariance property of the RKDG approximations.

4.1. The main difficulty: the loss of well-posedness

Devising numerical methods for nonlinear hyperbolic problems is dramatically different from devising methods for linear symmetric hyperbolic problems. This is due to the fact that whereas linear, symmetric hyperbolic problems are well posed, nonlinear hyperbolic problems are not.

This difficulty was uncovered first in the framework of the Euler equations of gas dynamics; indeed, this equation has several nonphysical *weak* solutions. This happens because the Euler equations of gas dynamics are obtained from the compressible Navier-Stokes by simply dropping from the equations, the terms *modeling viscosity* and *heat transfer effects*. As a consequence, the information concerning the second law of thermodynamics is completely lost and discontinuous solutions, which violate such a law suddenly appear. To devise numerical schemes that are guaranteed to converge to the entropy solution and not to any other weak solution constitutes the main difficulty of devising numerical methods for nonlinear hyperbolic problems.

This difficulty is present even in the simplest hyperbolic problem, namely, the scalar hyperbolic conservation law

$$\begin{aligned} u_t + (f(u))_x &= 0 \quad \text{in } (0,1)\times(0,T) \\ u(t=0) &= u_0 \quad \text{on } (0,1) \end{aligned}$$

with periodic boundary conditions. To illustrate this phenomenon, consider the well-known Engquist-Osher and Lax-Wendroff schemes and let us apply them to the above equation for $f(u) = u^2/2$ and $u_0(x) = 1$ on $(0.4, 0.6)$ and $u_0(x) = 0$ otherwise. In the Figure 5, we see that the approximation given by the Engquist-Osher scheme converges to the entropy solution, whereas that given by the Lax-Wendroff scheme does not. The Lax-Wendroff scheme lacks a

Encyclopedia of Computational Mechanics. Edited by Erwin Stein, René de Borst and Thomas J.R. Hughes.
 ISBN: 0-470-84699-2

Table 1. The effect of post-processing the approximate solution. (From Cockburn B, Luskin M, Shu C-W and Süli E. Enhanced accuracy by postprocessing for finite element methods for hyperbolic equations. *Math. Comput.* 2003; **72**:577-606.)

Mesh	Before postprocessing				After postprocessing			
	L^2 error	Order	L^∞ error	Order	L^2 error	Order	L^∞ error	Order
				P^1				
10	3.29E-02	-	5.81E-02	-	3.01E-02	-	4.22E-02	-
20	5.63E-03	2.55	1.06E-02	2.45	3.84E-03	2.97	5.44E-03	2.96
40	1.16E-03	2.28	2.89E-03	1.88	4.79E-04	3.00	6.78E-04	3.01
80	2.72E-04	2.09	8.08E-04	1.84	5.97E-05	3.00	8.45E-05	3.00
160	6.68E-05	2.03	2.13E-04	1.93	7.45E-06	3.00	1.05E-05	3.00
320	1.66E-05	2.01	5.45E-05	1.96	9.30E-07	3.00	1.32E-06	3.00
				P^2				
10	8.63E-04	-	2.86E-03	-	2.52E-04	-	3.57E-04	-
20	1.07E-04	3.01	3.69E-04	2.95	5.96E-06	5.40	8.41E-06	5.41
40	1.34E-05	3.00	4.63E-05	3.00	1.53E-07	5.29	2.16E-07	5.28
80	1.67E-06	3.00	5.78E-06	3.00	4.22E-09	5.18	5.97E-09	5.18
160	2.09E-07	3.00	7.23E-07	3.00	1.27E-10	5.06	1.80E-10	5.06
				P^3				
10	3.30E-05	-	9.59E-05	-	1.64E-05	-	2.31E-05	-
20	2.06E-06	4.00	6.07E-06	3.98	7.07E-08	7.85	1.00E-07	7.85
40	1.29E-07	4.00	3.80E-07	4.00	2.91E-10	7.92	4.15E-10	7.91
50	5.29E-08	4.00	1.56E-07	4.00	5.03E-11	7.87	7.24E-11	7.83
				P^4				
10	1.02E-06	-	2.30E-06	-	1.98E-06	-	2.81E-06	-
20	3.21E-08	5.00	7.30E-08	4.98	2.20E-09	9.82	3.11E-09	9.82
30	4.23E-09	5.00	9.66E-09	4.99	4.34E-11	9.68	6.66E-11	9.48

mechanism that ensures its convergence towards the entropy solution and, as a consequence, can converge to a weak solution, which is not the entropy solution.

4.2. Tools for capturing the entropy solution: heuristics

The DG methods try to ensure convergence towards the entropy solution by using the so-called *Riemann solvers* and either a *shock-capturing term* or a *slope limiter*. To describe the heuristics behind their construction, we consider the parabolic problem

$$\begin{aligned} u_t + (f(u))_x &= \nu\, u_{xx} \quad \text{in } (0,1)\times(0,T) \\ u(t=0) &= u_0 \quad \text{on } (0,1) \end{aligned}$$

Encyclopedia of Computational Mechanics. Edited by Erwin Stein, René de Borst and Thomas J.R. Hughes.
 ISBN: 0-470-84699-2

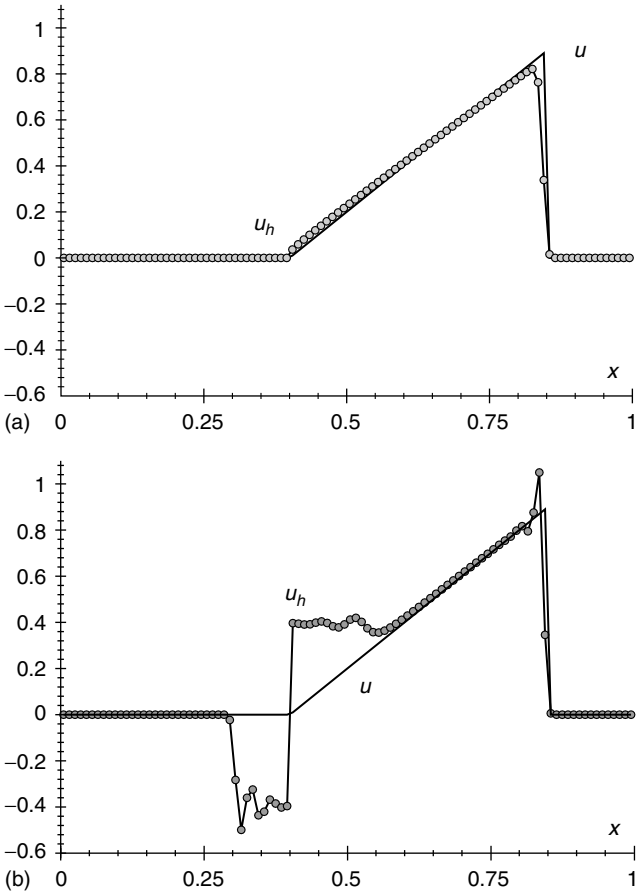

Figure 5. The entropy solution, u, and its approximation u_h at time $T = 1/2$: Engquist-Osher scheme (a) and Lax-Wendroff scheme (b). (From Cockburn B. Continuous dependence and error estimation for viscosity methods. *Acta Numer.* 2003a; **12**:127-180.)

since it is known that as the viscosity coefficient ν goes to zero, the solution of the above problem converges to the entropy solution of our scalar hyperbolic conservation law.

Given this property, our strategy is to use the weak formulation of the parabolic problem to see what the tools are that should be used to devise DG methods that converge to the entropy solution. Thus, multiplying the parabolic equation by a test function φ, and integrating over the space-time element K, we get

$$\int_{\partial K} (f(u) - \nu\, u_x, u) \cdot (n_x, n_t)\, \varphi \mathrm{d}s$$
$$- \int_K (f(u) - \nu\, u_x, u) \cdot (\varphi_x, \varphi_t) \mathrm{d}x\mathrm{d}t = 0$$

Encyclopedia of Computational Mechanics. Edited by Erwin Stein, René de Borst and Thomas J.R. Hughes.
 ISBN: 0-470-84699-2

Now, if we set $F_{\boldsymbol{n}_K}(u) = (f(u) - \nu\, u_x, u) \cdot (n_x, n_t)$, on ∂K, we end up with

$$\int_{\partial K} F_{\boldsymbol{n}_K}(u)\, \varphi \mathtt{d}s - \int_K (f(u), u) \cdot (\varphi_x, \varphi_t) + \int_K \nu\, u_x\, \varphi_x \mathtt{d}x\mathtt{d}t = 0$$

Finally, noting that we have

$$\nu\, u_x(x,t) = \int_{x(t)}^{x} R(u)(y,t)\mathtt{d}y$$

where $R(u) = u_t + (f(u))_x$ and $x(t)$ is such that $u_x(x(t),t) = 0$ (such a point always exists because we have periodic boundary conditions), this suggests the so-called shock-capturing DG methods:

$$\int_{\partial K} \widehat{F}_{\boldsymbol{n}_K}(u_h)\, \varphi \mathtt{d}s - \int_K (f(u_h), u_h) \cdot (\varphi_x, \varphi_t) + \int_K \widehat{\nu}\, (u_h)_x \varphi_x \mathtt{d}x\mathtt{d}t = 0$$

where $\widehat{F}_{\boldsymbol{n}_K}(u_h)$ is the approximate Riemann solver and the last term is the shock-capturing term.

The approximate Riemann solver is nothing but a numerical trace for the function $F_{\boldsymbol{n}_K}(u)$; it only depends on the two traces of the function u, that is, $\widehat{F}_{\boldsymbol{n}_K}(u_h) = \widehat{g}(u_h^-, u_h^+)$. The main examples are the following:

(i) The Godunov flux:

$$\widehat{g}^G(a,b) = \begin{cases} \min_{a \le u \le b}\, g(u), & \text{if } \ a \le b \\ \max_{b \le u \le a}\, g(u), & \text{otherwise} \end{cases}$$

(ii) The Engquist-Osher flux:

$$\widehat{g}^{EO}(a,b) = \int_0^b \min(g'(s), 0)\mathtt{d}s + \int_0^a \max(g'(s), 0)\mathtt{d}s + g(0)$$

(iii) The Lax-Friedrichs flux:

$$\begin{aligned} \widehat{g}^{\mathrm{LF}}(a,b) &= \tfrac{1}{2}\, [g(a) + g(b) - C(b-a)] \\ C &= \max_{\inf u^0(x) \le s \le \sup u^0(x)} |g'(s)| \end{aligned}$$

The shock-capturing term has the same structure as the corresponding term for the parabolic equation and typically, has a viscosity coefficient $\widehat{\nu}$ that depends on the residual as follows:

$$\widehat{\nu} = \delta^\alpha\, \frac{|\, R(u_h)\,|}{|\, (u_h)_x\,| + \epsilon}$$

Encyclopedia of Computational Mechanics. Edited by Erwin Stein, René de Borst and Thomas J.R. Hughes.
 ISBN: 0-470-84699-2

where the auxiliary parameter δ is usually taken to be of the order of the diameter of K and α is a parameter usually bigger than one and smaller than two. The purpose of the small number ϵ is to prevent a division by zero when $(u_h)_x = 0$. The shock-capturing DG methods considered by Jaffré et al. (1995 and by Cockburn and Gremaud (1996 for the scalar hyperbolic conservation law in several space dimensions are of this form.

The DG methods that do not have a shock-capturing term *must* have a slope limiter in order to ensure that the information about the entropy solution is incorporated into the scheme. In fact, as we argue next, the slope limiters and the shock-capturing terms have exactly the same origin. The DG methods with a slope limiter are obtained as follows. Instead of keeping the shock-capturing term in a single equation, that term is *split-off* in a way typical of operator splitting techniques. Take $K = I \times (t^n, t^{n+1})$. To march from time t^n to t^{n+1}, we first compute $u_h^{n+1/2}$ from u_h^n by using the scheme

$$\int_{\partial K} (\widehat{f}_h, \widehat{u}_h) \cdot (n_x, n_t)\, \varphi \mathsf{d}s - \int_K (f(u_h), u_h) \cdot (\varphi_x, \varphi_t) \mathsf{d}x\mathsf{d}t = 0$$

for some numerical flux $(\widehat{f}_h, \widehat{u}_h) \cdot (n_x, n_t)$, and then, compute u_h^{n+1} from $u_h^{n+1/2}$ by using

$$\int_I (u_h^{n+1} - u_h^{n+1/2})\, \varphi \mathsf{d}x - (t^{n+1} - t^n) \int_I \nu\, (u_h^{n+1/2})_x\, \varphi_x \mathsf{d}x = 0$$

We thus see that the function u_h^{n+1} captures the information contained in the shock-capturing term. The link between this second step and the so-called slope limiters can be easily established if we realize that, if we write,

$$u_h^{n+1} = \Lambda\Pi_h u_h^{n+1/2}$$

then, the operator $\Lambda\Pi_h$ is actually a (generalized) slope limiter. For details, see the work by Cockburn (2001.

Let us illustrate this fact on a simple case. Consider the piecewise linear function v_h and set $u_h = \Lambda\Pi(v_h)$, that is, u_h is the piecewise linear function defined by

$$\int_I u_h\, \varphi \mathsf{d}x = \int_I v_h\, \varphi \mathsf{d}x - \int_I \mathsf{slc}\, (v_h)_x\, \varphi_x \mathsf{d}x$$

where $\mathsf{slc} := (t^{n+1} - t^n)\, \nu$, for all linear functions φ. If we write

$$v_h(x) = \overline{v}_j + (x - x_j)\, v_{x,j}$$

on each interval I_j, and take

$$\mathsf{slc} = \begin{cases} 0 & \text{if } v_{x,j} = 0 \\ \frac{h_j^2}{12}\left[1 - m\left(1, \frac{2}{h_j}\frac{\overline{v}_j - \overline{v}_{j-1}}{v_{x,j}}, \frac{2}{h_j}\frac{\overline{v}_{j+1} - \overline{v}_j}{v_{x,j}}\right)\right] & \text{otherwise} \end{cases}$$

Encyclopedia of Computational Mechanics. Edited by Erwin Stein, René de Borst and Thomas J.R. Hughes.
 ISBN: 0-470-84699-2

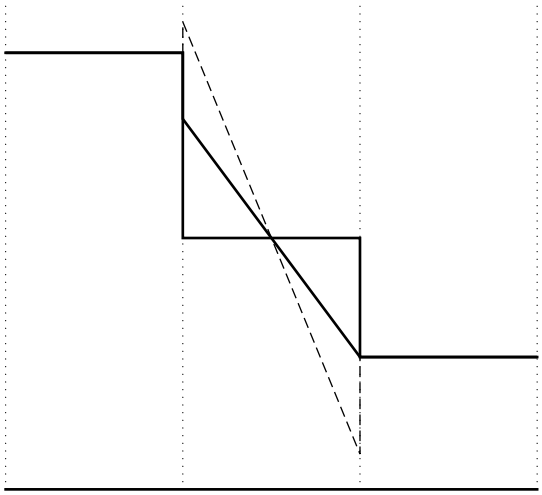

Figure 6. The $\Lambda\Pi_h^O$ limiter: an example. Displayed are the local means of u_h (——), the linear function u_h in the element of the middle before limiting (- - - -) and the resulting function after limiting (——).

where the *minmod* function m is defined by

$$m\,(a_1, a_2, a_3) = \begin{cases} s\ \min_{1\le n\le 3}\ |\,a_n\,| \text{ if } s = sign(a_1) \\ \qquad = sign(a_2) = sign(a_3) \\ 0 \text{ otherwise} \end{cases}$$

we obtain that

$$\overline{u}_j = \overline{v}_j, \quad \text{and} \quad u_{x,j} = m(v_{x,j}, \overline{v}_j - \overline{v}_{j-1}, \overline{v}_{j+1} - \overline{v}_j)$$

We thus see that the mean of u_h coincides with that of v_h. Moreover, since, by definition of the function m, we have

$$|\,u_{x,j}\,| \le |\,v_{x,j}\,|$$

it is reasonable to call the operator $\Lambda\Pi$ a slope limiter. This slope limiter, which we denote by $\Lambda\Pi_h^O$, is due to Osher (1984; see Figure 6. It is less restrictive than the limiters originally considered by van Leer (1974 and by van Leer (1979.

Next, we show computational results for some shock-capturing DG methods and then study the main example of DG methods using slope limiters, namely, the Runge-Kutta discontinuous Galerkin (RKDG) methods.

4.3. Shock-capturing DG methods

There are only two theoretical results concerning shock-capturing methods, and those concern the scalar hyperbolic conservation law. The first is by Jaffré et al. (1995, who proved convergence to the entropy solution. The second is by Cockburn and Gremaud (1996, who

Encyclopedia of Computational Mechanics. Edited by Erwin Stein, René de Borst and Thomas J.R. Hughes.
 ISBN: 0-470-84699-2

obtained a priori error estimates showing that this convergence takes place at rate of at least $h^{1/4}$ in the $L^\infty(0,T;L^1(\mathbb{R}^N))$-norm, as well as a posteriori error estimates which can be used for adaptivity purposes.

Space-time DG methods for nonlinear hyperbolic conservation laws were considered by Lowrie et al. (1995 (Lowrie et al. (1995, Lowrie et al. (1998) and Lowrie (1996. DG shock-capturing methods have been considered by Hartmann and Houston (2002a (Hartmann and Houston (2002a,b) for adaptively solving for values of linear functionals of solutions of *steady state* nonlinear hyperbolic conservation laws with remarkable success; see also Süli and Houston (2002. More recently, shock-capturing DG methods with PDE-based artificial viscosity were considered by Barter and Darmofal (2010. See also the shock-capturing DG method by Huerta et al. (2012.

To give an example, let us consider the Burger's equation

$$u_t + \tfrac{1}{2}\left(u^2\right)_x = 0, \quad \text{in } \Omega \times (0,T)$$

where $\Omega = (0,3)$ and $T = 2$, subject to the initial condition

$$u(x,0) = \begin{cases} 2\,\sin^2(\pi x), & 0 \le x \le 1 \\ \sin^2(\pi x), & 1 \le x \le 2 \\ 0, & 2 \le x \le 3 \end{cases}$$

and boundary condition $u(0,t) = 0$, for $t \in [0,T]$; see Figure 7. The exact solution develops two shocks, which eventually merge. The functional of interest $J(\cdot)$ is the value of the solution before these two shocks collapse into each other. We thus take,

$$J(u) = u(2.3, 1.5) = 0.664442403975254670$$

see Figure 7.

In Figure 8, we compare the performance of the h- and hp-mesh refinement algorithms for this problem. Again, we observe exponential convergence of the error in the computed functional using hp-refinement; on the linear-log scale, the convergence line is straight. On the final mesh the true error between $J(u)$ and $J(u_{\mathrm{DG}})$ using hp-refinement is almost five orders of magnitude smaller than the corresponding quantity when h-refinement is employed alone. Furthermore, in Figure 8, we observe that the hp-refinement algorithm also outperforms the h-refinement strategy, when comparing the error in the computed target functional with respect to the computational cost. Indeed, Figure 9 clearly shows that for the hp-DGFEM the cost per degree of freedom when hp-refinement is employed is comparable to that of using h-refinement.

Finally, in Figure 10, we show the primal mesh after 11 adaptive hp-mesh refinements. Here, we see that the h-mesh has been refined in the region upstream of the point of interest, thereby isolating the smooth region of u from the two interacting shock waves; this renders the subsequent p-refinement in this region much more effective.

Now, let us consider the problem of computing the drag coefficient, $J(\boldsymbol{u})$, of the NACA0012 airfoil for two flows. The first is subsonic and is obtained by imposing on the outer boundary

Encyclopedia of Computational Mechanics. Edited by Erwin Stein, René de Borst and Thomas J.R. Hughes.
 ISBN: 0-470-84699-2

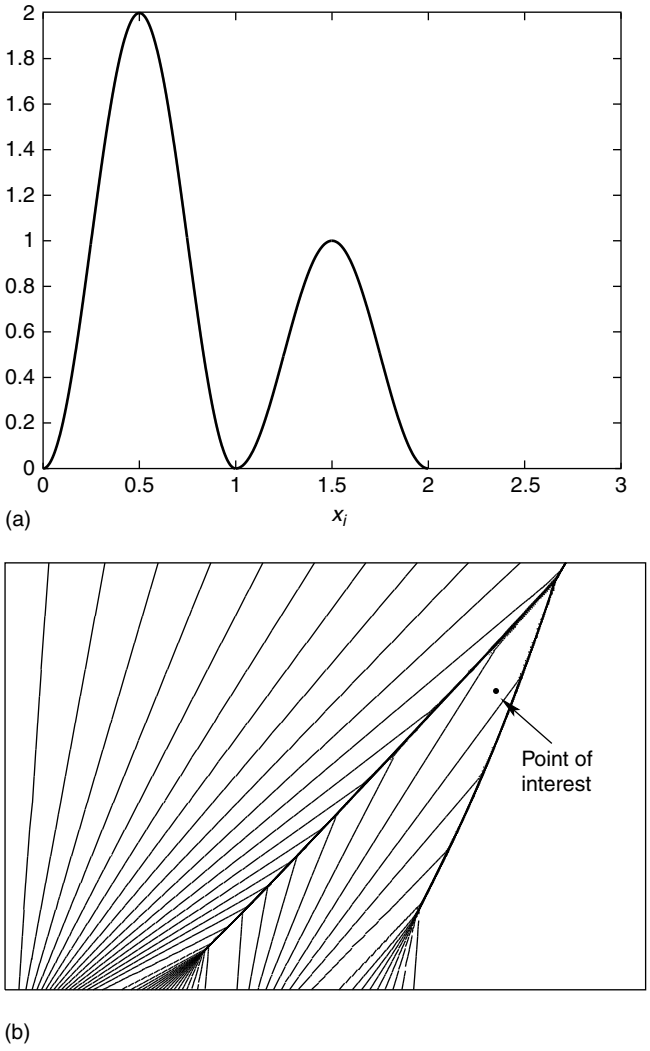

Figure 7. Burgers' problem initial condition (a) and isolines for the exact solution (b). (From Süli E and Houston P. Adaptive finite element approximation of hyperbolic problems. In *Error Estimation and Adaptive Discretization Methods in Computational Fluid Dynamics*, Volume 25 of *Lecture Notes in Computational Science and Engineering*, Barth T and Deconink H (eds). Springer-Verlag: Berlin, 2002; 269-344.)

Encyclopedia of Computational Mechanics. Edited by Erwin Stein, René de Borst and Thomas J.R. Hughes.

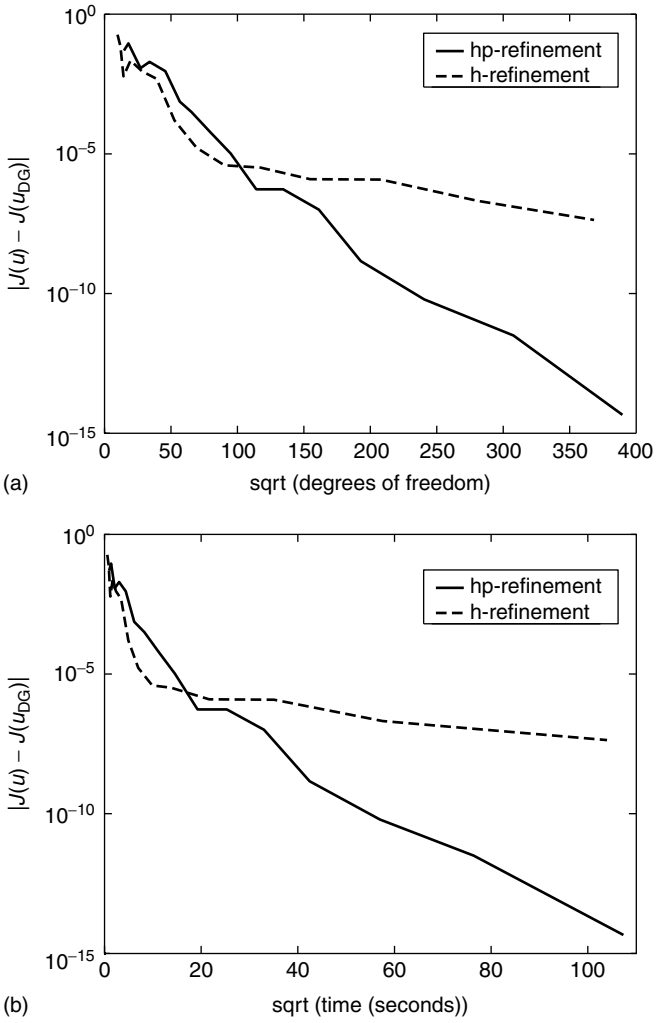

Figure 8. Burgers' equation. Comparison between h- and hp-adaptive mesh refinement: $|J(u)-J(u_{\mathrm{DG}})|$ versus number of degrees of freedom (a); $|J(u) - J(u_{\mathrm{DG}})|$ versus computational time (b). (From Süli E and Houston P. Error Estimation and Adaptive Discretization Methods in Computational Fluid Dynamics, Volume 25 of Lecture Notes in *Computational Science and Engineering, Adaptive finite element approximation of hyperbolic problems*, Barth T and Deconink H (eds). 269-344, 2002, Copyright Springer-Verlag Gmbh & Co.KG, Berlin.)

Encyclopedia of Computational Mechanics. Edited by Erwin Stein, René de Borst and Thomas J.R. Hughes.

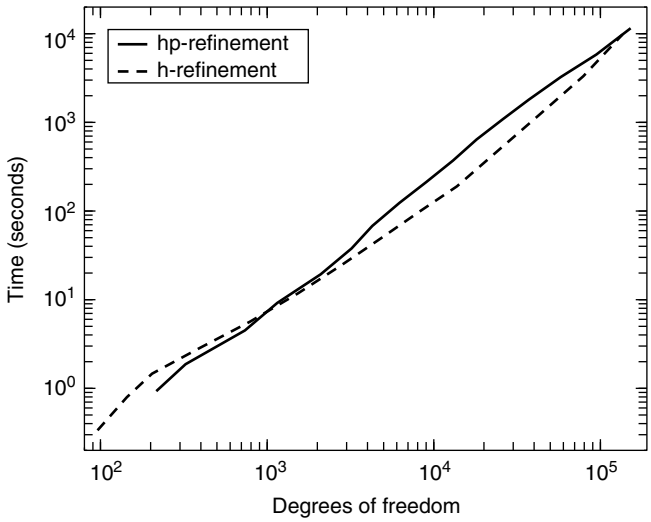

Figure 9. Burgers' equation. Computational time versus number of degrees of freedom. (From Süli E and Houston P. Error Estimation and Adaptive Discretization Methods in Computational Fluid Dynamics, Volume 25 of Lecture Notes in *Computational Science and Engineering, Adaptive finite element approximation of hyperbolic problems*, Barth T and Deconink H (eds). 269-344, 2002, Copyright Springer-Verlag Gmbh & Co.KG, Berlin.)

a Mach 0.5 flow at a zero angle of attack, and a far-field density $\varrho = 1$ and pressure $p = 1$. In this case, no shock-capturing term is used since the solution is very smooth. The second flow is obtained by imposing this time a Mach 0.8 flow and an angle of attack $\alpha = 1.25°$. Since in this case, the solution presents a shock, the shock-capturing term is turned on. In Figure 11, we see how easily the DG method handles meshes with hanging nodes and with different polynomials degrees in different elements. In Figure 12, we also see that *hp*-adaptivity is more efficient than *h*-adaptivity even in the presence of shocks.

In van der Vegt and van der Ven (2002b (see also the paper by van der Ven and van der Vegt (2002) have considered shock-capturing DG methods for the time-dependent compressible Euler equations of gas dynamics. Accordingly, they have used space-time elements, which allow them to easily deal with moving bodies. Their shock-capturing term uses both the local residuals as well as the jumps, which, as we have seen, are also related to the local residuals; for details, see van der Vegt and van der Ven (2002b. They have shown that this method can be efficiently used with mesh adaptation. As an example, we show in Figure 13, the approximation of the method with mesh adaptation on a time-dependent Mach 0.8 flow around an oscillating NACA 0012 airfoil. The pitching angle is between $-0.5°$ and $4.5°$, and the circular frequency is $\omega = \pi/10$. A more spectacular example is shown in Figures 14, 15, and 16, where their DG method is applied to helicopter flight.

Encyclopedia of Computational Mechanics. Edited by Erwin Stein, René de Borst and Thomas J.R. Hughes.
 ISBN: 0-470-84699-2

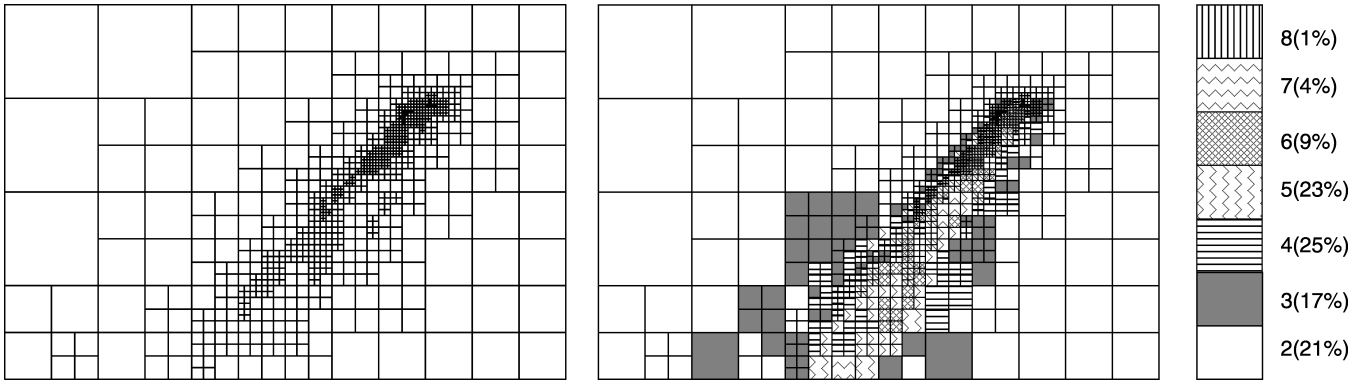

Figure 10. Burgers' equation. *h*- and *hp*-meshes after 11 refinements, with 999 elements and 26 020 degrees of freedom; here, $|J(u) - J(u_{\mathrm{DG}})| = 1.010 \times 10^{-7}$. (From Süli E and Houston P. Error Estimation and Adaptive Discretization Methods in Computational Fluid Dynamics, Volume 25 of Lecture Notes in *Computational Science and Engineering, Adaptive finite element approximation of hyperbolic problems*, Barth T and Deconink H (eds). 269-344, 2002, Copyright Springer-Verlag Gmbh & Co.KG, Berlin.)

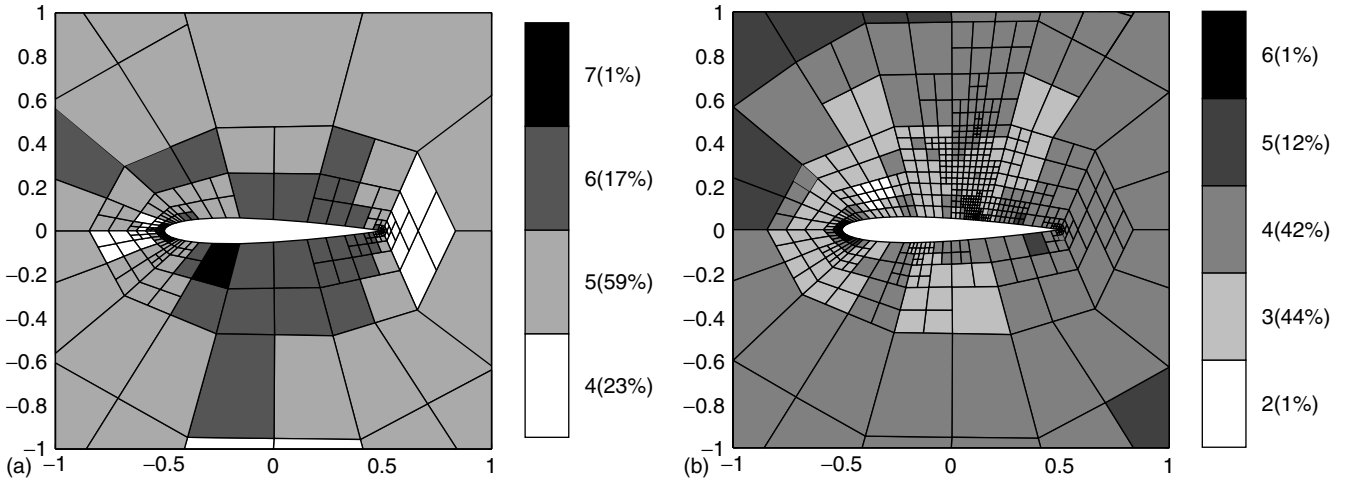

Figure 11. Flow around a NACA0012 airfoil sub-sonic (a) and supersonic (b). The actual *hp*-meshes after 10 refinements. For the subsonic flow, the *hp*-mesh has 325 elements, 45 008 degrees of freedom, and produces an error $|J(u) - J(u_h)| = 3.756 \times 10^{-7}$. For the transonic flow, it has 783 elements, 69 956 degrees of freedom, and produces an error of $|J(u) - J(u_{\mathrm{DG}})| = 1.311 \times 10^{-4}$. (From Süli E and Houston P. Error Estimation and Adaptive Discretization Methods in Computational Fluid Dynamics, Volume 25 of Lecture Notes in *Computational Science and Engineering, Adaptive finite element approximation of hyperbolic problems*, Barth T and Deconink H (eds). 269-344, 2002, Copyright Springer-Verlag Gmbh & Co.KG, Berlin.)

Encyclopedia of Computational Mechanics. Edited by Erwin Stein, René de Borst and Thomas J.R. Hughes.
 ISBN: 0-470-84699-2

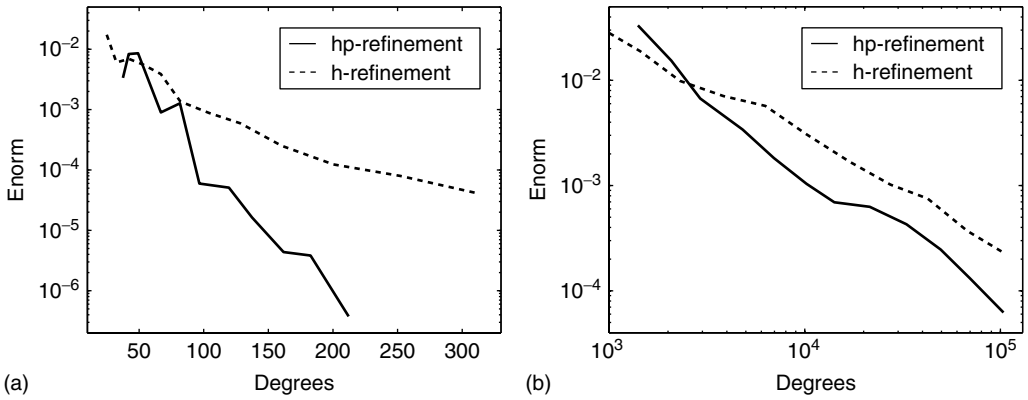

Figure 12. Flow around a NACA0012 airfoil sub-sonic (a) and supersonic (b). Comparison between *h*- and *hp*-adaptive mesh refinement. (From Süli E and Houston P. Error Estimation and Adaptive Discretization Methods in Computational Fluid Dynamics, Volume 25 of Lecture Notes in *Computational Science and Engineering, Adaptive finite element approximation of hyperbolic problems*, Barth T and Deconink H (eds). 269-344, 2002, Copyright Springer-Verlag Gmbh & Co.KG, Berlin.)

4.4. The RKDG methods

There are two main differences between the RKDG methods and the shock-capturing DG methods. The first is that the RKDG methods use an explicit Runge-Kutta scheme to evolve the approximate solution in time; this renders them very easy to implement and much more parallelizable. The second is that whereas the shock-capturing DG methods converge to the entropy solution, thanks to the inclusion in their weak formulation of the shock-capturing terms, the RKDG achieve this by using a slope limiters. Although these two techniques have the very same origin, as we showed in the previous section, the use of the slope limiters results in sharper approximations to the shocks and contact discontinuities.

In this section, we consider the Runge-Kutta discontinuous Galerkin (RKDG) methods for nonlinear hyperbolic systems in divergence form,

$$\boldsymbol{u}_t + \sum_{i=1}^{N} (\boldsymbol{f}_i(\boldsymbol{u}))_{x_i} = \boldsymbol{0}$$

To define the RKDG methods, we proceed in three steps. In the first, the conservation law is discretized in space by using a discontinuous Galerkin (DG) method. After discretization, the system of ordinary differential equations $(\mathrm{d}/\mathrm{d}t)\boldsymbol{u}_h = \boldsymbol{L}(\boldsymbol{u}_h)$ is obtained. Since the approximation is discontinuous, the so-called *mass matrix* is block diagonal and hence, easily invertible. In the second step, an *explicit* strong stability preserving (SSP) Runge-Kutta method is used to march in time. The distinctive feature of the strong stability preserving Runge-Kutta (SSP-RK) methods is that their stability follows from the stability of the forward Euler step. Finally, in the third step, a *generalized slope limiter* $\Lambda\Pi_h$ is introduced in order to *enforce* the above-mentioned stability property of the Euler forward step.

Encyclopedia of Computational Mechanics. Edited by Erwin Stein, René de Borst and Thomas J.R. Hughes.
 ISBN: 0-470-84699-2

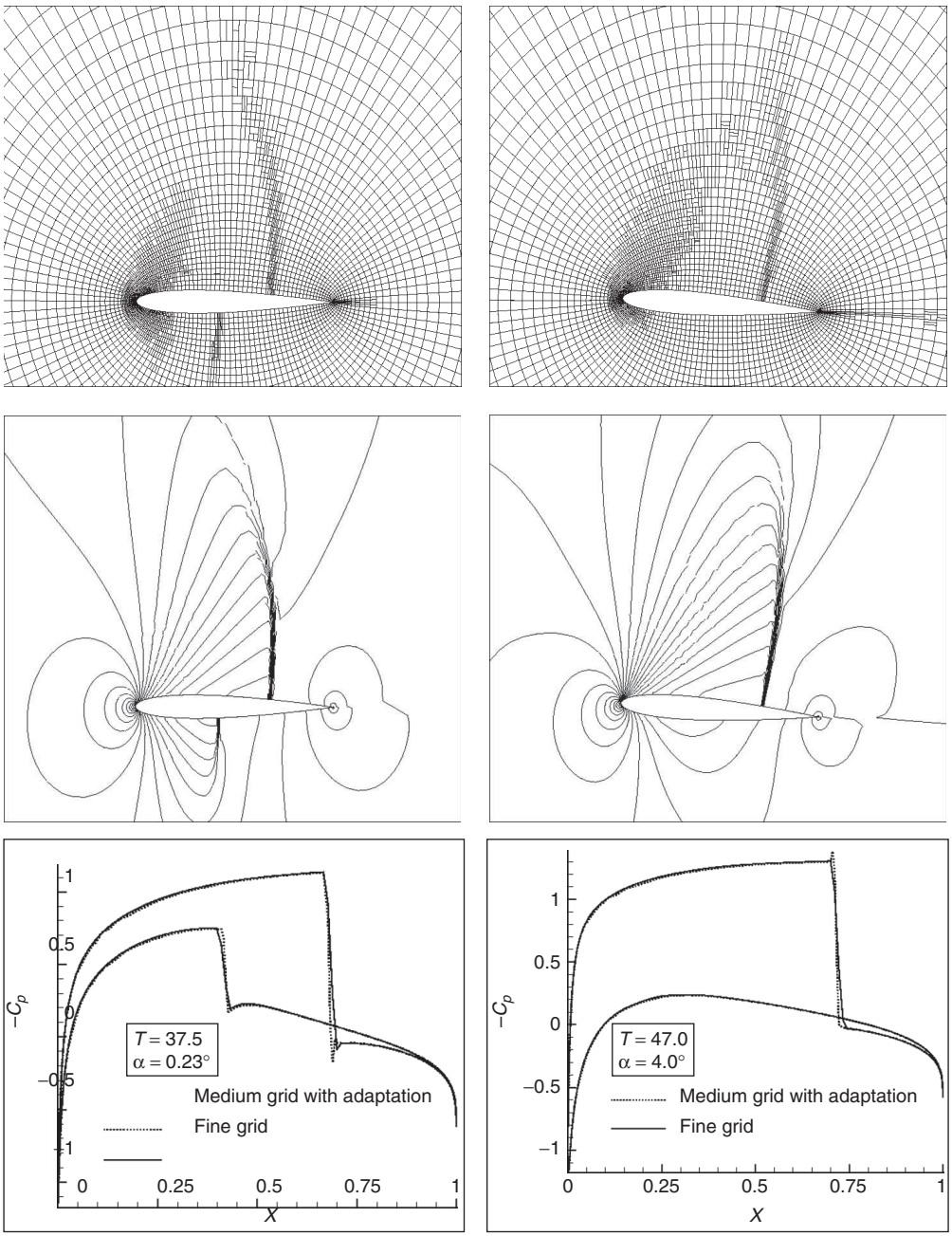

Figure 13. Adapted mesh around oscillating NACA 0012 airfoil, contours of density, and pressure coefficient C_p on the airfoil surface for $\alpha = 0.23^\circ$ (pitching upward) and $\alpha = 4.0^\circ$ (pitching downward) ($M_\infty = 0.8$, $\omega = \pi/10$, $\alpha = 2^\circ \pm 2.5^\circ$). (From van der Vegt JJW and van der Ven H. Space-time discontinuous Galerkin finite element method with dynamic mesh motion for inviscid compressible flows: I. General formulation. *J. Comput. Phys.* 2002b; **182**:546-585.)

Encyclopedia of Computational Mechanics. Edited by Erwin Stein, René de Borst and Thomas J.R. Hughes.
 ISBN: 0-470-84699-2

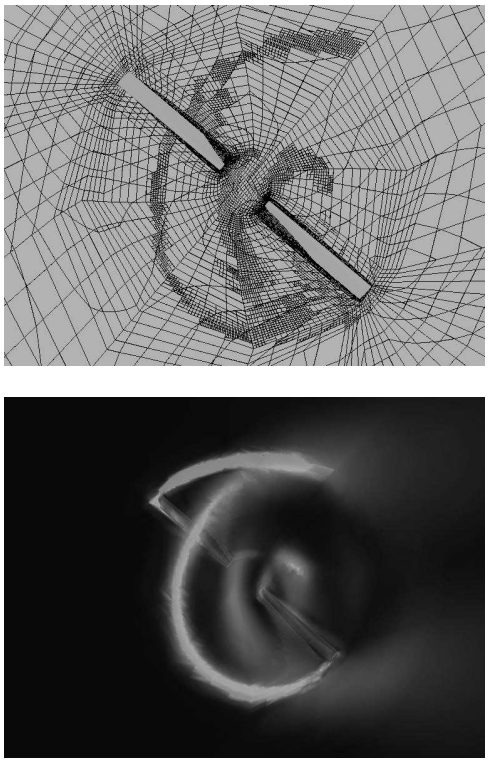

Figure 14. Four-dimensional simulation of the Operational Loads Survey rotor in forward flight. Grid cross-section at $z = 0$ (a) and vorticity levels (b) on adapted mesh at azimuth $\psi = 140°$. The tip vortex of the blade in the upper corner lies above the $z = 0$ plane. ($M_{\text{tip}} = 0.664$, advance ratio 0.164, and thrust 0.0054, flow is coming from the left). (Reproduced from van der Ven H and Boelens OJ. (2003). Towards affordable CFD simulations of rotors in forward flight, A feasibility study with future application to vibrational analysis. In *59th American Helicopter Society Forum*, Phoenix, Arizona, NLR-TP-2003-100, 6-8 May, 2003, by permission of American Helicopter Society.)

In what follows, we give a detailed construction of the RKDG method for the model problem of the scalar conservation law in one space dimension. Then, we briefly discuss the extension of the method to hyperbolic systems in several space dimensions and present numerical results showing the performance of the method.

4.5. RKDG methods for scalar hyperbolic nonlinear conservation laws

Let us define the RKDG method for the Cauchy problem for the scalar hyperbolic nonlinear conservation law

$$\begin{aligned} u_t + f(u)_x &= 0, \quad \text{in } (0,1) \times (0,T) \\ u(x,0) &= u_0(x), \quad \forall\, x \in (0,1) \end{aligned}$$

Encyclopedia of Computational Mechanics. Edited by Erwin Stein, René de Borst and Thomas J.R. Hughes.
 ISBN: 0-470-84699-2

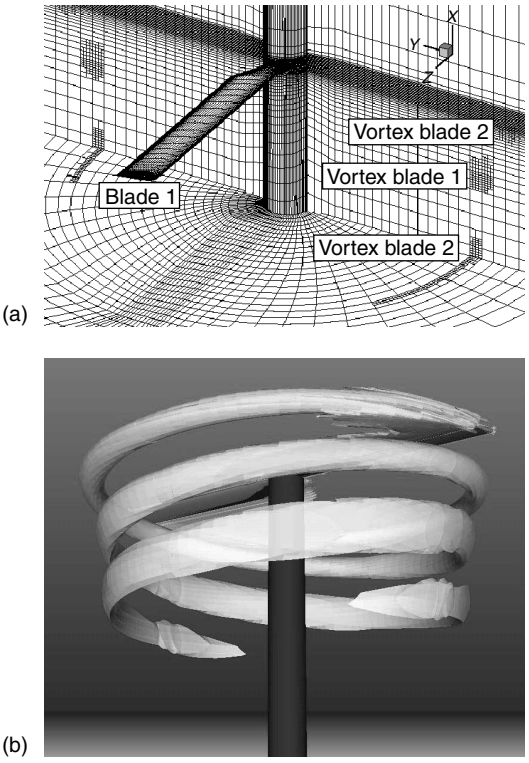

Figure 15. Adapted Caradonna-Tung rotor mesh (135.280 elements) with periodic plane at $z = 0$ and horizontal plane at $x = -3.6$, showing the refined regions at the vortex locations (a). Vorticity contours ($|\omega| = 0.175$) for the Caradonna-Tung rotor in hover, collective pitch 12°, and $M_{\text{tip}} = 0.61$ (b). (From Boelens OJ, van der Ven H, Oskam B and Hassan AA. The boundary conforming discontinuous Galerkin finite element approach for rotorcraft simulations. *J. Aircraft* 2002; **39**:776-785.)

with periodic boundary conditions.

4.5.1. The DG space discretization. Let us triangulate the domain $[0, 1)$ with the partition $\mathcal{T}_h = \{ I_j \}_{i=1}^{N}$ where $I_j = (x_{j-1/2}, x_{j+1/2})$. The initial data $u_h(\cdot, 0)|_{I_j}$ is simply the L^2-projection of $u_0|_{I_j}$ on the space $\mathbb{P}_k(I_j)$, that is, it is the only element of $\mathbb{P}_k(I_j)$ such that

$$(u_h(\cdot, 0), v)_{I_j} = (u_0, v)_{I_j} \tag{5}$$

for all $v \in \mathbb{P}_k(I_j)$. For $t > 0$, we take the approximate solution $u_h(\cdot, t)_{I_j}$ to be the element of $\mathbb{P}_k(I_j)$ such that

$$\begin{aligned} &(u_h(\cdot, t))_t, v)_{I_j} - (f(u_h(\cdot, t)), v_x)_{I_j} \\ &+ \left\langle \widehat{f}(u_h(\cdot, t))\, n_{I_j}, v \right\rangle_{\partial I_j} = 0 \end{aligned} \tag{6}$$

Encyclopedia of Computational Mechanics. Edited by Erwin Stein, René de Borst and Thomas J.R. Hughes.
 ISBN: 0-470-84699-2

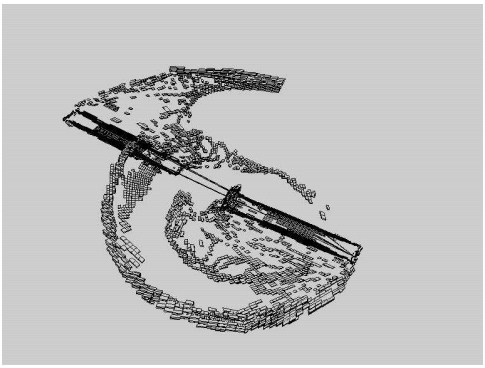

Figure 16. Four-dimensional simulation of the Operational Loads Survey rotor in forward flight. Full space mesh of adapted mesh in intermediate time level at azimuth $\psi = 151.25°$. This intermediate time level has completely been generated by local mesh refinement in time. ($M = 0.664$, advance ratio 0.164, and thrust 0.0054). (Reproduced from van der Ven H and Boelens OJ. Towards affordable CFD simulations of rotors in forward flight, A feasibility study with future application to vibrational analysis. In *59th American Helicopter Society Forum*, Phoenix, Arizona, NLR-TP-2003-100, 6-8 May, 2003, by permission of American Helicopter Society.)

for all $v \in \mathbb{P}_k(I_j)$, where $\widehat{f}(u_h)$ is the numerical flux, which can be taken as indicated in the previous section. This completes the definition of the DG space discretization.

Note that, thanks to the fact that the approximations are discontinuous, the mass matrix is block diagonal, each block being of order $(k+1)$. Moreover, this matrix can be rendered diagonal if we use (properly mapped) Legendre polynomials. Indeed, if, for $x \in I_j$, we write

$$\begin{aligned} u_h(x,t) &= \sum_{\ell=0}^{k} u_j^\ell \, \varphi_\ell^j(x), \quad \varphi_\ell^j(x) = P_\ell\left(\frac{2\,(x-x_j)}{\Delta x_j}\right) \\ \Delta x_j &= x_{j+1/2} - x_{j-1/2} \end{aligned}$$

then, the initial condition (5) becomes

$$u_j^\ell(0) = \frac{(2\ell+1)}{\Delta x_j} \int_{I_j} u_0(x)\, \varphi_\ell^j(x) \mathtt{d}x, \qquad \ell = 0, \ldots, k$$

and the weak formulation (6) takes the following simple form:

$$\begin{aligned} &\frac{\mathrm{d}}{\mathrm{d}t} u_j^\ell(t) + \frac{(2\ell+1)}{\Delta x_j}(-(f(u_h(\cdot,t))\,(\varphi_\ell^j)_x)_{I_j} \\ &\quad + \langle \widehat{f}(u_h(\cdot,t)), \varphi_\ell^j \rangle_{\partial I_j}) = 0 \end{aligned}$$

for $\ell = 0, \ldots, k$.

Encyclopedia of Computational Mechanics. Edited by Erwin Stein, René de Borst and Thomas J.R. Hughes.
 ISBN: 0-470-84699-2

Note that when $f(u) = u$, the system of equations for the degrees of freedom are:

$$\frac{\mathrm{d}}{\mathrm{d}t}u_j^\ell(t) + \frac{(2\ell+1)}{\Delta x_j}\left(\sum_{m=0}^{\ell-1}(-1)^{\ell+m}u_j^m + \sum_{m=\ell}^{k}u_j^m - \sum_{m=0}^{k}(-1)^\ell u_{j-1}^m\right) = 0$$

for $\ell = 0, \ldots, k$. The dissipation of this method was shown to be of order $2k+2$ and the dispersion of order $2k+3$ by Hu and Atkins (2002; Ainsworth (2004; see also Sherwin (2000). A sharp stability analysis of the method has been carried out by Krivodonova and Qin (2013a; Krivodonova and Qin (2013b.

Let us verify that the approximate solution remains bounded in the L^2-norm. It is easy to see that the exact solution satisfies

$$\frac{\mathrm{d}}{\mathrm{d}t}\| u(\cdot,t) \|^2_{L^2(0,1)} = 0$$

The approximate solution satisfies, instead

$$\frac{\mathrm{d}}{\mathrm{d}t}\| u_h(\cdot,t) \|^2_{L^2(0,1)} + \Theta_h(u_h(\cdot,t)) = 0$$

where

$$\Theta_h(v) = \sum_{i=1}^{N}\left(\int_{u_h^-}^{u_h^+}(f(s) - \widehat{f}(u_h^-, u_h^+))\mathtt{d}s\right)(x_{i+1/2}) \geq 0$$

For details, see Jiang and Shu (1994; see also Cockburn and Gremaud (1996.

4.5.2. The SSP-RK time discretization. We discretize in time by using the following $\mathcal{K}$-stage SSP-RK method:

1. Set $u_h^{(0)} = u_h^n$;
2. For $i = 1, \ldots, \mathcal{K}$ compute the intermediate functions:

$$u_h^{(i)} = \sum_{l=0}^{i-1}\alpha_{il}\, w_h^{il}, \quad w_h^{il} = u_h^{(l)} + \frac{\beta_{il}}{\alpha_{il}}\Delta t^n L_h(u_h^{(l)});$$

3. Set $u_h^{n+1} = u_h^{\mathcal{K}}$.

The method is called SSP if

(i) If $\beta_{il} \neq 0$ then $\alpha_{il} \neq 0$,
(ii) $\alpha_{il} \geq 0$,
(iii) $\sum_{l=0}^{i-1}\alpha_{il} = 1$.

Encyclopedia of Computational Mechanics. Edited by Erwin Stein, René de Borst and Thomas J.R. Hughes.
 ISBN: 0-470-84699-2

Table 2. TVD-RK time discretization parameters.

Order	α_{il}	β_{il}	$\max\{\beta_{il}/\alpha_{il}\}$
2	1	1	1
	$\frac{1}{2}\ \frac{1}{2}$	$0\ \frac{1}{2}$	
	1	1	
3	$\frac{3}{4}\ \frac{1}{4}$	$0\ \frac{1}{4}$	1
	$\frac{1}{3}\ 0\ \frac{2}{3}$	$0\ 0\ \frac{2}{3}$	

These methods were originally called TVD-RK methods as they preserved the TVD property of numerical schemes for nonlinear conservation laws. They were introduced by Shu (1988 and by Shu and Osher (1988. Examples are displayed in Table 2; more can be found in the paper by Gottlieb and Shu (1998. See also the recent review by Gottlieb et al. (2000.

The main property of these methods is that their stability *follows* from the stability of the forward Euler steps $w_h^{il} = u_h^{(l)} + (\beta_{il}/\alpha_{il})\Delta t^n$. Indeed, assume that each of the Euler steps satisfy the following stability property

$$|\, w_h^{il}\,| \leq |\, u_h^{(l)}\,|$$

for some seminorm $|\cdot|$. Then

$$\begin{aligned}
|\, u_h^{(i)}\,| &= \left|\sum_{l=0}^{i-1} \alpha_{il}\, w_h^{il}\right| \\
&\leq \sum_{l=0}^{i-1} \alpha_{il}\, |\, w_h^{il}\,| \quad \text{by the positivity property (ii)} \\
&\leq \sum_{l=0}^{i-1} \alpha_{il}\, |\, u_h^{(l)}\,| \quad \text{by the stability assumption} \\
&\leq \max_{0\leq l\leq i-1} |\, u_h^{(l)}\,| \quad \text{by the consistency property (iii)}
\end{aligned}$$

It is clear now that the inequality $|u_h^n| \leq |\mathbb{P}_h u_0|, \forall\, n \geq 0$, follows from the above inequality by a simple induction argument.

It is well known that the L^2-stability of the method (in the linear case) is necessary in order to prevent the growth of the round-off errors. Such a stability property is usually achieved under a condition of the form

$$|\, c|\frac{\Delta t}{\Delta x} \leq \mathrm{CFL}_{L^2}$$

In Table 3, we display the numbers CFL_{L^2} for a wide variety of time and space discretizations; they have been obtained by numerically. The symbol '$\star$' indicates that the method is *unstable*

Encyclopedia of Computational Mechanics. Edited by Erwin Stein, René de Borst and Thomas J.R. Hughes.
 ISBN: 0-470-84699-2

Table 3. The CFL_{L^2} numbers for polynomials of degree k and RK methods of order ν.

k	0	1	2	3	4	5	6	7	8
$\nu = 1$	1.000	$\star$	$\star$	$\star$	$\star$	$\star$	$\star$	$\star$	$\star$
$\nu = 2$	1.000	0.333	$\star$	$\star$	$\star$	$\star$	$\star$	$\star$	$\star$
$\nu = 3$	1.256	0.409	0.209	0.130	0.089	0.066	0.051	0.040	0.033
$\nu = 4$	1.392	0.464	0.235	0.145	0.100	0.073	0.056	0.045	0.037
$\nu = 5$	1.608	0.534	0.271	0.167	0.115	0.085	0.065	0.052	0.042
$\nu = 6$	1.776	0.592	0.300	0.185	0.127	0.093	0.072	0.057	0.047
$\nu = 7$	1.977	0.659	0.333	0.206	0.142	0.104	0.080	0.064	0.052
$\nu = 8$	2.156	0.718	0.364	0.225	0.154	0.114	0.087	0.070	0.057
$\nu = 9$	2.350	0.783	0.396	0.245	0.168	0.124	0.095	0.076	0.062
$\nu = 10$	2.534	0.844	0.428	0.264	0.182	0.134	0.103	0.082	0.067
$\nu = 11$	2.725	0.908	0.460	0.284	0.195	0.144	0.111	0.088	0.072
$\nu = 12$	2.911	0.970	0.491	0.303	0.209	0.153	0.118	0.094	0.077

when the ratio $\Delta t/\Delta x$ is held constant. For DG discretizations using polynomials of degree k and a $k+1$ stage RK method of order $k+1$ (which give rise to an $(k+1)$-th order accurate method), we can take

$$\mathrm{CFL}_{L^2} = \frac{1}{2k+1}$$

The issue of the stability of the Euler forward step $w_h = u_h + \delta\,\Delta t^n\,L(u_h)$, where δ is a positive parameter, is by far more delicate. Indeed, from Table 3, we see that this step is *always unstable* in L^2. On the other hand, when the method uses piecewise-constant approximations, then the forward Euler step is nothing but a monotone scheme, which is total variation diminishing (TVD), that is,

$$|\,w_h\,|_{\mathrm{TV}(0,1)} \leq |\,u_h\,|_{\mathrm{TV}(0,1)}$$

where

$$|\,u_h\,|_{\mathrm{TV}(0,1)} \equiv \sum_{1\leq j\leq N} |\,u_{j+1} - u_j\,|$$

is the total variation of u_h. Hence, if we use piecewise polynomial approximations, it is reasonable to try to see if the Euler forward step under consideration is stable for the following seminorm

$$|\,u_h\,|_{\mathrm{TVM}(0,1)} \equiv \sum_{1\leq j\leq N} |\,\overline{u}_{j+1} - \overline{u}_j\,|$$

where $\overline{u}_j$ is the mean of u_h in the interval I_j. Thus, this seminorm is the total variation of the local means of u_h. The following result gives the conditions for the Euler forward step to be nonexpansive with respect to this seminorm.

Proposition 1. (The sign conditions) *We have*

$$|\,w_h\,|_{\mathrm{TVM}(0,1)} \leq |\,u_h\,|_{\mathrm{TVM}(0,1)}$$

Encyclopedia of Computational Mechanics. Edited by Erwin Stein, René de Borst and Thomas J.R. Hughes.
 ISBN: 0-470-84699-2

provided that

$$\begin{aligned} \operatorname{sign}(u^+_{j+1/2} - u^+_{j-1/2}) &= \operatorname{sign}(u^0_{j+1} - u^0_j) \\ \operatorname{sign}(u^-_{j+1/2} - u^-_{j-1/2}) &= \operatorname{sign}(u^0_j - u^0_{j-1}) \end{aligned}$$

and provided that

$$|\,\delta\,| \left(\frac{|\,\widehat{f}(a,\cdot)\,|_{\mathrm{Lip}}}{\Delta_{j+1}} + \frac{|\,\widehat{f}(\cdot,b)\,|_{\mathrm{Lip}}}{\Delta x_j} \right) \leq 1$$

This result states that a discretization in space by the DG method and an SSP-RK time discretization of the resulting system of ordinary differential equations does not guarantee a nonexpansive total variation in the local means. Fortunately, the sign conditions can be *enforced* by a generalized slope limiter, $\Lambda\Pi_h$.

4.5.3. The generalized slope limiter. Next, we construct the operator $\Lambda\Pi_h$. To do that, let us denote by v_h^1 the L^2-projection of v_h into the space of piecewise-linear functions. We then define $u_h = \Lambda\Pi_h(v_h)$ on the interval I_j, as follows:

(i) Compute

$$\begin{aligned} u^-_{j+1/2} &= \overline{v}_j + m\,(\,v^-_{j+1/2} - \overline{v}_j,\, \overline{v}_j - \overline{v}_{j-1},\, \overline{v}_{j+1} - \overline{v}_j) \\ u^+_{j-1/2} &= \overline{v}_j - m\,(\,\overline{v}_j - v^+_{j-1/2},\, \overline{v}_j - \overline{v}_{j-1},\, \overline{v}_{j+1} - \overline{v}_j) \end{aligned}$$

(ii) If $u^-_{j+1/2} = v^-_{j+1/2}$ and $u^+_{j-1/2} = v^+_{j-1/2}$, set $u_h|_{I_j} = v_h|_{I_j}$,
(iii) If not, take $u_h|_{I_j}$ equal to $\Lambda\Pi^O_h(v^1_h)$.

This generalized slope limiter does not degrade the accuracy of the scheme, except at critical points. In order to avoid that, we replace the *minmod* function m by the *corrected minmod* function $\overline{m}_j$ defined by

$$\overline{m}_j\,(a_1,a_2,a_3) = \begin{cases} a_1 & \text{if } |a_1| \leq M\Delta x_j^2 \\ m\,(a_1,a_2,a_3) & \text{otherwise} \end{cases}$$

where M is an upper bound of the absolute value of the second-order derivative of the solution at local extrema.

We have the following result.

Proposition 2. (The TVBM property) *Suppose that for* $j = 1,\ldots,N$

$$|\,\delta\,| \left(\frac{|\,\widehat{f}(a,\cdot)\,|_{\mathrm{Lip}}}{\Delta_{j+1}} + \frac{|\,\widehat{f}(\cdot,b)\,|_{\mathrm{Lip}}}{\Delta x_j} \right) \leq \frac{1}{2}$$

Then, if $u_h = \Lambda\Pi_{h,M} v_h$, *then*

$$|\,\overline{w}_h\,|_{\mathrm{TVM}(0,1)} \leq |\,\overline{u}_h\,|_{\mathrm{TVM}(0,1)} + CM\Delta x$$

Encyclopedia of Computational Mechanics. Edited by Erwin Stein, René de Borst and Thomas J.R. Hughes.
 ISBN: 0-470-84699-2

Note that the condition on δ is *independent* of the form that the approximate solution has in space.

4.5.4. The nonlinear boundedness of the RKDG method. For this method, we have the following boundedness result.

Theorem 3. *(TVBM-stability of the RKDG method) Let each time step Δt^n satisfy the following* CFL *condition:*

$$\max_{il} \left| \frac{\beta_{il}}{\alpha_{il}} \right| \Delta t^n \left(\frac{|\, \widehat{f}(a,\cdot)\,|_{Lip}}{\Delta_{j+1}} + \frac{|\, \widehat{f}(\cdot,b)\,|_{Lip}}{\Delta x_j} \right) \leq \frac{1}{2} \tag{7}$$

Then we have

$$|\, \overline{u}_h^n\,|_{\mathrm{TVM}(0,1)} \leq |\, u_0\,|_{\mathrm{TV}(0,1)} + CMQ \quad \forall\, n = 0, \ldots, L$$

where $L\,\Delta x \leq Q$.

Let us emphasize that, as we have seen, the DG space discretization, the RK time discretization, and the generalized slope limiter are intertwined just in the right way to achieve the above nonlinear stability result. Thus, although the DG space discretization of this method is an essential distinctive feature, the other two ingredients are of no less relevance.

Note that the above result holds for any polynomial degree and for any order of accuracy in time. This shows that this stability result does not impose an accuracy barrier to the method, as happens with many other methods. The RKDG method can actually achieve high-order accuracy when the exact solution is smooth because the generalized slope limiter does not degrade the high-order accuracy of the space and time discretizations. Although there are no theoretical error estimates that justify this above statement, it is actually supported by overwhelming practical evidence.

Note also that for the linear case $f(u) = c\,u$, the CFL condition (7) becomes

$$|\, c\,| \frac{\Delta t}{\Delta x} \leq \mathrm{CFL}_{\mathrm{TV}} \equiv \frac{1}{2 \max \frac{\beta_{il}}{\alpha_{il}}}$$

In general, the restriction of the time step imposed by the TVBM property is *much weaker* than that required to achieve L^2-stability. However, it is the condition for L^2 stability that needs to be respected; otherwise, the round-off errors would get amplified and the high-order accuracy of the method would degenerate even though the RKDG method remains TVBM-stable.

4.5.5. Generalized slope limiters, discontinuity detection and artificial viscosity techniques. Although the generalized slope limiter just discussed is fairly simple to implement, how to estimate the constant M is not easy. The generalized slope limiters by Biswas et al. (1994; Burbeau et al. (2001, see also Krivodonova (2007, bypass this difficulty but they can still modify the approximation and degrade the original accuracy of the method. A new approach which

Encyclopedia of Computational Mechanics. Edited by Erwin Stein, René de Borst and Thomas J.R. Hughes.
 ISBN: 0-470-84699-2

overcomes this problem, based on seeing the slope limiter as an artificial diffusion operator (see Cockburn (2001) was proposed in Casoni et al. (2013.

Another approach is the essentially non-oscillatory and weighted essentially non-oscillatory techniques, see Zhu et al. (2013 and the references therein, which maintain nonlinear boundedness and maintains the formal order of accuracy of the method. However, they are very involved, especially for high-degree polynomial approximations and require structured meshes. On the other hand, the limiter proposed in Zhu et al. (2013 works for unstructured triangular meshes. To render the generalized slope limiters more efficient, a popular approach is to apply them only at the elements at which the approximate solution might be capturing a discontinuity of the exact solution. In this way, a sophisticated generalized slope limiter could be applied there. See the comparison carried out by Qiu and Shu (2005.

4.5.6. Convergence properties. It is not difficult to use Theorem 3 to conclude, by using a discrete version of the Ascoli-Arzelá theorem, that from the sequence $\{\,\overline{u}_h\,\}_{\Delta x>0}$, it is possible to extract a subsequence strongly converging in $L^\infty(0,T;\mathrm{L}^1(0,1))$ to a limit $u^\star$. That this limit is a weak solution of the nonlinear conservation law can be easily shown. However, while there is ample numerical evidence that suggests that $u^\star$ is actually the entropy solution, this fact is still a challenging theoretical open problem.

In the one-dimensional case of the transport equation with an initial condition displaying a discontinuity, it was shown by Cockburn and Guzmán (2008 that the RKDG with $k = 1$ and a second-order time-marching RK method that, at time T, the L^2-error is second order in the size of the mesh, h, *outside* a region of size $O(T^{1/2}\,h^{1/2}\ \log 1/h)$ to the right of the discontinuity and of size $O(T^{1/3}\,h^{2/3}\ \log 1/h)$ to the left. For any polynomial degree $k \geq 1$ and a third-order time-marching RK method , it was shown by Zhang and Shu (2014 that the L^2-error is of order $\min\{k+1,3\}$ in the size of the mesh, *outside* a region of size $O(T^{1/2}\,h^{1/2}\ \log 1/h)$ to both the right and the left of the location of the discontinuity. In both cases, the standard CFL condition is assumed.

Error estimates for $k = 1$ elements and a second-order time-marching RK method are obtained in the $L^\infty(0,T;L^2(\mathbb{R}^d))$-norm for nonlinear conservation laws in one-space dimension and for linear conservation laws in multiple space dimensions by Shu and Zhang (2004. The order of convergence of $\min\{k+1/2,2\}$ is obtained for general monotone numerical fluxes, and that of $\min\{k+1,2\}$ for upwind numerical fluxes; the minimal CFL condition for stability of the method. is assumed. The extension to symmetrizable hyperbolic systems was carried out by Zhang and Shu (2006. Results for the case in which the time-marching RK is of order three have been done by Zhang and Shu (2010a; Luo et al. (2015; Meng et al. (2016.

Encyclopedia of Computational Mechanics. Edited by Erwin Stein, René de Borst and Thomas J.R. Hughes.
 ISBN: 0-470-84699-2

4.6. RKDG methods for multidimensional hyperbolic systems

The extension of the RKDG methods to the model multidimensional hyperbolic system

$$\boldsymbol{u}_t + \sum_{i=1}^{N} (\boldsymbol{f}_i(\boldsymbol{u}))_{x_i} = \boldsymbol{0}$$

deserves comments on a few key points.

4.6.1. The basis functions. Just as in the one dimensional case, the mass matrix is block-diagonal; the block associated with the element K is a square matrix of order equal to the dimension of the local space and hence, can be easily inverted. Moreover, for a variety of elements and spaces, a basis can be found, which is orthonormal in L^2. This is the case, for example, of rectangles and tensor product polynomials, in which case, the orthonormal basis is a properly scaled tensor product of Legendre polynomials. For simplices and polynomials of a given total degree, there is also an orthonormal basis; see the work by Dubiner (1991, Karniadakis and Sherwin (1999, and Warburton (1998, and the recent implementations by Aizinger et al. (2000 and Hesthaven and Warburton (2002.

4.6.2. Quadrature rules. In practice, the integrals appearing in the weak formulation need to be approximated by quadrature rules. It was proven by Cockburn et al. (1990 that

$$\|L_h(u) + \nabla \cdot f(u)\|_{L^\infty(K)} \leq C\ h^{k+1} |f(u)|_{W^{k+2,\infty}(K)}$$

if the quadrature rules over each of the faces of the border of the element K are exact for polynomials of degree $2k+1$, and if the one over the element is exact for polynomials of degree $2k$. The fact that these requirements are also necessary, can be easily numerically verified; moreover, the method is more sensitive to the quality of the quadrature rules used on the boundary of the elements than to that used in their interior.

Finally, let us point out that a quadrature-free version of the method was devised by Atkins and Shu (1998, which results in a very efficient method for linear problems and certain nonlinear problems such as Euler equations of gas dynamics. A very efficient quadrature rule was obtained by van der Ven and van der Vegt (2002 for the Euler equations of gas dynamics by suitably exploiting the structure of the equations.

4.6.3. Numerical fluxes. When dealing with multidimensional hyperbolic systems, the so-called local Lax-Friedrichs numerical flux is a particularly convenient choice of numerical flux. Indeed, it can be easily applied to any nonlinear hyperbolic system, it is simple to compute, and yields good results. This numerical flux is defined as follows. If we set $\boldsymbol{f}_{\boldsymbol{n}_K} = \sum_{i=1}^{N} n_i \boldsymbol{f}_i(\boldsymbol{u})$, we define the local Lax-Friedrichs numerical flux as

$$\widehat{\boldsymbol{f}}^{\mathrm{LLF}}_{\boldsymbol{n}_K}(\boldsymbol{u}_h) = \{\boldsymbol{f}_{\boldsymbol{n}_K}(\boldsymbol{u}_h)\} - \frac{C}{2} [\![\boldsymbol{u}_h]\!]_{\boldsymbol{n}_K}$$

Encyclopedia of Computational Mechanics. Edited by Erwin Stein, René de Borst and Thomas J.R. Hughes.
 ISBN: 0-470-84699-2

where $C = C(K^{\pm})$ is the larger one of the largest eigenvalue (in absolute value) of $\partial/(\partial \boldsymbol{u}^{\pm})\boldsymbol{f}_{\boldsymbol{n}_{K^{\pm}}}(\boldsymbol{u}^{\pm})$, or, in practice, of $\partial/(\partial \overline{\boldsymbol{u}}^{\pm})\boldsymbol{f}_{\boldsymbol{n}_{K^{\pm}}}(\overline{\boldsymbol{u}}_{K^{\pm}}$, where $\overline{\boldsymbol{u}}_{K^{\pm}}$ are the means of the approximate solution $\boldsymbol{u}_h$ in the elements $K^{\pm}$.

For symmetric hyperbolic systems, it is possible to devise numerical fluxes that render the method of lines (or the space-time methods) L^2-stable; see Barth (2000.

4.6.4. The slope limiter $\Lambda\Pi_h$. When we dealt with the scalar one-dimensional conservation law, the role of the generalized slope limiter $\Lambda\Pi_h$ was to enforce the TVBM property of a typical Euler forward time step. In the case of multidimensional scalar conservation laws, we cannot rely anymore on the TVBM property of the Euler forward step because such a property does not hold for monotone schemes on general meshes; it has been proven only for monotone schemes in nonuniform Cartesian meshes by Sanders (1983. We can, instead, rely on a local maximum principle; see the paper by Cockburn et al. (1990.

A practical and effective generalized slope limiter $\Lambda\Pi_{h,M}$ was later developed by Cockburn and Shu (1998b. To apply it to the function v_h, we proceed on the element K as follows:

(i) Compute the L^2-projection of v_h into the linear functions on K, $v_h^1|_K$,
(ii) Compute $r_h|_K = \Lambda\Pi_{h,M}^1 v_h^1|_K$,
(iii) If $r_h|_K = v_h^1|_K$, set $u_h|_K = v_h|_K$,
(iv) If not, set $u_h|_K = r_h|_K$.

Note that in order to use this generalized slope limiter, one only needs to know how to slope limit piecewise linear functions; for the details of the definition of $\Lambda\Pi_{h,M}^1$, we refer the reader to the paper by Cockburn and Shu (1998b.

An interesting limiter has been proposed by Wierse (1997. Kershaw et al. (1998 introduced a limiter based on quadratic programming. Biswas et al. (1994 devised a limiter based on local moments, rather than on slopes, and used it for adaptivity purposes. Burbeau et al. (2001 proposed what they call a *problem-independent* slope limiter.

4.6.5. Characteristic variables. For systems, limiting in the local characteristic variables gives remarkably superior results than doing it component-by-component.

To limit the vector $\tilde{v}_h(m_i, K_0)$ in the element K_0 (see Figure 4.6.5), we proceed as follows:

- Find the matrix R and its inverse R^{-1}, which diagonalizes the Jacobian

$$J = \frac{\partial}{\partial u} f(\overline{v}_{K_0}) \cdot \frac{m_i - b_0}{|m_i - b_0|}$$

Encyclopedia of Computational Mechanics. Edited by Erwin Stein, René de Borst and Thomas J.R. Hughes.
 ISBN: 0-470-84699-2

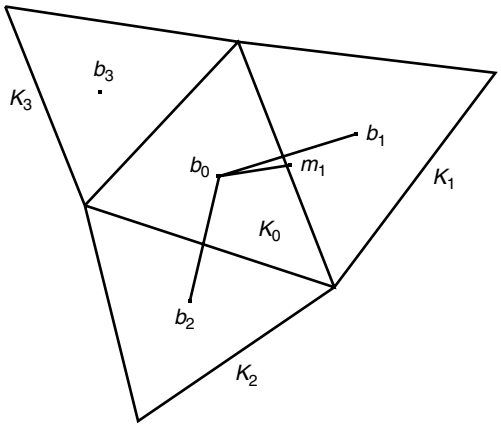

Figure 17. Illustration of limiting.

that is, $R^{-1}JR = \Lambda$, where Λ is a diagonal matrix containing the eigenvalues of J. Notice that the columns of R are the right eigenvectors of J and the rows of R^{-1} are the left eigenvectors.

- Transform $\widetilde{v}_h(m_i, K_0)$ and $\Delta\overline{v}(m_i, K_0)$ to the characteristic fields. This is achieved by left multiplying these vectors by R^{-1}.
- Apply the scalar limiter to each of the components of the transformed vectors.
- Multiply by R on the left to transform the result back to the original space.

4.7. Computational results

In this section, we display computational results that show that the RKDG method can achieve exponential convergence when the solution is very smooth and that it can perform as well as the high-resolution methods when discontinuities are present. We also show results showing its excellent handling of boundary conditions and its remarkable parallelization properties. Finally, we also show that the use of higher-degree polynomials results in a more efficient method, even in the presence of discontinuities.

4.7.1. Exponential convergence. To show that exponential convergence can be achieved and that it is always more efficient to use higher-degree polynomials when the exact solution is very smooth, we consider

$$u_t + \nabla \cdot (\boldsymbol{v}\, u) = 0$$

where $\boldsymbol{v} = 2\pi\,(-y, x)$ and the initial condition is a Gaussian hill. In Figure 4.7.1, we see the L^2-error at time $T = 1$ versus the CPU time for the four different successively refined meshes described below and for polynomials of degree up to six. The refinement of the mesh is obtained by dividing the triangles in four congruent triangles. Each line corresponds to a different mesh,

Encyclopedia of Computational Mechanics. Edited by Erwin Stein, René de Borst and Thomas J.R. Hughes.
 ISBN: 0-470-84699-2

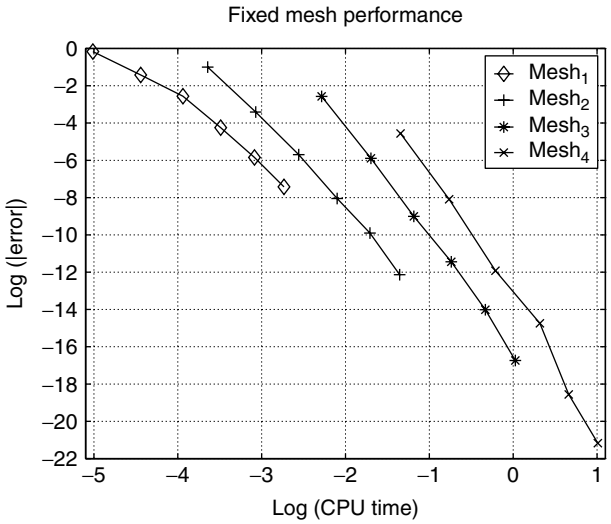

Figure 18. Spectral convergence and comparison of L^2-error versus CPU time for 4 successively refined meshes and polynomials of degree 1 to 6. (From Aizinger V, Dawson CN, Cockburn B and Castillo P. Local discontinuous Galerkin method for contaminant transport. *Adv. Water Res.* 2000; **24**:73-87.)

with the symbols on each line representing the error for the six different approximating spaces. We easily observe that exponential convergence is achieved and that it is always more efficient to use a coarser mesh with a higher-order polynomial approximation.

4.7.2. Treatment of the boundary conditions. To show the ease with which the method deals with the boundary conditions, we consider a variation of the above problem

$$u_t + \nabla \cdot (\boldsymbol{v}\, u) = 0$$

where $\boldsymbol{v} = (-y + 1/2, x - 3/4)$ and the initial data is

$$u(\boldsymbol{x}, t = 0) = \begin{cases} \exp\left(8 - \frac{8}{1 - 8|\boldsymbol{x} - (3/4, 1)|^2}\right), & \text{if } 8\left|\boldsymbol{x} - \left(\frac{3}{4}, 1\right)\right|^2 < 1 \\ 0, & \text{otherwise} \end{cases}$$

An RKDG method using quadratic polynomial approximations and a SSP-RK method of order three is used. Note that, unlike the previous example, only part of the initial data is in the computational domain. The boundary conditions are taken by using the Lax-Friedrichs flux and by giving the exact solution as the exterior trace. In Table 4, we see that the full order three has been achieved, as expected. In Figure 19, we also see that the boundary conditions have been captured very well by the RKDG method.

Encyclopedia of Computational Mechanics. Edited by Erwin Stein, René de Borst and Thomas J.R. Hughes.
 ISBN: 0-470-84699-2

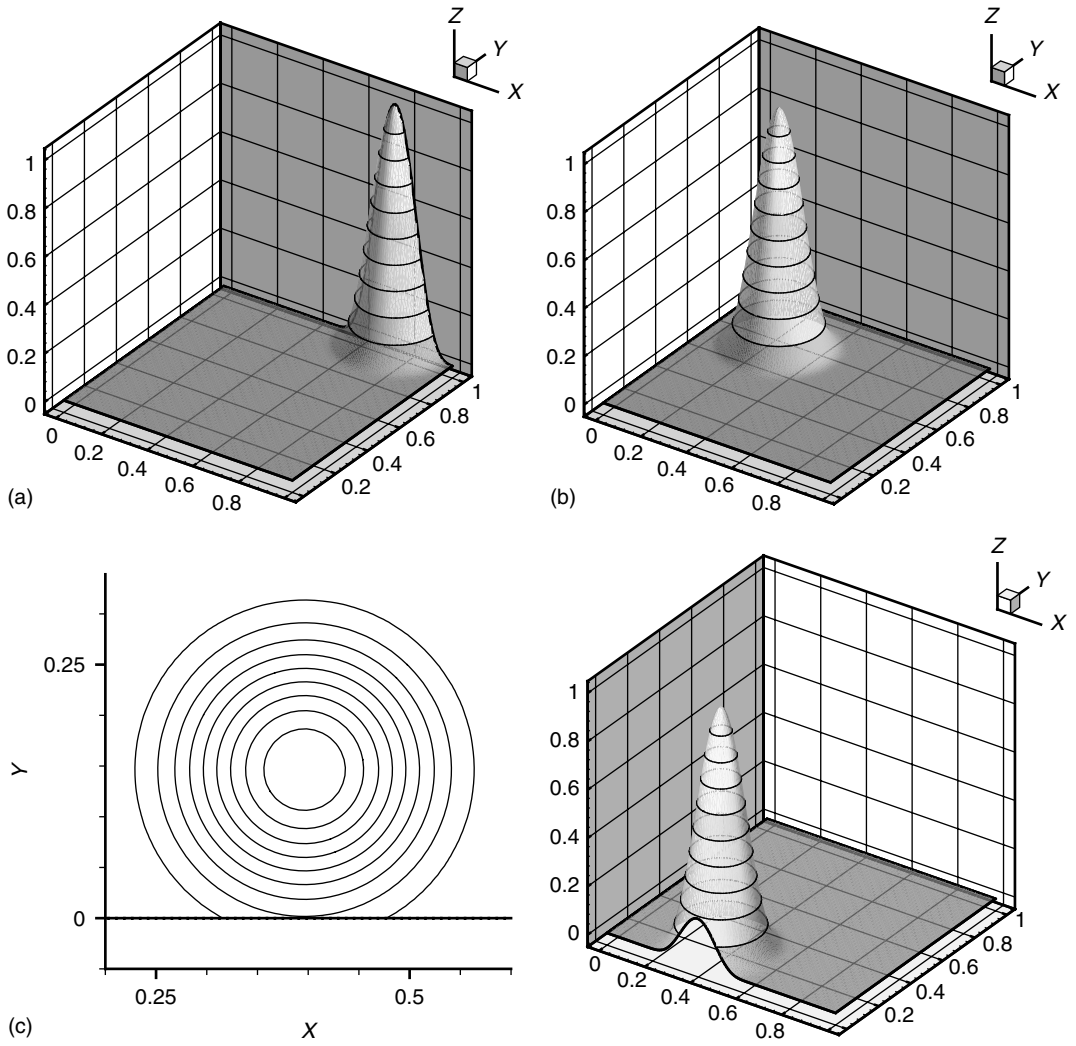

Figure 19. Approximate solution at $T = 0.0$ (a), $T = (3/8)\pi$ (b) and $T = (3/4)\pi$ (c). The mesh is a uniform 64×64 of triangles.

Table 4. Errors at $T = (3/4)\pi$.

Mesh	$\| e_u(T) \|_{L^\infty(\Omega)}$	Order	$\| e_u(T) \|_{L^1(\Omega)}$	Order
16×16	0.21E-01	2.01	0.42E-03	3.32
32×32	0.25E-02	3.07	0.42E-04	3.31
64×64	0.32E-03	2.96	0.49E-05	3.11
128×128	0.52E-04	2.64	0.60E-06	3.01

Encyclopedia of Computational Mechanics. Edited by Erwin Stein, René de Borst and Thomas J.R. Hughes.

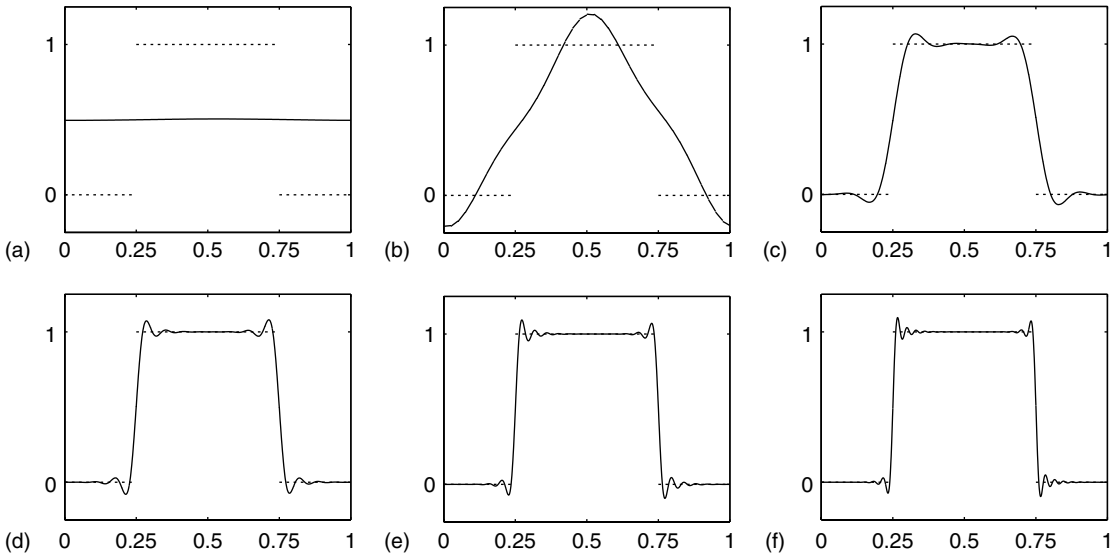

Figure 20. Effect of the order of the RKDG method on the approximation of discontinuities. The exact solution at time $T = 100$, u (----), is contrasted against the approximate solution u_h (———) obtained with the RKDG method of order $k + 1$ on a mesh of 40 elements for the values $k = 0$ (a), $k = 1$ (b), $k = 2$ (c), $k = 3$ (d), $k = 4$ (e), and $k = 5$ (f). No limiter was used.

4.7.3. Approximation of contact discontinuities. Let us now show how the contact discontinuities are approximates by the RKDG methods. To do that, we consider the problem

$$u_t + u_x = 0, \quad \text{in } [0,1) \times (0,T)$$

with periodic boundary conditions and initial condition

$$u(x,0) = \begin{cases} 1, & \text{if } x \in (0.25, 0.75) \\ 0, & \text{otherwise} \end{cases}$$

In Figures 20 and 21, we show the results given by RKDG methods using polynomials of degree k and a $(k+1)$-stage, $(k+1)$th-order accurate SSP-RK method. We see that as the polynomials degree increases, so does the quality of the approximation of the contact discontinuity, except, perhaps for the unwanted oscillations near them.

4.7.4. Approximation of shocks. First, let us show in a simple example that the RKDG methods can capture shocks as well as any high-resolution finite difference or finite volume scheme. Consider the approximation of the entropy solution of the inviscid Burgers equation

$$u_t + \left(\frac{u^2}{2}\right)_x = 0$$

on the domain $(0,1)\times(0,T)$ with initial condition $1/4+\sin(\pi(2\,x-1))/2$ and periodic boundary conditions. In Figure 22, we display the RKDG solution using piecewise linear and piecewise

Encyclopedia of Computational Mechanics. Edited by Erwin Stein, René de Borst and Thomas J.R. Hughes.

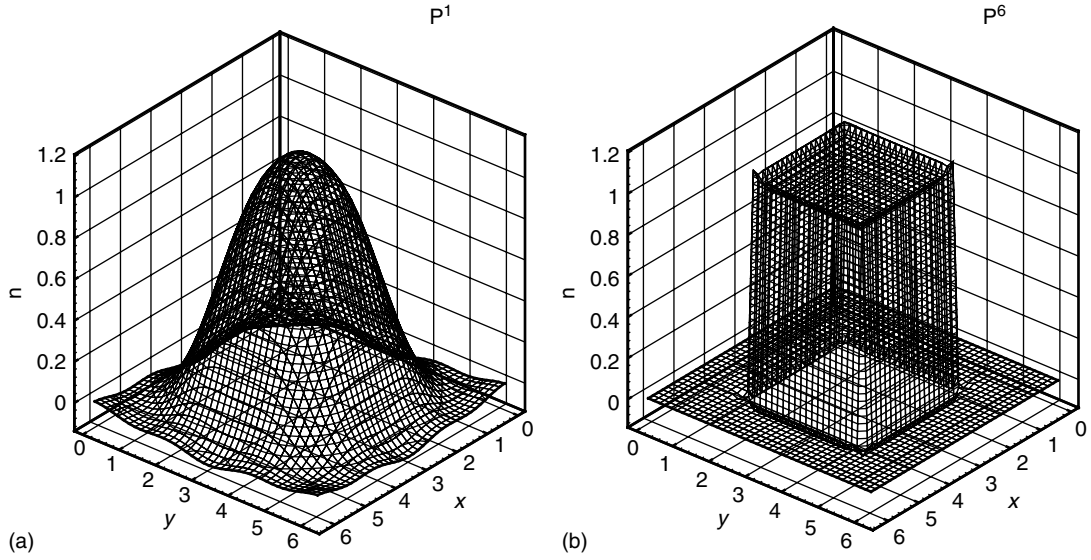

Figure 21. Effect of the order of the RKDG method on the approximation of discontinuities. Comparison of the exact and the RKDG solutions at $T = 100\pi$ with $k = 1$ (a) and $k = 6$ (b). Two dimensional results with 40×40 squares. No limiter was used. (Reproduced from Cockburn B and Shu C-W. Runge-Kutta discontinuous Galerkin methods for convection-dominated problems. *J. Sci. Comput.* 2001; **16**:173-261, by permission of Kluwer Academic/Plenum Publishers.)

quadratic approximations; note how, in both cases, the shock has been captured within three elements as would be expected of any high-resolution scheme.

4.7.5. Parallelizability. Let us address the parallelizability of the RKDG method. In Table 5 below, we display the results obtained by Biswas et al. (1994; we see the solution time and total execution time for the two-dimensional problem

$$u_t + u_x + u_y = 0$$

on the domain $(-\pi, \pi)^2 \times (0, T)$ with initial condition $u(x, y, 0) = \sin(\pi x)\, \sin(\pi y)$ and periodic boundary conditions. Biswas et al. (1994 used 256 elements per processor and ran the RKDG method with polynomials of degree two and eight time steps; the work per processor was kept constant. Note how the solution time increases only slightly with the number of processors and the remarkable parallel efficiency of the method.

4.7.6. Approximation of complex solutions. Let us show that the RKDG method can handle solutions with very complicated structure. Consider the classical double-Mach reflection problem for the Euler equations of gas dynamics. In Figure 23, details of the approximation of the density are shown. Note that the strong shocks are very well resolved by the RKDG solution using piecewise linear and piecewise quadratic polynomials defined on *squares*. Also,

Encyclopedia of Computational Mechanics. Edited by Erwin Stein, René de Borst and Thomas J.R. Hughes.
 ISBN: 0-470-84699-2

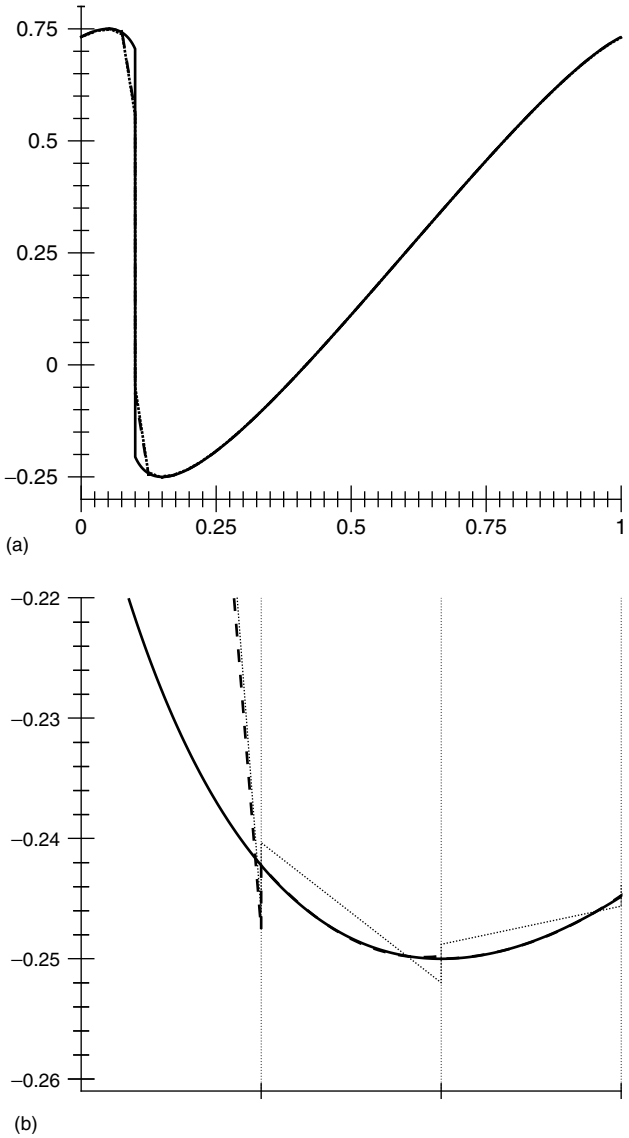

Figure 22. Burgers equation: Comparison of the exact and the RKDG solutions obtained with $\Delta x = 1/40$ at $T = 0.40$. Full domain (a) and zoom on three elements (b) the first of which contains the exact shock. Exact solution (———), piecewise linear approximation (. . . . . .), and piecewise quadratic approximation (- - - -). (From Cockburn B. High-Order Methods for Computational Physics, Volume 9 of Lecture Notes in *Computational Science and Engineering, Discontinuous Galerkin methods for convection-dominated problems*, Barth T and Deconink H (eds), 69-224, 1999, Copyright Springer-Verlag Gmbh & Co.KG, Berlin.)

Encyclopedia of Computational Mechanics. Edited by Erwin Stein, René de Borst and Thomas J.R. Hughes.
 ISBN: 0-470-84699-2

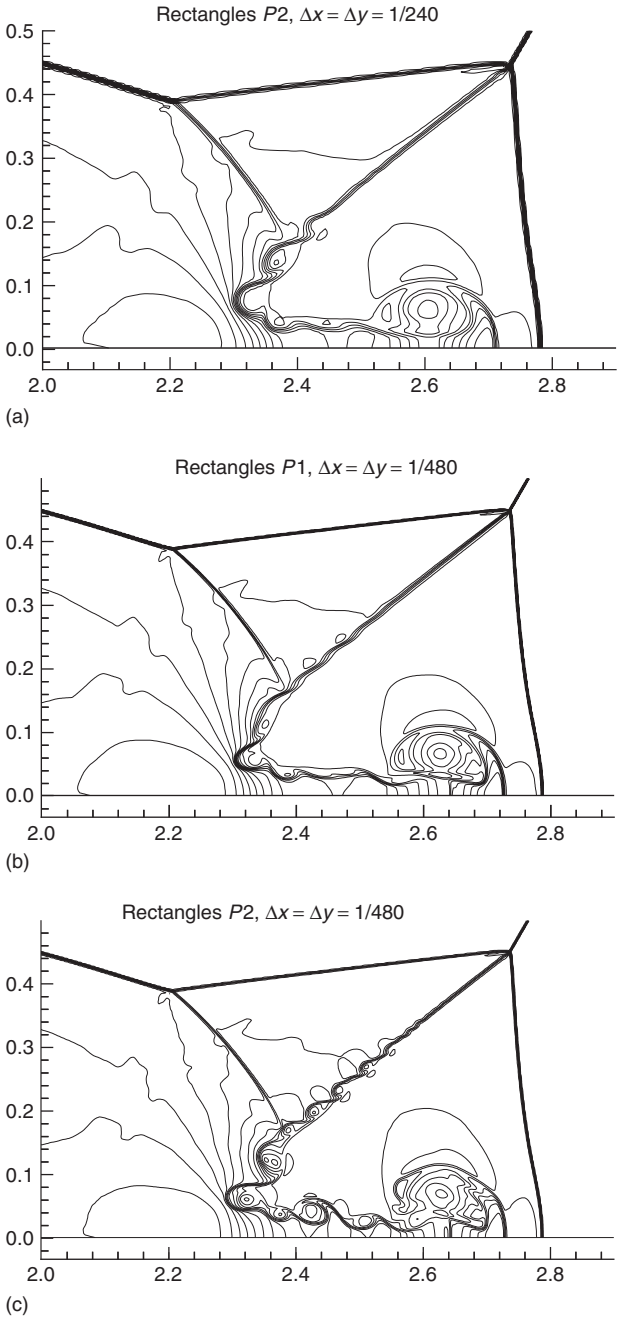

Figure 23. Euler equations of gas dynamics double Mach reflection problem. Isolines of the density around the double Mach stems. Quadratic polynomials on squares $\Delta x = \Delta y = (1/240)$ (a); linear polynomials on squares $\Delta x = \Delta y = (1/480)$ (b); and quadratic polynomials on squares$\Delta x = \Delta y = (1/480)$ (c). (From Cockburn B and Shu C-W. The Runge-Kutta discontinuous Galerkin finite element method for conservation laws V: multidimensional systems. *J. Comput. Phys.* 1998b; **141**:199-224.)

Encyclopedia of Computational Mechanics. Edited by Erwin Stein, René de Borst and Thomas J.R. Hughes.

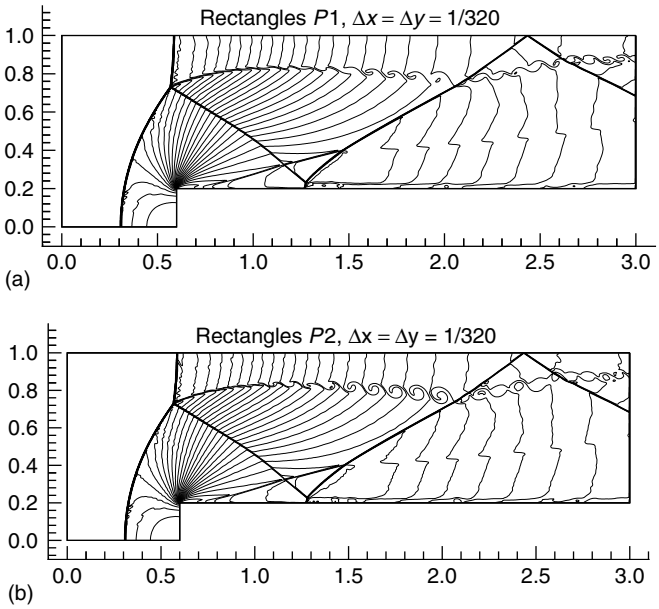

Figure 24. Forward facing step problem. Approximation of the density ϱ. 30 equally spaced contour lines from $\varrho = 0.090338$ to $\varrho = 6.2365$. (From Cockburn B and Shu C-W. The Runge-Kutta discontinuous Galerkin finite element method for conservation laws V: multidimensional systems. *J. Comput. Phys.* 1998b; **141**:199-224.)

note that there is a remarkable improvement in the approximation of the density near the contacts when going from linear to quadratic polynomials.

A similar conclusion can be drawn in the case of the flow of a gas past a forward facing step (see Figure 24); see, also, the study by Woodward and Colella (1984.

4.7.7. Problems with curved boundaries. Bassi and Rebay (1997b showed the importance of approximating as accurately as possible the boundaries of the physical domain and the ease with which this is achieved by using the RKDG methods. Indeed, for the classical two-dimensional isentropic flow around a circle, they showed that approximating the circle by a polygon results in nonphysical entropy production at each of the kinks, which is then carried downstream and accumulates into a nonphysical wake, which does not disappear by further refining the mesh. However, by simply taking into account the exact shape of the boundary, a remarkably improved approximation is obtained; see Figure 25.

On the other hand, van der Vegt and van der Ven (2002a have shown that the high-order accurate representation of the curved boundary can be avoided by using local mesh refinement.

Encyclopedia of Computational Mechanics. Edited by Erwin Stein, René de Borst and Thomas J.R. Hughes.
 ISBN: 0-470-84699-2

Table 5. Scaled parallel efficiency. Solution times (without I/O) and total execution times measured on the nCUBE/2. (From Biswas R, Devine KD and Flaherty J. Parallel, adaptive finite element methods for conservation laws. *Appl. Numer. Math.* 1994; **14**:255-283.)

Number of processors	Work (W)	Solution time (secs.)	Solution parallel efficiency (%)	Total time (secs.)	Total parallel efficiency (%)
1	18 432	926.92	-	927.16	-
2	36 864	927.06	99.98	927.31	99.98
4	73 728	927.13	99.97	927.45	99.96
8	147 456	927.17	99.97	927.58	99.95
16	294 912	927.38	99.95	928.13	99.89
32	589 824	927.89	99.89	929.90	99.70
64	1 179 648	928.63	99.81	931.28	99.55
128	2 359 296	930.14	99.65	937.67	98.88
256	4 718 592	933.97	99.24	950.25	97.57

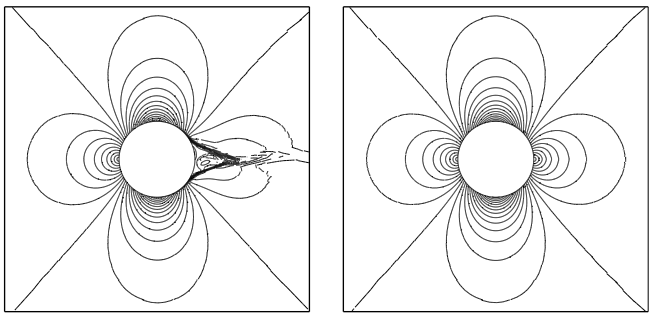

Figure 25. Mach isolines of the DG approximation with P^1 elements the circle is approximated by a polygonal (a) and rendered exactly (b). (From Bassi F and Rebay S. High-order accurate discontinuous finite element solution of the 2-D Euler equations. *J. Comput. Phys.* 1997b; **138**:251-285.)

4.7.8. Adaptivity for the Euler equations of gas dynamics. Next, we give examples of adaptivity using the RKDG method with anisotropic mesh refinement. The first two examples illustrate the use of conforming mesh refinement. For the first example, two Sedov-type explosions in an open square domain develop and interact while bouncing on square obstacles and interacting with each other; see Figure 26. In the second example, the blast of a cannon is simulated in order to understand the shape of the blast waves around the muzzle break; see Figure 27.

Finally, we present an example of a steady state computation on an ONERA M6 wing for which nonconforming refinement has been employed; see Figure 28.

Encyclopedia of Computational Mechanics. Edited by Erwin Stein, René de Borst and Thomas J.R. Hughes.

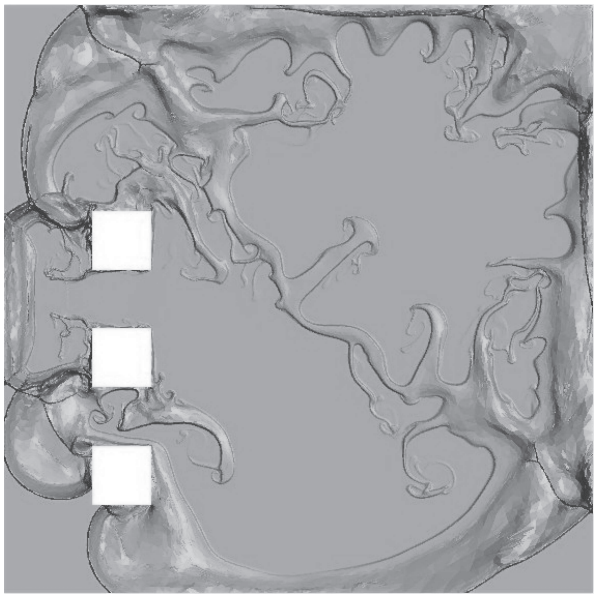

(a)

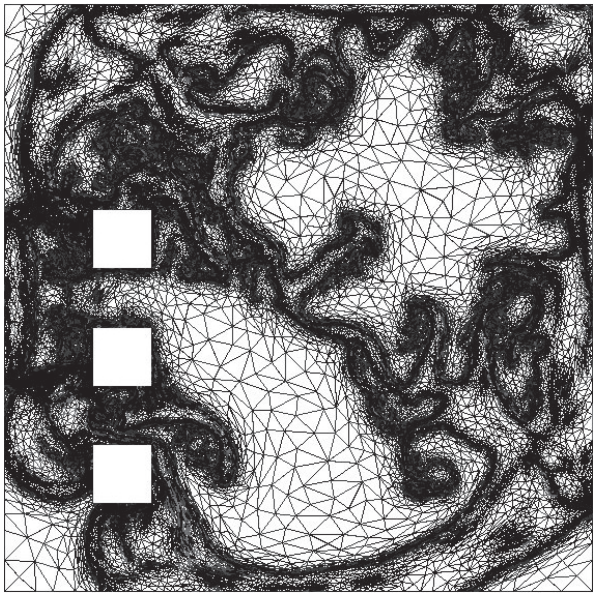

(b)

Figure 26. Two explosions in a square domain with obstacle density (a), and the corresponding mesh (b) after 1 second. (From Remacle J-F, Li X, Chevaugeon N, Shephard MS and Flaherty JE. (2003). Anisotropic Adaptive Simulation of Transient Flows Using Discontinuous Galerkin Methods, 2003, Submitted.)

Encyclopedia of Computational Mechanics. Edited by Erwin Stein, René de Borst and Thomas J.R. Hughes.
 ISBN: 0-470-84699-2

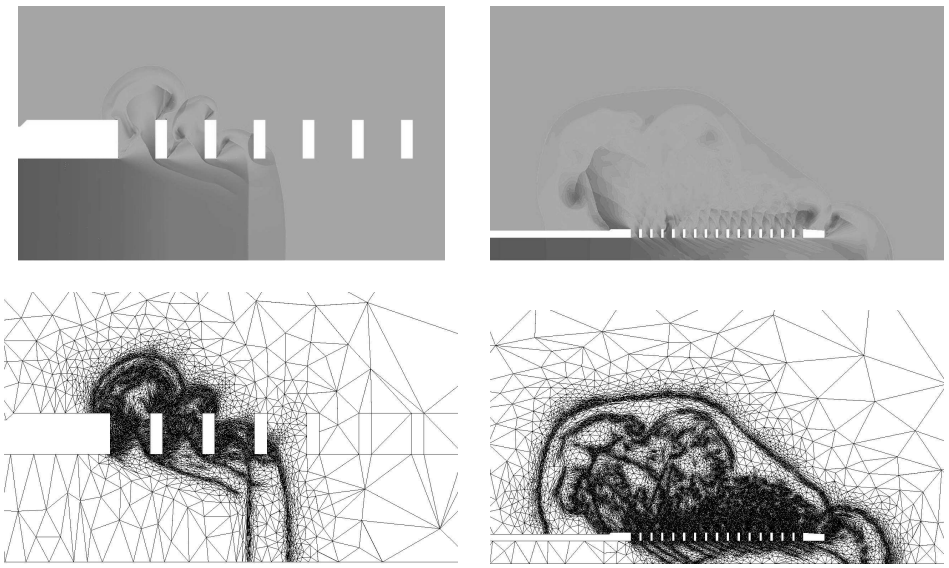

Figure 27. Cannon-blast simulation density and the corresponding mesh. Close up on the muzzle break at an early stage (a), and after the main blast wave left the muzzle (b). (From Remacle J-F, Li X, Chevaugeon N, Shephard MS and Flaherty JE. (2003). Anisotropic Adaptive Simulation of Transient Flows Using Discontinuous Galerkin Methods. 2003, Submitted.)

4.7.9. Simulation of inertial confinement fusion. Our final example is the simulation of the implosion of a NIF capsule which consists of a nearly vacuous inner region enclosed by two spherical shells. For details, see Shestakov et al. (2001. This is a complicated and very difficult problem which involves the simulation of hydrodynamics, heat conduction and radiation transport phenomena. Only the hydrodynamics part of the problem is simulated by using a *one-step* ALE, RKDG method proposed by Kershaw et al. (1998 and implemented in the ICF3D code by Shestakov et al. (2000. In Figure 31, we see the mesh and several physical quantities after 8 nanoseconds of having deposited energy on the outer surface of the capsule. Note the near spherical symmetry of the implosion.

4.8. Enforcing range invariance of the DG approximations

To end this section, we describe a technique for enforcing a range-invariance property of the RKDG methods was introduced by Zhang and Shu (2010b in the framework of nonlinear scalar hyperbolic conservation laws.

For the sake of clarity, we describe this technique for RKDG methods for the initial-value problem:

$$u_t + f(u)_x = 0 \quad \text{in } (0,T)\times\mathbb{R} \qquad u = u_0 \quad \text{on } \{T\}\times\mathbb{R}.$$

Encyclopedia of Computational Mechanics. Edited by Erwin Stein, René de Borst and Thomas J.R. Hughes.
 ISBN: 0-470-84699-2

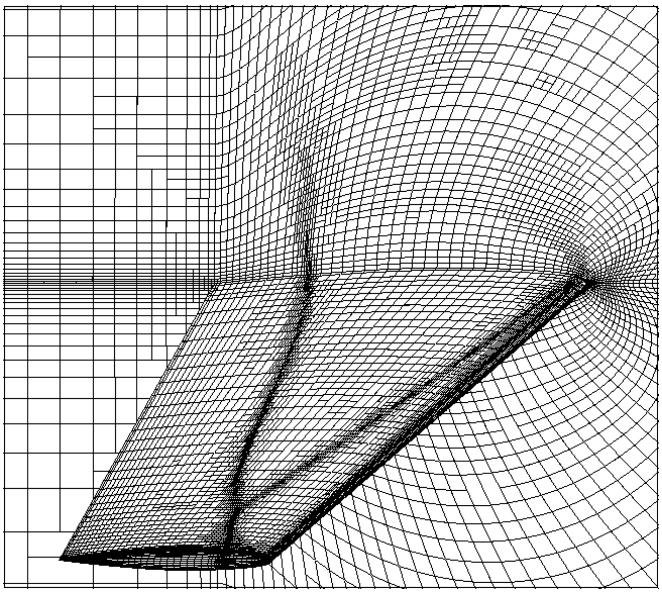

Figure 28. Final adapted mesh on ONERA M6 wing, clearly showing the lambda shock (flow conditions $M_\infty = 0.84$, $\alpha = 3.06^\circ$). (From van der Vegt JJW and van der Ven H. Discontinuous Galerkin finite element method with anisotropic local mesh refinement for inviscid compressible flows. *J. Comput. Phys.* 1998; **182**:46-77.)

In this case, it is well known that the exact solution satisfies the range-invariance (or maximum principle) property

$$u(t,x) \in [m,M] \quad \text{for all } (t,x) \in (0,T)\times\mathbb{R},$$

where $m := \inf_{x\in\mathbb{R}} u_0(x)$ and $M := \sup_{x\in\mathbb{R}} u_0(x)$.

Suppose that we are given the RKDG approximation at the i-th intermediate stage *after* the application of the generalized slope limiter $\Lambda\Pi_{h,M}$. Then, on the element $I_j := (x_{j-1/2}, x_{j+1/2})$, we modify the function as follows:

$$u_h^{(i)} := \theta(u_h^{(i)} - \overline{u}_h^{(i)}) + \overline{u}_h^{(i)},$$

where

$$\theta := \left\{ \left| \frac{M - \overline{u}_h^{(i)}}{M_j - \overline{u}_h^{(i)}} \right|, \left| \frac{m - \overline{u}_h^{(i)}}{m_j - \overline{u}_h^{(i)}} \right|, 1 \right\},$$

and $m_j := \inf_{x\in S_j} u_h^{(i)}(x)$ and $M_j := \sup_{x\in S_j} u_h^{(i)}(x)$. Here S_j denotes a set of suitably chosen points lying on $[x_{j-1/2}, x_{j+1/2}]$. Typically, they are chosen as Gauss-Lobatto quadrature points. This modification does not alter the high-order accuracy of the method and enforces the range-invariance property

$$u_h(t^n,x) \in [m,M] \quad \text{for all } (t,x) \in (0,T)\times S_j \quad \forall j \in \mathbb{Z}.$$

Encyclopedia of Computational Mechanics. Edited by Erwin Stein, René de Borst and Thomas J.R. Hughes.
 ISBN: 0-470-84699-2

under a suitable CFL condition. An illustration is provided in Figures 29 and 30. Therein, the slope limiter $\Lambda\Pi_{h,M}$ has not been applied since it is not needed to enforce convergence to the physically relevant solution.

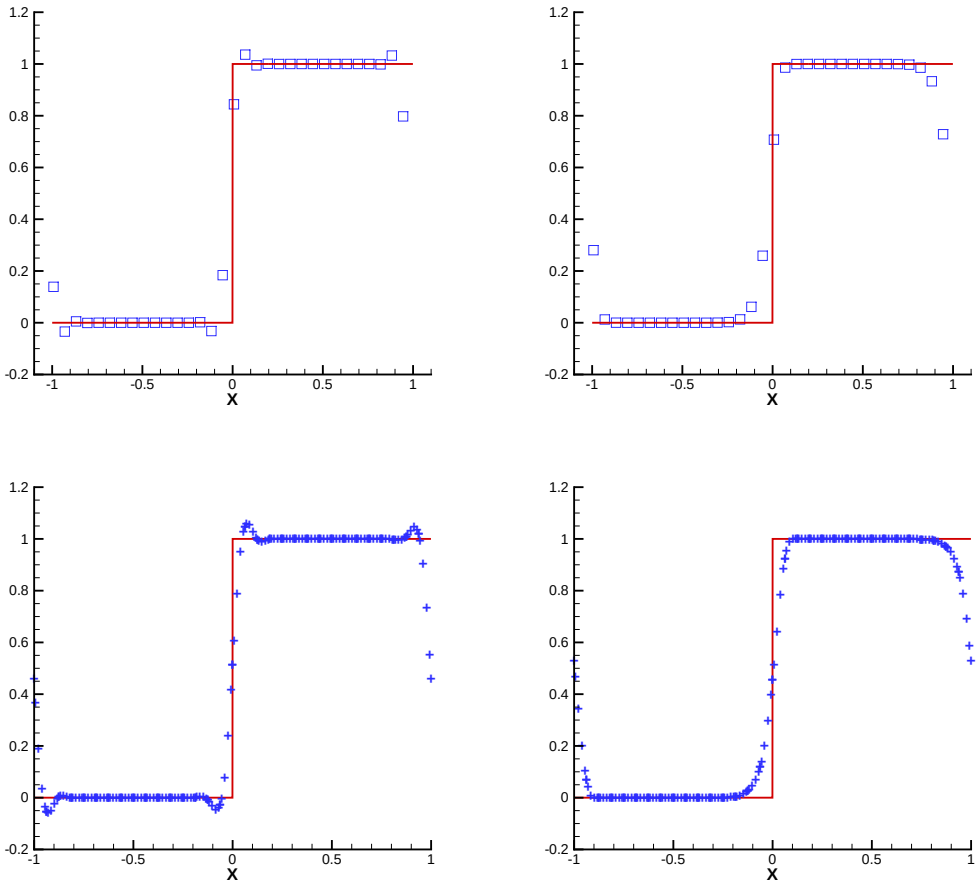

Figure 29. Approximations provided by the RKDG method at time $T = 100$ of the solution of the transport equation $u_t + u_x = 0$ with an initial condition $u_0(x) = 0$ for $x \leq 0$ and $u_0(x) = 1$ for $x > 0$ defined on the interval $(-1, 1)$ with periodic boundary conditions. Here, $k = 5, \Delta t = \frac{1}{16}\Delta x, \Delta x = 1/16$ and the time-marching method is the SSP RK method or order 3. Without (left) and with (right) bound-preserving limiter. Cell averages (top) and Gauss-Lobatto points (bottom) are plotted. Note how the limiter enforces strict maximum principle for all Gauss-Lobatto point values and cell averages of the numerical polynomial solution. Courtesy of Chi-Wang Shu and Xiongxiang Zhang.

Applications and extensions of this technique were carried out by Zhang and Shu (2010c; Zhang and Shu (2011; Hu et al. (2013 to the compressible Euler equations, by Zhang et al. (2012; Zhang et al. (2013 for triangular meshes, by Qin et al. (2016 to relativistic hydrodynamics, and by Vilar et al. (2016b; Vilar et al. (2016a to multimaterial compressible

Encyclopedia of Computational Mechanics. Edited by Erwin Stein, René de Borst and Thomas J.R. Hughes.
 ISBN: 0-470-84699-2

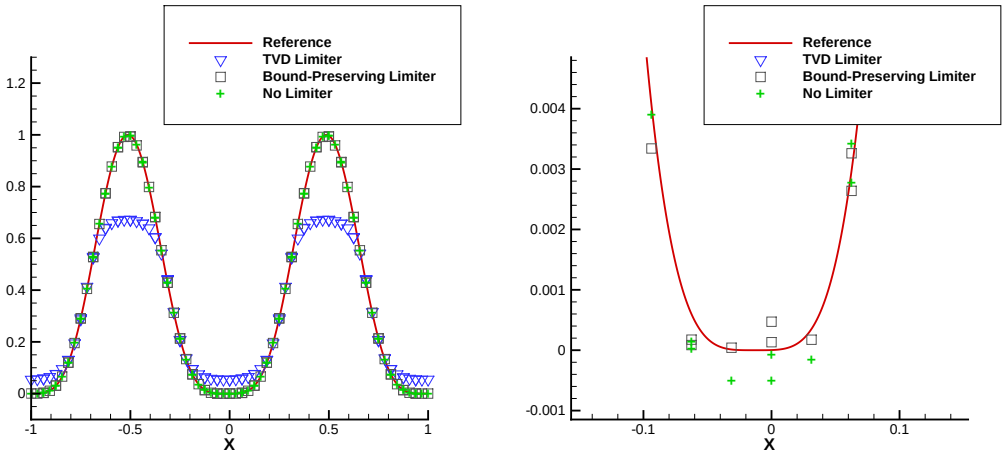

Figure 30. Approximations provided by the RKDG method at time $T = 2$ of the solution of the transport equation $u_t + u_x = 0$ with an initial condition $u_0(x) = \sin^4(\pi x)$ defined on the interval $(-1, 1)$ with periodic boundary conditions. Here, $k = 2, \Delta t = \frac{1}{5}\Delta x, \Delta x = 1/16$ and the time-marching method is the SSP RK method or order 3. Three Gauss-Lobatto point values are ploted for each element. Note how the limiter does not "clip" a smooth extremum, unlike the TVD limiter. Courtesy of Chi-Wang Shu and Xiongxiang Zhang.

flows.

4.9. A posteriori error estimation and adaptivity

For pioneering work on adaptivity for nonlinear problems , see the papers by Biswas et al. (1994, Devine et al. (1995, Devine and Flaherty (1996, Flaherty et al. (1997; Flaherty et al. (1998; Flaherty et al. (1999, Flaherty et al. (2000.

The only rigorous a posteriori error estimate in the $L^\infty(0, T; L^1(\mathbb{R}^N))$-norm was obtained by Cockburn and Gremaud (1996. It holds for the approximation given by an space-time, shock-capturing DG method for nonlinear hyperbolic conservation laws in multiple-space dimensions. The entropy solution can display discontinuities. For more recent work on the subject see the review by Ohlberger (2009. See also the paper by Giesselmann et al. (2015 on a posteriori error estimates for the semidiscrete version of DG methods for *smooth* solutions of nonlinear systems of conservation laws.

Encyclopedia of Computational Mechanics. Edited by Erwin Stein, René de Borst and Thomas J.R. Hughes.
 ISBN: 0-470-84699-2

5. Steady-state diffusion

In this section, we consider DG methods for a second-order elliptic model problem, steady-state diffusion. We do this not only because this also has direct applications to fluid flow (in porous media, for example) but mainly as a much needed transition towards the devising of DG methods for convection-dominated flows. The emphasis here is on the fact that the numerical fluxes used in the framework of hyperbolic conservation laws are not associated to approximate Riemann solvers anymore. Instead, they are better understood if they are considered to be *numerical traces* that must be chosen in order to render the DG method both stable and accurate. We show that, also in this context, the stability of the DG methods is enhanced by the jumps of the approximate solution and that they are a particular case of stabilized mixed methods. We also show that the inter-element jumps control the quality of the approximate solution and discuss the convergence properties of the methods for various choices of numerical traces.

We present these ideas for the second-order elliptic model problem:

$$-\Delta u \quad = \quad f \quad \text{in } \Omega, \quad u = u_D \quad \text{on } \partial\Omega,$$

where Ω is a bounded domain of $\mathbb{R}^N$ and $\boldsymbol{n}$ is the outward unit normal to its boundary.

5.1. General form of the DG methods

5.1.1. Definition. A way to define a DG method consists in rewriting the elliptic model problem as a system of first-order equations, namely,

$$\boldsymbol{q} = \nabla u, \quad -\nabla \cdot \boldsymbol{q} = f \quad \text{in } \Omega, \quad u = u_D \quad \text{on } \partial\Omega$$

and then applying to it a DG discretization. Thus, the approximate solution $(\boldsymbol{q}_h, u_h)$ on the element K is taken in the space $\boldsymbol{V}(K) \times W(K)$ and is defined as the solution, for all $(\boldsymbol{v}, w) \in \boldsymbol{V}(K) \times W(K)$, of the equations

$$\begin{aligned} (\boldsymbol{q}_h, \boldsymbol{v})_K + (u_h, \nabla \cdot \boldsymbol{v})_K - \langle \widehat{u}_h, \boldsymbol{n}_K \cdot \boldsymbol{v} \rangle_{\partial K} &= 0, \\ (\boldsymbol{q}_h, \nabla v)_K - \langle \widehat{\boldsymbol{q}}_h \cdot \boldsymbol{n}_K, v \rangle_{\partial K} &= (f, v)_K. \end{aligned}$$

The Dirichlet boundary condition is enforced by requiring that $\widehat{u}_h = u_D$ on $\partial K \cap \partial\Omega$. All the DG methods are generated by choosing the local spaces $\boldsymbol{V}(K) \times W(K)$ and the numerical traces $\widehat{\boldsymbol{q}}_h \cdot \boldsymbol{n}_K$ and $\widehat{u}_h$. This completes the definition of the DG methods.

Next, we discuss some simple properties that hold for all of them.

5.1.2. The numerical traces. Just as for DG methods for hyperbolic problems, the definition of the numerical traces $\widehat{\boldsymbol{q}}_h$ and $\widehat{u}_h$ strongly influences the properties of the corresponding DG method. In this context, we also require that the numerical traces be linear functions of the traces of $\boldsymbol{q}_h \cdot \boldsymbol{n}_K$ and u_h (on the boundary of the element ∂K) which are consistent and

Encyclopedia of Computational Mechanics. Edited by Erwin Stein, René de Borst and Thomas J.R. Hughes.
 ISBN: 0-470-84699-2

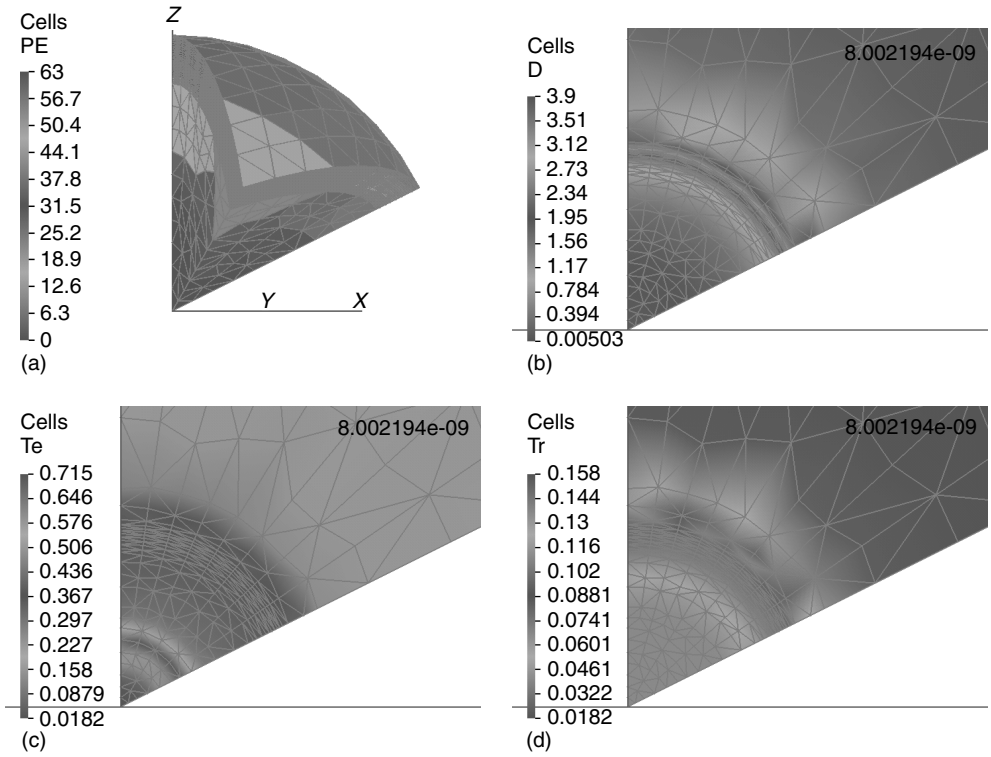

Figure 31. ICF capsule implosion mesh (a) with colors indicating to which processor the element belongs. Density (b), matter temperature (c), and radiation temperature (d) at 8 nanoseconds. (From Shestakov AI, Milovich JL and Prasad MK. Combining cell- and point-centered methods in 3-D, unstructured-mesh hydrodynamics codes. *J. Comput. Phys.* 2001; **170**:81-111.)

single valued. As for the original DG method, the first property renders the numerical traces easy to evaluate and ensures a high degree of locality of the method. The very form of the numerical traces also influences the way the DG methods can be implemented, as we will see. The consistency of the traces ensures the convergence of the method to the correct solution. The single-valuedness property, which is highly valued in computational fluid dynamics, is also very important in this context. If violated, the method produces a stiffness matrix for the primal variable, which is not symmetric; see the paper by Arnold et al. (2002 for a complete discussion. More importantly, it induces a loss in the rate of convergence in u_h as well as a significant degradation in the quality of the approximation of linear functionals as shown by Harriman et al. (2003.

5.1.3. Energy identities. If we take $(\boldsymbol{v}, w) := (\boldsymbol{q}_h, u_h)$ and add the resulting equations, we obtain what we could call the local energy identity, namely,

$$(\boldsymbol{q}_h, \boldsymbol{q}_h)_K + \Theta_K = \langle \widehat{\boldsymbol{q}}_h \cdot \boldsymbol{n}_K, \widehat{u}_h \rangle_{\partial K} + (f, u_h)_K,$$

Encyclopedia of Computational Mechanics. Edited by Erwin Stein, René de Borst and Thomas J.R. Hughes.
 ISBN: 0-470-84699-2

where

$$\Theta_K := \langle (\boldsymbol{q}_h - \widehat{\boldsymbol{q}}_h) \cdot \boldsymbol{n}_K, u_h - \widehat{u}_h \rangle_{\partial K}.$$

By adding on all the elements these equations, we obtain the global energy identity

$$(\boldsymbol{q}_h, \boldsymbol{q}_h)_\Omega + \Theta_h = \langle \widehat{\boldsymbol{q}}_h \cdot \boldsymbol{n}, \widehat{u}_h \rangle_{\partial\Omega} + (f, u_h)_\Omega,$$

where $\Theta_h := \sum_{K \in \mathcal{T}_h} \Theta_K$. We see that the jumps $(\boldsymbol{q}_h - \widehat{\boldsymbol{q}}_h) \cdot \boldsymbol{n}_K$ and $u_h - \widehat{u}_h$ can stabilize the method it they are chosen in such a way that $\Theta_h \geq 0$.

5.1.4. Residuals and jumps. Let us next show that the method establishes linear relations between the residuals in the interior of the element K

$$R_{\boldsymbol{r}} := \boldsymbol{q}_h - \nabla u_h \quad \text{and} \quad R_v := -\nabla \cdot \boldsymbol{q}_h - f,$$

and the residuals on its boundary ∂K,

$$r_{\boldsymbol{r}} := \widehat{u}_h - u_h \quad \text{and} \quad r_v := (\widehat{\boldsymbol{q}}_h - \boldsymbol{q}_h) \cdot \boldsymbol{n}_K$$

Indeed, a simple integration by parts gives that for all $(\boldsymbol{v}, w) \in \boldsymbol{V}(K) \times W(K)$,

$$\begin{aligned} (R_{\boldsymbol{v}}, \boldsymbol{v})_K &= \langle r_{\boldsymbol{r}}, \boldsymbol{n}_K \cdot \boldsymbol{v} \rangle_{\partial K}, \\ (R_w, w)_K &= \langle r_w, w \rangle_{\partial K}. \end{aligned}$$

Taking $\boldsymbol{v} := \mathsf{P}_{\boldsymbol{V}} R_{\boldsymbol{v}}$ and $w := \mathsf{P}_W$, where P_N denotes the $L^2(K)$-projection into the finite dimensional space $N(K)$, we obtain that

$$\begin{aligned} \|\mathsf{P}_{\boldsymbol{V}} R_{\boldsymbol{v}}\|_K &\leq C\, h_K^{-1/2} \|r_{\boldsymbol{r}}\|_{\partial K}, \\ \|\mathsf{P}_W R_w\|_K &\leq C\, h_K^{-1/2} \|r_w\|_{\partial K}. \end{aligned}$$

If we assume that $\nabla W(K) \subset \boldsymbol{V}(K)$ so that $\mathsf{P}_{\boldsymbol{V}} R_{\boldsymbol{r}} = R_{\boldsymbol{r}}$, these inequalities say that the jumps $(\widehat{\boldsymbol{q}}_h - \boldsymbol{q}_h) \cdot \boldsymbol{n}_K$ and $\widehat{u}_h - u_h$, and $f - \mathsf{P}_W f$, control the size of the residuals, and hence the quality of the approximation. This implies that any a posteriori error estimate for DG methods should only depend on those quantities.

5.1.5. An example. Let us consider the numerical traces proposed in Cockburn and Shu (1998a and Castillo et al. (2000. With the notation

$$\begin{aligned} & & [\![u_h]\!] &= u_h^+ \boldsymbol{n}^+ + u_h^- \boldsymbol{n}^- \\ \text{and} & & [\![\boldsymbol{q}_h]\!] &= \boldsymbol{q}_h^+ \cdot \boldsymbol{n}^+ + \boldsymbol{q}_h^- \cdot \boldsymbol{n}^+ \\ \text{where} & & \omega_h^\pm(\boldsymbol{x}) &= \lim_{\epsilon \downarrow 0} \omega_h(\boldsymbol{x} - \epsilon\, \boldsymbol{n}^\pm) \end{aligned}$$

the numerical traces are defined as follows. Inside the domain Ω, we take

$$\begin{aligned} \widehat{\boldsymbol{q}}_h &:= \{\boldsymbol{q}_h\} - C_{\mathbf{qq}} [\![\boldsymbol{q}_h]\!] - C_{\mathbf{q}u} [\![u_h]\!] \\ \widehat{u}_h &:= \{u_h\} - C_{uu} \cdot [\![u_h]\!] - C_{u\boldsymbol{q}} [\![\boldsymbol{q}_h]\!] \end{aligned}$$

Encyclopedia of Computational Mechanics. Edited by Erwin Stein, René de Borst and Thomas J.R. Hughes.
 ISBN: 0-470-84699-2

and on its boundary, we take

$$\begin{aligned} \widehat{\boldsymbol{q}}_h &:= \boldsymbol{q}_h - C_{\mathbf{q}u}(u_h - u_D)\,\boldsymbol{n} \\ \widehat{u}_h &:= u_D. \end{aligned}$$

In this case, assuming that $C_{\mathbf{qq}} + C_{uu} = 0$, a simple computation gives us that the global energy identity is

$$(\boldsymbol{q}_h, \boldsymbol{q}_h)_\Omega + \Theta_h = \langle \widehat{\boldsymbol{q}}_h \cdot \boldsymbol{n}, u_D\rangle_{\partial\Omega} + (f, u_h)_\Omega,$$

where

$$\Theta_h(\boldsymbol{q}_h, u_h) := \langle C_{u\mathbf{q}}[\![\boldsymbol{q}_h]\!], [\![\boldsymbol{q}_h]\!]\rangle_{\mathcal{F}_h^i} + \langle C_{\mathbf{q}u}\,[\![u_h]\!], [\![u_h]\!]\rangle_{\mathcal{F}_h^i} + \langle C_{\mathbf{q}u}(u_h - u_D), u_h - u_D\rangle_{\partial\Omega}.$$

We see that, if we assume that $C_{u\mathbf{q}}$ and $C_{\mathbf{q}u}$ are nonnegative, the quantity Θ_h can be interpreted as the term capturing the energy of the inter-element jumps $[\![\boldsymbol{q}_h]\!]$ and $[\![u_h]\!]$, and the jumps $u_h - u_D$ on $\partial\Omega$. This suggests that the role of $C_{u\mathbf{q}}$ and $C_{\mathbf{q}u}$ is to stabilize the method. The role of the other coefficient $C_{\mathbf{qq}} = -C_{uu}$, *can* be that of maximizing the sparsity of the matrices, see Cockburn et al. (2001, or even that of enforcing the stability and convergence properties of the DG method resulting when $C_{u\mathbf{q}} = C_{\mathbf{q}u} = 0$ on $\mathcal{F}_h^i$, see Cockburn and Dong (2007.

We can use the above global energy identity to obtain the existence and uniqueness of the approximate solution in the simple but important case in which

$$\begin{aligned} &\text{(i)} && C_{u\mathbf{q}} \geq 0 && \text{on } \mathcal{F}_h^i, \\ &\text{(ii)} && C_{\mathbf{q}u} > 0 && \text{on } \mathcal{F}_h^i \cup \partial\Omega, \\ &\text{(iii)} && \nabla W(K) \subset \boldsymbol{V}(K) && \forall K \in \mathcal{T}_h. \end{aligned}$$

Again, we only have to show that, when we set the data f and u_D to zero, the only solution is the trivial one. But in this case, the above energy identity gives that

$$(\boldsymbol{q}_h, \boldsymbol{q}_h)_\Omega + \langle C_{u\mathbf{q}}[\![\boldsymbol{q}_h]\!], [\![\boldsymbol{q}_h]\!]\rangle_{\mathcal{F}_h^i} + \langle C_{\mathbf{q}u}\,[\![u_h]\!], [\![u_h]\!]\rangle_{\mathcal{F}_h^i} + \langle C_{\mathbf{q}u}u_h, u_h\rangle_{\partial\Omega} = 0,$$

which implies, by (i) and (ii), that $\boldsymbol{q}_h = \boldsymbol{0}$ on Ω, that $[\![u_h]\!] = 0$ on $\mathcal{F}_h^i$, and that $C_{\mathbf{q}u}u_h = 0$ on $\partial\Omega$. As a consequence, we have that $\widehat{u}_h = u_h$ on $\mathcal{F}_h^i \cup \partial\Omega$, and the first equation defining the DG method reads

$$-(\nabla u_h, \boldsymbol{r})_K = 0$$

for all $\boldsymbol{r} \in \boldsymbol{V}(K)$. By (iii) we can take $\boldsymbol{r} := \nabla u_h$ and conclude that u_h is a constant on the element K. Since $u_h = \widehat{u}_h$ on the interelement boundaries, u_h is a constant on Ω, and since $u_h = 0$ on $\partial\Omega$, we get that $u_h = 0$ on Ω. This completes the proof.

Let us end by pointing out that this DG method is in fact a stabilized mixed finite element method whenever we require that $C_{uu} + C_{\mathbf{qq}} = 0$ and $C_{\mathbf{q}u}$ and $C_{u\mathbf{q}}$ are non-negative. To see this, we only have to notice that $(\boldsymbol{q}_h, u_h)$ is the element of $\boldsymbol{V}_h \times W_h$, where

$$\begin{aligned} \boldsymbol{V}_h &= \{\boldsymbol{v} \in \boldsymbol{L}^2(\Omega) : \boldsymbol{v} \in \boldsymbol{V}(K)\ \forall\ K \in \mathcal{T}_h\} \\ W_h &= \{w \in L^2(\Omega) : w \in W(K)\ \forall\ K \in \mathcal{T}_h\} \end{aligned}$$

Encyclopedia of Computational Mechanics. Edited by Erwin Stein, René de Borst and Thomas J.R. Hughes.
 ISBN: 0-470-84699-2

that solves the equations

$$\begin{aligned} a_h(\boldsymbol{q}_h, \boldsymbol{v}) + b_h(u_h, \boldsymbol{v}) &= \langle u_D, \boldsymbol{v}\cdot\boldsymbol{n}\rangle_{\partial\Omega} \\ -b_h(w, \boldsymbol{q}_w) + c_h(u_h, w) &= (f, v)_\Omega + \langle C_{\mathbf{qu}} u_D, v\rangle_{\partial\Omega} \end{aligned}$$

for all $(\boldsymbol{v}, w) \in \mathcal{Q}_h \times \mathcal{U}_h$, where

$$\begin{aligned} a_h(\boldsymbol{q}, \boldsymbol{r}) &:= (\boldsymbol{q}, \boldsymbol{r})_\Omega + \langle C_{u\mathbf{q}} [\![\boldsymbol{q}_h]\!], [\![\boldsymbol{r}]\!]\rangle_{\mathcal{F}_h^i} \\ b_h(u, \boldsymbol{r}) &:= (u, \nabla\cdot\boldsymbol{r})_{\mathcal{T}_h} - \langle \{u\} - C_{uu}\cdot[\![u]\!], [\![\boldsymbol{r}]\!]\rangle_{\mathcal{F}_h^i} \\ c_h(u, v) &:= \langle C_{\mathbf{q}u}\,[\![u]\!], [\![v]\!]\rangle_{\mathcal{F}_h^i} + \langle C_{\mathbf{q}u} u, v\rangle_{\partial\Omega}, \end{aligned}$$

where $(\cdot,\cdot)_{\mathcal{T}_h} := \sum_{K\in\mathcal{T}_h}(\cdot,\cdot)_K$ and $(\cdot,\cdot)_{\mathcal{F}_h^i} := \sum_{F\in\mathcal{F}_h^i}(\cdot,\cdot)_F$, where $\mathcal{F}_h^i$ is the set of faces F of the triangulation $\mathcal{T}_h$. Note that $C_{\mathbf{qq}}$ does not appear in the definition of these bilinear forms because we are assuming that $C_{uu} + C_{\mathbf{qq}} = 0$. Note that the method has *two* stabilization terms, namely, the one associated to the jumps in the normal component of the flux, $[\![\boldsymbol{q}_h]\!]$, and the other asociated to the jumps of the scalar vairable, $[\![u_h]\!]$. Both have important effects on the accuracy of the method.

Indeed, some convergence properties of these methods in terms of the spaces and numerical traces are given in the Table 6; for a proof, see Castillo et al. (2000. The so-called minimal dissipation DG method takes $C_{\boldsymbol{q}u} = 0$ and $C_{u\boldsymbol{q}} = 0$ on the interior faces, and $C_{\boldsymbol{q}u} = 1/h$ and $C_{u\boldsymbol{q}} = 0$ on the boundary faces. For simplexes, it has the same order of convergence that the third method in Table 6. This can be achieved by taking a special choice of C_{uu} and $C_{\boldsymbol{qq}}$; see the work by Cockburn and Dong (2007.

Table 6. Orders of convergence of the DG methods in terms of the local spaces and the stabilization parameters. We assume that C_{uu} and $C_{\boldsymbol{qq}}$ are uniformly bounded and that $C_{uu} + C_{\boldsymbol{qq}} = 0$. The meshes are made of shape-regular elements of arbitrary shape. The space of vector-valued functions $\boldsymbol{\mathcal{P}}_\ell(K)$ can be replaced by the space $\nabla\mathcal{P}_{\ell+1}(K)$ without altering the orders of covergence.

$\boldsymbol{V}(K)$	$W(K)$	$C_{\boldsymbol{q}u}$	$C_{u\boldsymbol{q}}$	$\boldsymbol{q}_h$	u_h
$\boldsymbol{\mathcal{P}}_k(K)$	$\mathcal{P}_k(K)$	h	1/h	$k+1$	k
$\boldsymbol{\mathcal{P}}_k(K)$	$\mathcal{P}_k(K)$	1	1	$k+1/2$	$k+1$
$\boldsymbol{\mathcal{P}}_k(K)$	$\mathcal{P}_k(K)$	1/h	h, 0	k	$k+1$
$\boldsymbol{\mathcal{P}}_{k-1}(K)$	$\mathcal{P}_k(K)$	1/h	h, 0	k	$k+1$

5.2. DG methods allowing for an easy elimination of $\mathbf{q}_h$

Let us consider DG methods having a numerical trace $\widehat{u}_h$ *independent* of $\boldsymbol{q}_h$. This allows for the easy elimination of the variable $\boldsymbol{q}_h$, which can now be expressed in terms of u_h in an elementwise manner, and results in the so-called *primal* formulation of the method. The main DG methods

Encyclopedia of Computational Mechanics. Edited by Erwin Stein, René de Borst and Thomas J.R. Hughes.

of this type are displayed in Table 7. There, $\alpha^j([\![u_h]\!]) := C_{\mathbf{q}u}[\![u_h]\!]$ and $\alpha^r([\![u_h]\!])$ denotes the stabilization introduced by Bassi et al. (1997 and later studied by Brezzi et al. (2000. The effect of both stabilizations is essentially the same; however, that latter produces a method with a more sparse stiffness matrix for u_h. Note that the methods proposed by Cockburn and Shu (1998a are called the local DG (LDG) methods, whereas the methods by Baker (1977; Arnold (1982 are called the IP (IP) methods. Let us note that the so-called compact DG method proposed by Peraire and Persson (2008 increases the sparsity of the matrix for u_h of the LDG method while maintaining the same orders of convergence. In Castillo (2010, an algorithm to increase the sparsity of the LDG method wss introduced.

Not all DG methods were originally proposed in the form we have used to present them. Many of them were proposed directly in the primal form

$$B_h(u_h, v) = (f\, v)_\Omega - \langle u_D, \nabla v \cdot \boldsymbol{n} + C_{\mathbf{q}u}\, v\rangle_{\partial\Omega}$$

The two main examples are the IP method, proposed by Arnold (1982, see also Baker (1977 where the biharmonic problem was considered, for which we have

$$\begin{aligned} B_h(u_h, v) \;=\; & (\nabla u_h, \nabla v)_{\mathcal{T}_h} \\ & -\langle [\![u_h]\!], \{\nabla v\}\rangle_{\mathcal{F}_h^i} - \langle u_h, \nabla v \cdot \boldsymbol{n}\rangle_{\partial\Omega} \\ & -\langle \{\nabla u_h\}, [\![v]\!]\rangle_{\mathcal{F}_h^i} - \langle \nabla u_h \cdot \boldsymbol{n}, v\rangle_{\partial\Omega} \\ & +\langle C_{\mathbf{q}u}[\![u_h]\!], [\![v]\!]\rangle_{\mathcal{F}_h^i} + \langle C_{\mathbf{q}u} u_h, v\rangle_{\partial\Omega}, \end{aligned}$$

and the method proposed by Baumann and Oden (1999, for which we have

$$\begin{aligned} B_h(u_h, v) \;=\; & (\nabla u_h, \nabla v)_{\mathcal{T}_h} \\ & -\langle [\![u_h]\!], \{\nabla v\}\rangle_{\mathcal{F}_h^i} - \langle u_h, \nabla v \cdot \boldsymbol{n}\rangle_{\partial\Omega} \\ & +\langle \{\nabla u_h\}, [\![v]\!]\rangle_{\mathcal{F}_h^i} + \langle \nabla u_h \cdot \boldsymbol{n}, v\rangle_{\partial\Omega} \\ & +\langle C_{\mathbf{q}u}[\![u_h]\!], [\![v]\!]\rangle_{\mathcal{F}_h^i} + \langle C_{\mathbf{q}u} u_h, v\rangle_{\partial\Omega}, \end{aligned}$$

where $C_{\mathbf{q}u} = 0$.

A theoretical study of the main DG methods introduced up to the end of last century for the elliptic model problem is carried out in a single, unified approach by Arnold et al. (2002. Here, the mixed formulation is not used to carry out the analysis. Instead, the variable $\boldsymbol{q}_h$ is eliminated from the equations. A primal formulation is thus obtained, which is used to analyze the method. In Table 8, we have summarized the properties of various DG methods. We display the properties of consistency and conservativity of the numerical fluxes, of stability of the method, of the type of stability (the symbol α^{j} is used to denote the stabilization associated with the terms $C_{\mathbf{q}u}\,[\![u_h]\!]^2$), the condition on $C_{\mathbf{q}u}$ for achieving stability, and the corresponding rates of convergence.

Error estimates in the L^∞-norm for the IP methods have been obtained in Kanschat and Rannacher (2002 and Chen and Chen (2004. For the other DG methods displaying consistent and single-valued numerical traces, see Guzmán (2006. The sub-optimal convergence, for odd polynomial approximations, in the L^2-norm of the error of the scalar approximation of the

Encyclopedia of Computational Mechanics. Edited by Erwin Stein, René de Borst and Thomas J.R. Hughes.
 ISBN: 0-470-84699-2

Table 7. Some DG methods and their numerical traces. The elements K are simplexes, the spaces are $\boldsymbol{V}(K) = [\mathbb{P}_k(K)]^d$, $W(K) = \mathbb{P}_k(K)$. We also have that $C_{uu} + C_{\mathbf{qq}} = 0$.

Method	$\widehat{\boldsymbol{q}}_{h,K}$	$\widehat{u}_{h,K}$
Bassi and Rebay (1997a	$\{\boldsymbol{q}_h\}$	$\{u_h\}$
Cockburn and Shu (1998a	$\{\boldsymbol{q}_h\} - C_{\mathbf{qq}}[\![\boldsymbol{q}_h]\!] - C_{\mathbf{q}u}[\![u_h]\!]$	$\{u_h\} - C_{uu} \cdot [\![u_h]\!]$
Brezzi et al. (2000	$\{\boldsymbol{q}_h\} - \alpha^r([\![u_h]\!])$	$\{u_h\}$
Baker (1977,Arnold (1982	$\{\nabla u_h\} - C_{\mathbf{q}u}[\![u_h]\!]$	$\{u_h\}$
Bassi et al. (1997	$\{\nabla u_h\} - \alpha^r([\![u_h]\!])$	$\{u_h\}$
Baumann and Oden (1999	$\{\nabla u_h\}$	$\{u_h\} - \boldsymbol{n}_K \cdot [\![u_h]\!]$
Rivière et al. (1999	$\{\nabla u_h\} - C_{\mathbf{q}u}[\![u_h]\!]$	$\{u_h\} - \boldsymbol{n}_K \cdot [\![u_h]\!]$
Babuška and Zlámal (1973	$-C_{\mathbf{q}u}[\![u_h]\!]$	$u_h\|_K$
Brezzi et al. (2000	$-\alpha^r([\![u_h]\!])$	$u_h\|_K$

(Modified from Arnold DN, Brezzi F, Cockburn B and Marini D. SIAM Journal on Numerical Analysis, Unified analysis of discontinuous Galerkin methods for elliptic problems, **39**:1749-1779, 2001, Copyright Society for Industrial and Applied Mathematics, Philadelphia.)

Table 8. Properties of the DG methods. The elements K are simplexes, the spaces are $\boldsymbol{V}(K) = [\mathbb{P}_k(K)]^d$, $W(K) = \mathbb{P}_k(K)$. We also have $C_{uu} + C_{\mathbf{qq}} = 0$.

Method	Consistency	Conservativity	Stability	Type	$\eta_0 = h\,C_{\mathbf{q}u}$	H^1	L^2
Brezzi et al. (1999	$\surd$	$\surd$	$\surd$	α^{r}	$\eta_0 > 0$	h^p	h^{p+1}
Cockburn and Shu (1998a	$\surd$	$\surd$	$\surd$	α^{j}	$\eta_0 > 0$	h^p	h^{p+1}
Baker (1977,Arnold (1982	$\surd$	$\surd$	$\surd$	α^{j}	$\eta_0 > \eta^*$	h^p	h^{p+1}
Bassi et al. (1997	$\surd$	$\surd$	$\surd$	α^{r}	$\eta_0 > 3$	h^p	h^{p+1}
Rivière et al. (1999	$\surd$	$\times$	$\surd$	α^{j}	$\eta_0 > 0$	h^p	h^p
Babuška and Zlámal (1973	$\times$	$\times$	$\surd$	α^{j}	$\eta_0 \approx h^{-2p}$	h^p	h^{p+1}
Brezzi et al. (2000	$\times$	$\times$	$\surd$	α^{r}	$\eta_0 \approx h^{-2p}$	h^p	h^{p+1}
Baumann and Oden (1999 ($p = 1$)	$\surd$	$\times$	$\times$	-	-	$\times$	$\times$
Baumann and Oden (1999 ($p \geq 2$)	$\surd$	$\times$	$\times$	-	-	h^p	h^p
Bassi and Rebay (1997a	$\surd$	$\surd$	$\times$	-	-	$[h^p]$	$[h^{p+1}]$

(Modified from Arnold DN, Brezzi F, Cockburn B and Marini D. SIAM Journal on Numerical Analysis, Unified analysis of discontinuous Galerkin methods for elliptic problems, **39**:1749-1779, 2001, Copyright Society for Industrial and Applied Mathematics, Philadelphia.)

Encyclopedia of Computational Mechanics. Edited by Erwin Stein, René de Borst and Thomas J.R. Hughes.

DG methods proposed in Baumann and Oden (1999 and Rivière et al. (1999 was proven in Guzmán and Rivière (2009.

Superconvergence results for the approximation inside the elements have been obtained by Adjerid and Baccouch (2012 and for the numerical traces by Celiker and Cockburn (2007.

A numerical study of various of these methods was carried out in Castillo (2002. He found, in particular, that $\boldsymbol{q}_h$ is a much better approximation to $\boldsymbol{q}$ than ∇u_h; that the penalization parameter $C_{\mathbf{q}u}$ must be taken as η_0/h, where h is a measure of the diameters of the elements, to obtain a condition number of the matrix for u_h of order h^{-2}; and that when η_0 is taken to be too big, all the DG methods give similar approximations. The hp-version of the IP method on general computational meshes consisting of polygonal/polyhedral elements of arbitrary shapes was considered by Cangiani et al. (2014; the elements are also allowed to have degenerating faces.

A posteriori error estimates for the IP method were obtained by Karakashian and Pascal (2003; Houston et al. (2007; Ainsworth (2007; Cochez-Dhondt and Nicaise (2008; R. Lazarov and Tomar (2009; Creusé and Nicaise (2010 for the symmetric IP methods, in Becker et al. (2003; A. Ern and Vohralík (2007; Ainsworth and Rankin (2010 for the symmetric and non-symmetric IP methods, in Bustinza et al. (2005 for the local DG methods, and in Juntunen and Stenberg (2008 for the Bassi-Rebay DG methods. For the L^2-norm of the error in the scalar variable, they have been obtained in Rivière and Wheeler (2003 for the non-symmetric IP method and in Castillo (2005 for the local DG method. A unified a posteriori error analysis of all the DG methods for second-order elliptic problems considered in Arnold et al. (2002 was carried out in Carstensen et al. (2009. Another unified a posteriori error analysis, based on the point of view proposed in Brezzi et al. (2006, was carried out in Lovadina and Marini (2009.

The convergence of an adaptive algorithm for the IP method was proved by Karakashian and Pascal (2007; Hoppe et al. (2008; Bonito and Nochetto (2010.

5.3. The HDG methods

The DG methods just considered have numerical traces which allow for the elimination of the variable $\boldsymbol{q}_h$ in order to obtain a formulation of the method in terms of u_h only. The HDG methods have numerical traces which allow for the elimination of both $\boldsymbol{q}_h$ and u_h in order to obtain a formulation of the method in terms of $\widehat{u}_h$ only. The size of the stiffness matrix of the HDG methods are thus significantly smaller than those of the previously mentioned methods. The HDG methods are also more accurate, as we are going to see. We follow closely the work done by Cockburn (2015.

5.3.1. Definition. The HDG methods are obtained as a discrete version of the following characterization of the exact solution. On the element K, for any given $f|_K$ and Dirichlet

Encyclopedia of Computational Mechanics. Edited by Erwin Stein, René de Borst and Thomas J.R. Hughes.
 ISBN: 0-470-84699-2

boundary data $\widehat{u}\,|_{\partial K}$, we take $(\boldsymbol{q}, u)$ to be the solution of the *local problem*

$$\boldsymbol{q} = \nabla u, \quad -\nabla \cdot \boldsymbol{q} = f \quad \text{in } K, \quad u = \widehat{u} \quad \text{in } \partial K.$$

Then the single-valued function $\widehat{u}$ is determined by solving the *global problem* obtained by imposing the following transmission and boundary conditions:

$$[\![\boldsymbol{q}]\!] = 0 \quad \text{on } \mathcal{F}_h^i \quad \text{and} \quad \widehat{u} = u_D \quad \text{in } \partial\Omega.$$

To obtain the HDG methods, we solve the local problem on each element $K \in \mathcal{T}_h$ by using a DG method. We solve the global problem by imposing the transmission and boundary conditions weakly. So, on the element $K \in \mathcal{T}_h$, for any given $f|_K$ and Dirichlet boundary data $\widehat{u}_h|_{\partial K}$,we define $(\boldsymbol{q}_h, u_h) \in \boldsymbol{V}(K) \times W(K)$ as the solution of the local problem

$$\begin{aligned}(\boldsymbol{q}_h, \boldsymbol{v})_K + (u_h, \nabla \cdot \boldsymbol{v})_K - \langle \widehat{u}_h, \boldsymbol{v} \cdot \boldsymbol{n}\rangle_{\partial K} = 0 \qquad & \forall \boldsymbol{v} \in \boldsymbol{V}(K),\\ (\boldsymbol{q}_h, \nabla w)_K - \langle \widehat{\boldsymbol{q}}_h \cdot \boldsymbol{n}, w\rangle_{\partial K} = (f, w)_K \quad & \forall w \in W(K),\end{aligned}$$

where

$$\widehat{\boldsymbol{q}} \cdot \boldsymbol{n} := \boldsymbol{q}_h \cdot \boldsymbol{n} - \tau(u_h - \widehat{u}_h) \quad \text{on } \partial K,$$

where the function τ is linear. Note that here we consider $\widehat{u}_h|_{\partial K}$ to be *data* of this problem. To determine it, we take the numerical trace $\widehat{u}_h$ in the space

$$M_h := \{\mu \in L^2(\mathcal{F}_h) : \ \mu_F \in M(F) \ \forall F \in \mathcal{F}_h\},$$

where $M(F)$ is a suitably chosen finite dimensional space, and require that it be determined as the solution of the following global problem consisting in weakly imposed transmission and boundary conditions:

$$\begin{aligned}&\langle \mu, [\![\widehat{\boldsymbol{q}}_h]\!]\rangle_{\mathcal{F}_h^i} = \langle \mu, \widehat{\boldsymbol{q}}_h \cdot \boldsymbol{n}\rangle_{\partial\mathcal{T}_h \setminus \partial\Omega} = 0,\\ &\langle \mu, \widehat{u}_h\rangle_{\partial\Omega} = \langle \mu, u_D\rangle_{\partial\Omega},\end{aligned}$$

for all $\mu \in M_h$. This completes the definition of the HDG methods.

Notice that $\widehat{u}_h$ is the *data* of the local problems but is the *unknown* of the global problem. So, the only globally-coupled degrees of freedom are those of $\widehat{u}_h$. By solving the local problems, we express $\boldsymbol{q}_h, u_h$ and $\widehat{\boldsymbol{q}}_h$ in terms of $\widehat{u}_h$ and f. With these expressions, we construct the matrix equation associated to the global problem. After solving it, we can insert the actual values of $\widehat{u}_h$ in the expressions we had obtained for $\boldsymbol{q}_h, u_h$ and $\widehat{\boldsymbol{q}}_h$. Next, we describe this procedure more precisely.

5.3.2. The problem for $\widehat{u}_h$. We begin by introducing some notation associated to the local problems. On the element $K \in \mathcal{T}_h$, for any $\mu \in L^2(\partial K)$, the function $(\mathbf{Q}_\mu, \mathsf{U}_\mu) \in \boldsymbol{V}(K) \times W(K)$ is the solution of the local problem

$$\begin{aligned}(\mathbf{Q}_\mu, \boldsymbol{v})_K - (\mathsf{U}_\mu, \nabla \cdot \boldsymbol{v})_K + \langle \mu, \boldsymbol{v} \cdot \boldsymbol{n}\rangle_{\partial K} = 0 \quad & \forall \boldsymbol{v} \in \boldsymbol{V}(K),\\ -(\mathbf{Q}_\mu, \nabla w)_K + \langle \widehat{\mathbf{Q}}_\mu \cdot \boldsymbol{n}, w\rangle_{\partial K} = 0 \quad & \forall w \in W(K),\\ \widehat{\mathbf{Q}}_\mu \cdot \boldsymbol{n} := \mathbf{Q}_\mu \cdot \boldsymbol{n} + \tau(\mathsf{U}_\mu - \mu) \qquad & \text{on } \partial K,\end{aligned}$$

Encyclopedia of Computational Mechanics. Edited by Erwin Stein, René de Borst and Thomas J.R. Hughes.
 ISBN: 0-470-84699-2

and, for any $f \in L^2(K)$, the function $(\mathbf{Q}_f, \mathsf{U}_f) \in \boldsymbol{V}(K) \times W(K)$ is the solution of the local problem

$$\begin{aligned} (\mathbf{Q}_f, \boldsymbol{v})_K - (\mathsf{U}_f, \nabla \cdot \boldsymbol{v})_K = 0 \qquad & \forall \boldsymbol{v} \in \boldsymbol{V}(K), \\ -(\mathbf{Q}_f, \nabla w)_K + \langle \widehat{\mathbf{Q}}_f \cdot \boldsymbol{n}, w \rangle_{\partial K} = (f, w)_K \quad & \forall w \in W(K), \\ \widehat{\mathbf{Q}}_f \cdot \boldsymbol{n} := \mathbf{Q}_f \cdot \boldsymbol{n} + \tau(\mathsf{U}_f) \qquad & \text{on } \partial K. \end{aligned}$$

With this notation, we can write that

$$(\boldsymbol{q}_h, u_h) = (\mathbf{Q}_\mu, \mathsf{U}_\mu) + (\mathbf{Q}_f, \mathsf{U}_f),$$

where $\widehat{u}_h$ is the solution of the global problem. Next, we give a characterization of the problem for the globally-coupled unknown $\widehat{u}_h$ by suitably rewriting the transmission condition. We are now ready to state the result. Therein, we are going to use the following notation:

$$M_h(g) := \{\mu \in M_h : \langle \lambda, \mu \rangle_{\partial\Omega} = \langle \lambda, g \rangle_{\partial\Omega} \; \forall \lambda \in M_h\},$$

Theorem 4 (Characterization of $\widehat{u}_h$) *Assume that*

$$\begin{aligned} &\text{(i)} \quad \tau|_F \text{ is a strictly positive constant} \quad && \forall F \in \mathcal{F}_h, \\ &\text{(ii)} \quad \nabla W(K) \subset \mathbf{V}(K) && \forall K \in \mathcal{T}_h. \end{aligned}$$

Then, the function $\widehat{u}_h$ is the element of $M_h(u_D)$ such that

$$a_h(\widehat{u}_h, \mu) = \ell_h(\mu) \quad \forall \, \mu \in M_h(0),$$

where $a_h(\mu, \lambda) := -\langle \mu, \widehat{\mathbf{Q}}_\lambda \cdot \mathbf{n} \rangle_{\partial\mathcal{T}_h}$ and $\ell_h(\mu) := \langle \mu, \widehat{\mathbf{Q}}_f \cdot \mathbf{n} \rangle_{\partial\mathcal{T}_h}$. Moreover,

$$a_h(\mu, \lambda) = (\mathbf{Q}_\mu, \mathbf{Q}_\lambda)_{\mathcal{T}_h} + \langle \mathsf{U}_\mu - \mu, \tau(\mathsf{U}_\lambda - \lambda) \rangle_{\partial\mathcal{T}_h}, \quad \ell_h(\mu) = (f, \mathsf{U}_\mu),$$

and $a_h(\cdot, \cdot)$ is symmetric and positive definite on $M_h(0) \times M_h(0)$. Thus, $\widehat{u}_h$ minimizes *the* total energy *functional $J_h(\mu) := \frac{1}{2} a_h(\mu, \mu) - \ell_h(\mu)$ over $M_h(u_D)$.*

This result shows that the method can be implemented in a way typical of finite element methods. Note that the equation satisfied by $\widehat{u}_h$ is nothing but the transmission condition. Indeed, since $\widehat{\boldsymbol{q}}_h \cdot \boldsymbol{n} = \widehat{\mathbf{Q}}_{\widehat{u}} \cdot \boldsymbol{n} + \widehat{\mathbf{Q}}_f \cdot \boldsymbol{n}$, the transmission condition $\langle \mu, \widehat{\boldsymbol{q}}_h \cdot \boldsymbol{n} \rangle_{\partial\mathcal{T}_h \setminus \partial\Omega} = 0 \; \forall \mu \in M_h$, becomes

$$-\langle \mu, \widehat{\mathbf{Q}}_{\widehat{u}} \cdot \boldsymbol{n} \rangle_{\partial\mathcal{T}_h} = \langle \mu, \widehat{\mathbf{Q}}_f \cdot \boldsymbol{n} \rangle_{\partial\mathcal{T}_h} \quad \forall \mu \in M_h(0).$$

Note also that to obtain the matrix equation for the degrees of freedom of $\widehat{u}$, we only need to compute the mapping $\mu \mapsto (\mathbf{Q}_\mu, \mathsf{U}_\mu)$. The computation of the mapping is not $f \mapsto (\mathbf{Q}_f, \mathsf{U}_f)$ required. Finally, note that the fact that the bilinear for $a_h(\cdot, \cdot)$ is symmetric and positive definite on $M_h(0) \times M_h(0)$ is a reflection that it approximates the solution u of a strangle elliptic, self adjoint problem.

This result shows that the HDG methods are amenable to *static condensation*, see Guyan (1965, thanks to the fact that the method can be *hybridized*, see Fraejis de Veubeke (1977. The relation between static condensation, hybridization and the way the HDG methods are devised is explored by Cockburn (2015. Also there, one can find different ways of rewriting the HDG methods and how other characterizations of the exact solution can give rise to the same DHG methods.

Encyclopedia of Computational Mechanics. Edited by Erwin Stein, René de Borst and Thomas J.R. Hughes.
 ISBN: 0-470-84699-2

5.3.3. The numerical traces of the HDG methods. Suppose that the stabilization function τ is a constant on each face and that the local spaces are such that the numerical trace $\widehat{\boldsymbol{q}}_h \cdot \boldsymbol{n}|_F$ lies in the space $M(F)$ for all interior faces $F \in \mathcal{F}_h^i$. Then, the transmission condition is equivalent to

$$[\![\widehat{\boldsymbol{q}}_h]\!] = 0 \quad \text{on} \quad \mathcal{F}_h^i.$$

A simple calculation shows us that the above equation can take place if and only if

$$\widehat{u}_h = \frac{\tau^+ {u_h}^+ + \tau^- {u_h}^-}{\tau^+ + \tau^-} - \frac{1}{\tau^+ + \tau^-}[\![\boldsymbol{q}_h]\!],$$
$$\widehat{\boldsymbol{q}}_h = \frac{\tau^- {\boldsymbol{q}_h}^+ + \tau^+ {\boldsymbol{q}_h}^-}{\tau^+ + \tau^-} - \frac{\tau^+\tau^-}{\tau^+ + \tau^-}[\![u_h]\!],$$

provided, of course, that $\tau^+ + \tau^- \neq 0$. In other words, the DG methods proposed in Cockburn and Shu (1998a and Castillo et al. (2000 with

$$C_{u\mathbf{q}} = \frac{1}{\tau^+ + \tau^-},$$
$$C_{\mathbf{q}u} = \frac{\tau^+\tau^-}{\tau^+ + \tau^-},$$
$$-C_{\mathbf{qq}} = C_{uu} = \frac{\tau^+ \boldsymbol{n}^+ + \tau^- \boldsymbol{n}^-}{2(\tau^+ + \tau^-)}.$$

are also HDG methods. These are called LDG-H methods since the numerical method used to define the local problems is the local DG (LDG) method.

5.3.4. Mixed methods and superconvergent HDG methods. As pointed out in Cockburn et al. (2009b, when the stabilization function τ can be set *identically to zero*, we obtain nothing but the well known hybridized version of the well known mixed methods. In this case, the above expressions for the numerical traces are not valid anymore and, instead, we simply have that

$$\widehat{\boldsymbol{q}}_h \cdot \boldsymbol{n}^\pm = \boldsymbol{q}_h^- \cdot \boldsymbol{n}^\pm = \boldsymbol{q}_h^- \cdot \boldsymbol{n}^\pm,$$

on all interelement boundaries; the unknown $\widehat{u}_h$ can be characterized exactly as in Theorem 4. This suggests that the HDG methods might share with the mixed methods some of its convergence properties.

This was proven to be true by Cockburn et al. (2008b for a special LDG-H method obtained by setting $\tau = 0$ on all the faces of the simplex K except one. For this reason, it was called the single face-hybridizable (SFH) DG method. Moreover, it was shown that the bilinear forms $a_h(\cdot,\cdot)$ of the Raviart-Thomas (RT), Brezzi-Douglas-Marini (BDM) and SFH methods are the same, and that these three methods share the same superconvergence property (we describe below). A similar result was later obtained by Chung et al. (2014 who proved that the staggered discontinuous Galerkin (SDG) method, originally introduced in the framework of wave propagation in Chung and Engquist (2009, can be obtained as the limit when the non-zero values of the stabilization function, which must be defined in suitable manner, of the SFH method goes to infinity.

Encyclopedia of Computational Mechanics. Edited by Erwin Stein, René de Borst and Thomas J.R. Hughes.
 ISBN: 0-470-84699-2

By the above-mentioned superconvergence property we mean that the elemenwise averages of the error $u - u_h$, converge faster than the errors $u - u_h$ and $\boldsymbol{q} - \boldsymbol{q}_h$. As a consequence, we can define, on the each element K, the new approximation $u_h^\star \in W^*(K) := \mathcal{P}_{k+1}(K)$ as the solution of

$$\begin{aligned}(\nabla u_h^\star, \nabla w)_K &= -\left(\mathrm{c}\, \boldsymbol{q}_h, \nabla w\right)_K \qquad \text{for all } w \in W^*(K),\\ (u_h^\star, 1)_K &= (u_h, 1)_K,\end{aligned}$$

Then $u - u_h^\star$ will converge faster than $u - u_h$. Any HDG method with this property will be called a *superconvergent* method.

The orders of convergence, for conforming the meshes made of simplexes, are displayed in Tables 9 and 10. The symbol $\star$ indicates that the non-zero values of the stabilization function τ only need to be uniformly bounded by below.

Table 9. Examples of mixed and HDG methods defined on simplexes.

Method	$\boldsymbol{V}(K)$	$W(K)$	$M(F)$
RT Raviart and Thomas (1977	$\boldsymbol{\mathcal{P}}_k(K) + \boldsymbol{x}\widetilde{\mathcal{P}}_k(K)$	$\mathcal{P}_k(K)$	$\mathcal{P}_k(F)$
SFH Cockburn et al. (2008b	$\boldsymbol{\mathcal{P}}_k(K)$	$\mathcal{P}_k(K)$	$\mathcal{P}_k(F)$
SDG Chung and Engquist (2009	$\boldsymbol{\mathcal{P}}_k(K)$	$\mathcal{P}_k(K)$	$\mathcal{P}_k(F)$
LDG-H Cockburn et al. (2009b	$\boldsymbol{\mathcal{P}}_k(K)$	$\mathcal{P}_k(K)$	$\mathcal{P}_k(F)$
BDM Brezzi et al. (1985	$\boldsymbol{\mathcal{P}}_k(K)$	$\mathcal{P}_{k-1}(K)$	$\mathcal{P}_k(F)$

Table 10. Orders of convergence (in the corresponding L^2-norms) for simplicial, conforming meshes.

Method	τ	$\boldsymbol{q}_h$	u_h	$\overline{u}_h$	k
RT Arnold and Brezzi (1985	0	$k+1$	$k+1$	$k+2$	≥ 0
SFH Cockburn et al. (2008b	$\star$	$k+1$	$k+1$	$k+2$	≥ 1
SDG Chung et al. (2014	$0, \infty$	$k+1$	$k+1$	$k+2$	≥ 1
LDG-H Cockburn et al. (2010d	$\mathcal{O}(1)$	$k+1$	$k+1$	$k+2$	≥ 1
BDM Brezzi et al. (1985	0	$k+1$	k	$k+2$	≥ 2
LDG-H Castillo et al. (2000	$\mathcal{O}(1/h)$	k	$k+1$	$k+1$	≥ 1

The presence of hanging nodes in the meshes does not alter the superconvergence of the HDG methods, as shown by Chen and Cockburn (2012; Chen and Cockburn (2014. A posteriori error estimates were obtained by Cockburn and Zhang (2012; Cockburn and Zhang (2013. A proof of the convergence of an adaptive algorithm for the LDG-H method was obtained by Cockburn et al. (2016c. The performance of the LDG-H method (with τ of order one) for the p-Laplacian was numerically explored by Cockburn and Shen (2016. The superconvergence

Encyclopedia of Computational Mechanics. Edited by Erwin Stein, René de Borst and Thomas J.R. Hughes.
 ISBN: 0-470-84699-2

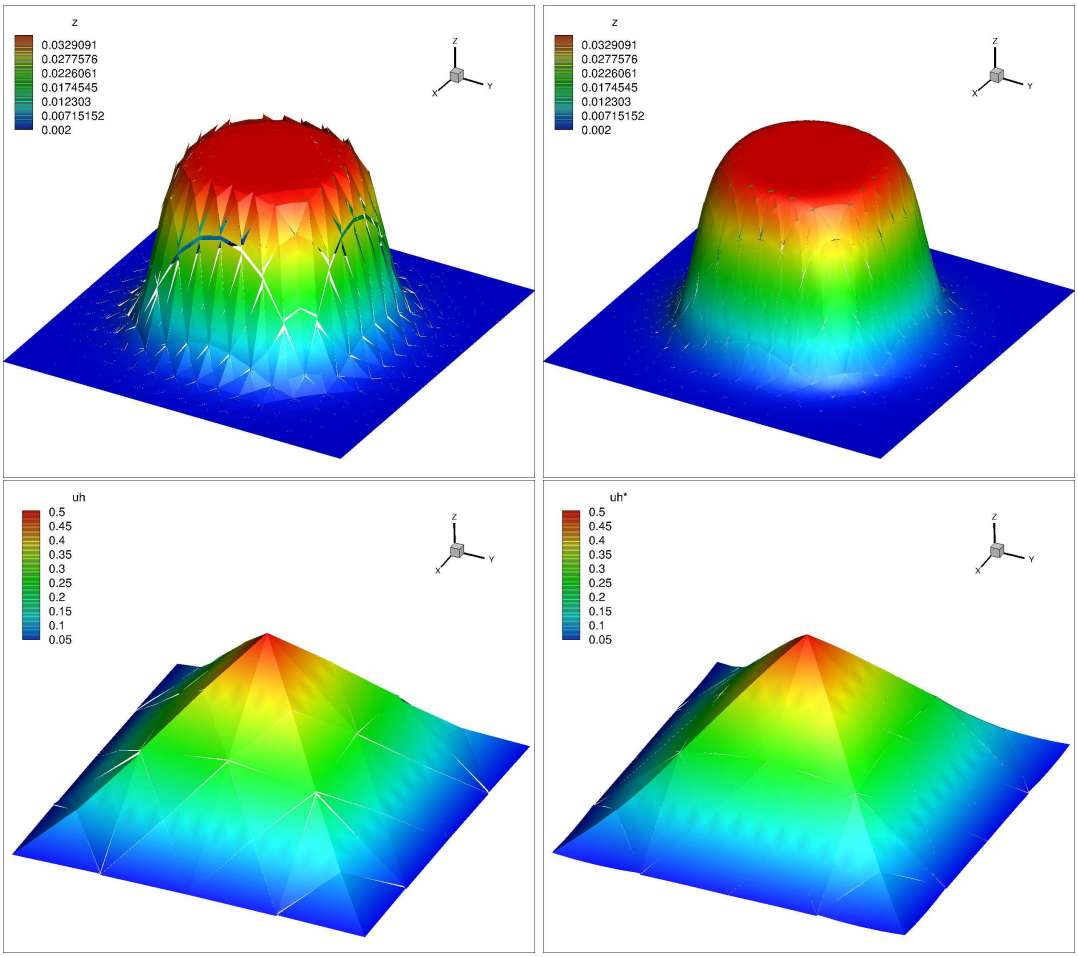

Figure 32. HDG approximations, on $\Omega := (0,1)^2$, of the p-Laplacian for $p = 1.05$ (top) and $p = 15$ with f equal to ten times the characteristic function of the square $(1/4, 3/4)^2$. The interelement jumps in the piecewise linear approximation u_h (left column) indicate the need of smaller meshes or higher-degree polynomials. The interelement jumps of the piecewise quadratic postprocessing u_h^* are smaller than those of u_h as the former function is usually a better approximation than the latter. Note the ability of the method to capture at the same time very strong and very weak gradients ($p = 1.05$), as well as functions displaying kinks ($p = 15$). Courtesy of Jiguang Shen.

properties for the case $p = 2$ were recovered. In Figure 5.3.4, examples of approximations u_h and the corresponding postprocessing u_h^* are provided. Notice how the size of the interelement jumps increases whenever the solution has steeper gradients, as expected.

The systematic construction of superconvergent HDG methods was undertaken in Cockburn

Encyclopedia of Computational Mechanics. Edited by Erwin Stein, René de Borst and Thomas J.R. Hughes.

et al. (2012a where the following sufficient conditions were found. The space $\boldsymbol{V}(K) \times W(K)$ must have a subspace $\widetilde{\boldsymbol{V}}(K) \times \widetilde{W}(K)$ satisfying inclusions

$$\begin{aligned} \boldsymbol{\mathcal{P}}_0(K) &\subset \nabla W(K) \subset \widetilde{\boldsymbol{V}}(K), \\ \mathcal{P}_0(K) &\subset \nabla \cdot \boldsymbol{V}(K) \subset \widetilde{W}(K), \\ \boldsymbol{V}(K) \cdot \boldsymbol{n}|_{\partial K} + W(K)|_{\partial K} &\subset M(\partial K). \end{aligned}$$

and whose orthogonal complement satisfies the identity

$$\widetilde{\boldsymbol{V}}^{\perp} \cdot \boldsymbol{n}|_{\partial K} \oplus \widetilde{W}^{\perp}|_{\partial K} = M(\partial K).$$

Many new superconvergence HDG and mixed methods were found for simplexes, squares, cubes and prisms; see also the related new commuting diagrams for the so-called **TNT** elements on cubes obtained by Cockburn and Qiu (2014 for the DeRham complex. For curved elements, see Cockburn et al. (2012b. This work was then further refined by Cockburn et al. (2016b who introduced the so-called M-decompositions as a tool for the systematic construction of superconvergent HDG and mixed methods. The actual construction for general polygonal elements was carried out in Cockburn and Fu (2016a and the actual construction for arbitrary pyramids, prisms and hexahedral was carried out in Cockburn and Fu (2016b.

5.3.5. Other stabilization functions. So far, we have only considered stabilization function τ which are simple mutiplication operators. A more sophisticated stabilization function was introduced in Lehrenfeld (2010, Remark 1.2.4 by Lehrenfeld and Schöberl, see also Lehrenfeld and Schöberl (2015, and independently by Oikawa (2015. The stabilization function is simply

$$\tau^{\mathrm{LS}}(u_h - \widehat{u}_h) := h^{-1} \cdot (P_M(u_h) - \widehat{u}_h),$$

and was introduced to deal with the case in which $W(K)|_{\partial K}$ is *not* included in $M(\partial K)$. Thanks to this choice of stabilization function *optimal* orders of convergence for both $\boldsymbol{q}_h$ and u_h for regular-shaped, general polyhedral elements can be obtained whenever we take $\boldsymbol{V}(K) := \boldsymbol{\mathcal{P}}_k(K), W(K) := \mathcal{P}_{k+1}(K)$ and $M(F) := \mathcal{P}_k(F)$; see the proof by Oikawa (2015.

The very *same* orders of convergence can actually be obtained with the much smaller local spaces $\boldsymbol{V}(K) := \nabla \mathcal{P}_{k+1}(K), W(K) := \mathcal{P}_k(K)$ and $M(F) := \mathcal{P}_k(F)$ if yet another more sophisticated stabilization function is properly constructed: See the so-called hybrid high-order (HHO) methods introduced by Di-Pietro and Ern (2015DiPietroErnLemaire14DiPietroErnCRAS14. Although these methods were originally introduced in a primal form, their relation to the HDG methods was recently established in Cockburn et al. (2015.

5.4. The embedded DG methods

An embedded DG (EDG) method is obtained by simply taking an already existing HDG method using the space M_h and requiring that its approximation $\widehat{u}_h$ lie in a space *embedded* in M_h. In this way, the computational complexity of the global problem can be greatly reduced.

Encyclopedia of Computational Mechanics. Edited by Erwin Stein, René de Borst and Thomas J.R. Hughes.
 ISBN: 0-470-84699-2

An important particular case is the case in which the above-mentioned subspace is $M_h \cap \mathcal{C}^0(\mathcal{F}_h)$. Note that the EDG has the very same local problems than the associated HDG method and a smaller matrix for the global system of the form $E^t AE$, where A is the matrix for the global system of the original HDG method and E is the matrix associated to the embedding.

Next consider the HDG method for which $\boldsymbol{V}(K) := \nabla \mathcal{P}_k(K), W(K) := \mathcal{P}_k(K)$ and $M(F) := \mathcal{P}_k(F)$ with $\tau = 1$, where the elements are simplexes. It was shown by Cockburn et al. (2009c that the corresponding EDG method with $M_h \cap \mathcal{C}^0(\mathcal{F}_h)$ as the embedded subspace looses the superconverence properties of the original HDG method. So, the reduction of computational complexity comes at a heavy price.

The EDG methods were introduced in the framework of linear shells by Güzey et al. (2007, see also Cockburn et al. (2009b. The method seems to be identical to the second version of the so-called multiscale DG method introduced by Hughes et al. (2006; the first version was introduced by Bochev et al. (2006.

5.5. Extensions

How to couple DG methods with the classical conforming methods was shown by Alotto et al. (2001 and Perugia and Schötzau (2001. Moreover, Perugia and Schötzau (2001 combined the theoretical framework developed by Arnold et al. (2002 with the techniques of analysis of nonconforming methods to obtain optimal error estimates for the resulting coupling. How to couple DG methods with mixed methods was shown by Cockburn and Dawson (2002. The coupling at a distance of HDG methods with BEM was carried out by Cockburn et al. (2012c.

DG methods for multiscale problems have been considered by Wang et al. (2011; Efendiev et al. (2015.

Extensions to the approximation of eigenvalues and eigenfunctions by using the LDG-H methods was explored by Gopalakrishnan et al. (2015; see also the corresponding work for the RT method by Cockburn et al. (2010c.

Extensions to the heat equation are straightforward; see, in particular, the HDG methods developed by Chabaud and Cockburn (2012. For the heat equation, the so-called direct DG (DDG) method has been developed by Liu and Yan (2010 which has the distinctive feature of bypassing the definition of an approximation for the flux and letting its numerical flux to depend of the interelement jumps of second and higher-order derivatives of the approximation to the scalar variable. The methods display an optimal order of convergence in an *energy*-like norm.

A comparison between the HDG and the continuous Galerkin method has been carried out by Kirby et al. (2012. See also the study by Huerta et al. (2013.

Encyclopedia of Computational Mechanics. Edited by Erwin Stein, René de Borst and Thomas J.R. Hughes.
 ISBN: 0-470-84699-2

5.6. Solvers

A domain decomposition preconditioner for DG approximations for purely elliptic problems was proposed by Feng and Karakashian (2001. The condition number of their nonoverlapping preconditioner grows linearly with the number of degrees of freedom in each subdomain. Later, Lasser and Toselli (2000 found an overlapping domain decomposition method for DG methods for linear advection-diffusion problems whose condition number is independent of the number of degrees of freedom and the number of subdomains.

Another significant result has been obtained by Gopalakrishnan and Kanschat (2003b who devised a multigrid method for solving the matrix equation of the IP method for elliptic problems. They proved that it convergences in a fixed number of iterations; they have also devised a method for the steady state convection-diffusion problem, which converges with a fixed number of iterations independently of the size of the convection coefficients. These solvers were generalized to the LDG method in primal form, the method by Bassi and Rebay (1997a, and the method by Brezzi et al. (1999 by Gopalakrishnan and Kanschat (2003a. On the basis of these solvers, preconditioners for the LDG saddle point systems arising from the mixed discretization of Poisson and Stokes equations were introduced by Kanschat (2003.

A a semi-algebraic multilevel preconditioner for the local discontinuous Galerkin method was proposed and studied in P. E. Castillo and Velázquez (2008; Castillo and Sequeira (2013. A nonnested multigrid V-cycle, with one smoothing per level for the HDG method was introduced in Cockburn et al. (2014 and proven to converge at a mesh-independent rate. Domain decomposition methods on complicated domains have been investigated by Antonietta et al. (2014.

6. The Stokes equations of incompressible fluid flow

In this section, we study the application of DG methods to the Stokes equations of incompressible fluid flow

$$\begin{aligned} \mathrm{L} - \nabla \boldsymbol{u} &= 0 && \text{in } \Omega, \\ -\nu \nabla \cdot \mathrm{L} + \nabla p &= \boldsymbol{f} && \text{in } \Omega, \\ \nabla \cdot \boldsymbol{u} &= 0 && \text{in } \Omega, \\ (p, 1)_\Omega &= 0, \\ \boldsymbol{u} &= \boldsymbol{u}_D, && \text{on } \partial\Omega, \end{aligned}$$

where Ω is a bounded domain in $\mathbb{R}^d$ with Lipschitz boundary $\partial\Omega$, ν is a viscosity. We assume that ν is a constant function on Ω and that $\boldsymbol{u}_D$ satisfies the compatibility condition $(\boldsymbol{u}_D \cdot \boldsymbol{n}, 1)_{\partial\Omega} = 0$.

Since the Laplace operator is applied to each of the components of the velocity, to devise a DG method, we can simply use any DG method for the steady-state diffusion equation by applying it to each component of the velocity. This does not present any major difficulty and

Encyclopedia of Computational Mechanics. Edited by Erwin Stein, René de Borst and Thomas J.R. Hughes.
 ISBN: 0-470-84699-2

so, here the novelty resides on how to carry out the DG-discretization of the incompressibility condition. In particular, we show that, even though the approximation of the velocity is discontinuous, it is possible to obtain an $\boldsymbol{H}(\mathrm{div},\Omega)$-conforming, divergence-free approximate velocities by means of an elementwise postprocessing. We also show how to devise DG methods with $\boldsymbol{H}(\mathrm{div},\Omega)$-conforming velocity spaces. Finally, we show how to use finite dimensional subspaces of divergence-free, $\boldsymbol{H}(\mathrm{div},\Omega)$-conforming without having to actually carry out the almost impossible construction of their bases. This can only be done in a few cases, see Thomasset (1981; Hecht (1981; Scott and Vogelius (1985.

6.1. The general form of the DG methods

6.1.1. Definition. The approximation $(\mathrm{L}_h, \boldsymbol{u}_h, p_h)$ on the element $K \in \mathcal{T}_h$ is taken in the space $\mathrm{G}(K) \times \boldsymbol{V}(K) \times Q(K)$ and is defined as the solution, for all $(\mathrm{G}, \boldsymbol{v}, q) \in \mathrm{G}(K) \times \boldsymbol{V}(K) \times Q(K)$, of the equations

$$\begin{aligned}(\mathrm{L}_h, \mathrm{G})_K + (\boldsymbol{u}_h, \nabla \cdot \mathrm{G})_K - \langle \widehat{\boldsymbol{u}}_h^{\mathrm{L}}, \mathrm{G}\boldsymbol{n}_K\rangle_{\partial K} &= 0,\\ \nu\,(\mathrm{L}_h, \nabla \boldsymbol{v})_K - (p_h, \nabla \cdot \boldsymbol{v})_K - \langle \nu\widehat{\mathrm{L}}_h\boldsymbol{n}_K - \widehat{p}_h\boldsymbol{n}_K, \boldsymbol{v}\rangle_{\partial K} &= (\boldsymbol{f}, \boldsymbol{v})_K,\\ -(\boldsymbol{u}_h, \nabla q)_K + \langle \widehat{\boldsymbol{u}}_h^{p} \cdot \boldsymbol{n}_K, q\rangle_{\partial K} &= 0.\end{aligned}$$

The average condition on the pressure is $(p_h, 1)_\Omega = 0$. Finally, the Dirichlet boundary condition is imposed by setting $\widehat{\boldsymbol{u}}_h^{\mathrm{L}} = \widehat{\boldsymbol{u}}_h^{p} = \boldsymbol{u}_D$ on $\partial\Omega$. To complete the definition of the DG method, we only need to define the numerical traces $\nu\widehat{\mathrm{L}}_h\boldsymbol{n} - \widehat{p}_h\boldsymbol{n}$, $\widehat{\boldsymbol{u}}_h^{\mathrm{L}}$ and $\widehat{\boldsymbol{u}}_h^{p}$.

6.1.2. The numerical traces. Taking advantage that the Laplacian operator acts on each component of the velocity, the numerical traces $\widehat{\mathrm{L}}_h\boldsymbol{n}$ and $\widehat{\boldsymbol{u}}_h^{\mathrm{L}}$ can be chosen by using, also in a componentwise manner, *any* of the numerical traces for the DG method for steady-state diffusion. The numerical traces $\widehat{p}_h\boldsymbol{n}$ and $\widehat{\boldsymbol{u}}_h^{p}$ can be picked independently.

6.1.3. Energy identities. Taking $(\mathrm{G}, \boldsymbol{v}, q) := (\nu\mathrm{L}_h, \boldsymbol{u}_h, p_h)$ and adding the resulting equations, we obtain the following local energy identity:

$$\nu(\mathrm{L}_h, \mathrm{L}_h)_K + \Theta_K = \langle \nu\widehat{\mathrm{L}}_h\boldsymbol{n}_K, \widehat{\boldsymbol{u}}_h^{\mathrm{L}}\rangle_{\partial K} - \langle \widehat{p}_h\boldsymbol{n}_K, \widehat{\boldsymbol{u}}_h^{p}\rangle_{\partial K} + (\boldsymbol{f}, \boldsymbol{u}_h)_K,$$

where

$$\begin{aligned}\Theta_K &:= \Theta_K^{\mathrm{L}} + \Theta_K^{p},\\ \Theta_K^{\mathrm{L}} &:= \langle \nu(\mathrm{L}_h - \widehat{\mathrm{L}}_h)\boldsymbol{n}_K, \boldsymbol{u}_h - \widehat{\boldsymbol{u}}_h^{\mathrm{L}}\rangle_{\partial K},\\ \Theta_K^{p} &:= -\langle (p_h - \widehat{p}_h)\boldsymbol{n}_K, \boldsymbol{u}_h - \widehat{\boldsymbol{u}}_h^{p}\rangle_{\partial K}.\end{aligned}$$

By adding on all the elements, we obtain the global energy identity

$$\nu(\mathrm{L}_h, \mathrm{L}_h)_\Omega + \Theta_h = \langle \nu\widehat{\mathrm{L}}_h\boldsymbol{n} - \widehat{p}_h\boldsymbol{n}, \widehat{\boldsymbol{u}}_D\rangle_{\partial\Omega} + (\boldsymbol{f}, \boldsymbol{u}_h)_\Omega,$$

where $\Theta_h := \sum_{K\in\mathcal{T}_h} \Theta_K$. We now see that, if the numerical traces have to be defined so that the term Θ_h is positive, it can be interpreted as the *energy* associated to the interelement jumps.

Encyclopedia of Computational Mechanics. Edited by Erwin Stein, René de Borst and Thomas J.R. Hughes.
 ISBN: 0-470-84699-2

6.1.4. Residuals and jumps. Let us show that the method establishes a linear relation between the residuals in the interior or the element K,

$$\mathrm{R_G} := \mathrm{L}_h - \nabla \boldsymbol{u}_h, \quad \boldsymbol{R_v} := -\nu \nabla \cdot \mathrm{L}_h + \nabla p_h - \boldsymbol{f}, \quad R_q := \nabla \cdot \boldsymbol{u}_h,$$

and the residuals on its boundaries ∂K,

$$\mathrm{r_G} := \widehat{\boldsymbol{u}}_h^{\mathrm{L}} - \boldsymbol{u}_h, \quad \boldsymbol{r_v} := \nu(\widehat{\mathrm{L}}_h - \mathrm{L}_h)\boldsymbol{n}_K - (\widehat{p}_h - p_h)\boldsymbol{n}_K, \quad r_q := (\widehat{\boldsymbol{u}}_h^p - \boldsymbol{u}_h) \cdot \boldsymbol{n}_K,$$

Simple integration by parts in the three equations defining the DG methods give us that, for all $(\mathrm{G}, \boldsymbol{v}, q) \in \mathrm{G}(K) \times \boldsymbol{V}(K) \times Q(K)$, we have that

$$\begin{aligned} (\mathrm{R_G}, \mathrm{G})_K &= \langle \mathrm{r_L}, \mathrm{G}\boldsymbol{n}_K \rangle_{\partial K}, \\ (\boldsymbol{R_v}, \boldsymbol{v})_K &= \langle \boldsymbol{r_v}, \boldsymbol{v} \rangle_{\partial K}, \\ (r_q, q)_K &= \langle r_q, q \rangle_{\partial K}. \end{aligned}$$

This immediately implies that

$$\begin{aligned} \|\mathsf{P}_{\mathrm{G}} \mathrm{R_G}\|_K &\leq C\, h_K^{-1/2}\, \|\mathrm{r_G}\|_{\partial K}, \\ \|\mathsf{P}_{\boldsymbol{V}} \boldsymbol{R_v}\|_K &\leq C\, h_K^{-1/2}\, \|\boldsymbol{r_v}\|_{\partial K}, \\ \|\mathsf{P}_Q R_q\|_K &\leq C\, h_K^{-1/2}\, \|r_q\|_{\partial K}, \end{aligned}$$

where P_{G}, $\mathsf{P}_{\boldsymbol{V}}$ and P_Q denote the $L^2(K)$-projections into the spaces $\mathrm{G}(K)$, $\boldsymbol{V}(K)$ and $Q(K)$, respectively. We thus see that, whenever

$$\nabla \boldsymbol{V}(K) \subset \mathrm{G}(K), \quad \nabla \cdot \mathrm{G}(K) \subset \boldsymbol{V}(K) \quad \text{and} \quad \nabla \cdot \boldsymbol{V}(K) \subset Q(K),$$

the quality of the approximation only depends on the residuals on the boundaries and on $\boldsymbol{f} - \mathsf{P}_{\boldsymbol{V}} \boldsymbol{f}$.

6.1.5. An example. Let us consider the numerical traces proposed in Cockburn et al. (2002; they use the numerical traces used for discretizing the Laplacian in Cockburn and Shu (1998a and Castillo et al. (2000. Le us begin with the traces associated to the discretization of the Laplacian. Inside the domain Ω, we take

$$\begin{aligned} \widehat{\mathrm{L}}_h &:= \{\mathrm{L}_h\} - [\![\mathrm{L}_h]\!] \otimes \boldsymbol{C}_{\mathrm{LL}} - C_{\mathrm{L}\boldsymbol{u}} [\![\boldsymbol{u}_h]\!], \\ \widehat{\boldsymbol{u}}_h &:= \{\boldsymbol{u}_h\} - [\![\boldsymbol{u}_h]\!] \boldsymbol{C}_{\boldsymbol{u}\boldsymbol{u}} - C_{\boldsymbol{u}\mathrm{L}} [\![\mathrm{L}_h]\!], \end{aligned}$$

where $[\![\mathrm{L}_h]\!] := \mathrm{L}_h^+ \boldsymbol{n}^+ + \mathrm{L}_h^- \boldsymbol{n}^-$ and $[\![\mathrm{u}_h]\!] := \boldsymbol{u}_h^+ \otimes \boldsymbol{n}^+ + \boldsymbol{u}_h^- \otimes \boldsymbol{n}^-$, and on its boundary, we take

$$\begin{aligned} \widehat{\mathrm{L}}_h &:= \mathrm{L}_h - C_{\mathrm{L}\boldsymbol{u}} (\boldsymbol{u}_h - \boldsymbol{u}_D) \otimes \boldsymbol{n} \\ \widehat{\boldsymbol{u}}_h &:= \boldsymbol{u}_D. \end{aligned}$$

Now, let us consider the traces associated to the pressure and the discretization of the divergence-free condition. On the interior faces, we take

$$\begin{aligned} \widehat{p}_h &:= \{p_h\} + \boldsymbol{D}_{pp} \cdot [\![p_h]\!] + D_{p\boldsymbol{u}} [\![\boldsymbol{u}_{h,n}]\!], \\ \widehat{\boldsymbol{u}}_h^p &:= \{\boldsymbol{u}_h\} + \boldsymbol{D}_{\boldsymbol{u}\boldsymbol{u}} [\![\boldsymbol{u}_{h,n}]\!] + \boldsymbol{D}_{\boldsymbol{u}p} \cdot [\![p_h]\!], \end{aligned}$$

Encyclopedia of Computational Mechanics. Edited by Erwin Stein, René de Borst and Thomas J.R. Hughes.
 ISBN: 0-470-84699-2

where $[\![\mathrm{u}_{h,n}]\!] := \boldsymbol{u}_h^+ \cdot \boldsymbol{n}^+ + \boldsymbol{u}_h^- \cdot \boldsymbol{n}^-$ and $[\![p_h]\!] := p_h^+ \boldsymbol{n}^+ + p_h^- \boldsymbol{n}^-$, and on the boundary,

$$\begin{aligned} \widehat{p}_h &:= p_h + D_{p\boldsymbol{u}}(\boldsymbol{u}_h - \boldsymbol{u}_D) \cdot \boldsymbol{n}, \\ \widehat{\boldsymbol{u}}_h^p &:= \boldsymbol{u}_D. \end{aligned}$$

In this case, a simple computation gives us that the global energy identity is

$$\nu(\mathrm{L}_h, \mathrm{L}_h)_\Omega + \Theta_h = \langle \nu \widehat{\mathrm{L}}_h \boldsymbol{n} - \widehat{p}_h \boldsymbol{n}, \boldsymbol{u}_D \rangle_{\partial\Omega} + (\boldsymbol{f}, \boldsymbol{u}_h)_\Omega,$$

where

$$\begin{aligned} \Theta_h = {} & \langle C_{\boldsymbol{u}\mathrm{L}} [\![\mathrm{L}_h]\!], [\![\mathrm{L}_h]\!] \rangle_{\mathcal{F}_h^i} + \langle C_{\mathrm{L}\boldsymbol{u}} [\![\boldsymbol{u}_h]\!], [\![\boldsymbol{u}_h]\!] \rangle_{\mathcal{F}_h^i} + \langle C_{\mathrm{L}\boldsymbol{u}} (\boldsymbol{u}_h - \boldsymbol{u}_D), \boldsymbol{u}_h - \boldsymbol{u}_D \rangle_{\partial\Omega} \\ & + \langle D_{\boldsymbol{u}p} [\![p_h]\!], [\![p_h]\!] \rangle_{\mathcal{F}_h^i} + \langle D_{p\boldsymbol{u}} [\![\boldsymbol{u}_{h,n}]\!], [\![\boldsymbol{u}_{h,n}]\!] \rangle_{\mathcal{F}_h^i} + \langle D_{p\boldsymbol{u}} (\boldsymbol{u}_h - \boldsymbol{u}_D), \boldsymbol{u}_h - \boldsymbol{u}_D \rangle_{\partial\Omega}, \end{aligned}$$

whenever $\boldsymbol{C}_{\mathrm{LL}} + \boldsymbol{C}_{\boldsymbol{u}\boldsymbol{u}} = \boldsymbol{0}$ and $\boldsymbol{D}_{pp} + \boldsymbol{D}_{\boldsymbol{u}\boldsymbol{u}} = \boldsymbol{0}$. We see that $C_{\boldsymbol{u}\mathrm{L}}, C_{\mathrm{L}\boldsymbol{u}}, C_{\boldsymbol{u}p}$ and $C_{p\boldsymbol{u}}$ stabilize the method.

Let us use the above global energy identity to obtain the existence and uniqueness of the approximate solution in the case in which

$$\begin{aligned} &\text{(i)} && C_{\boldsymbol{u}\mathrm{L}}, D_{p\boldsymbol{u}} \geq 0 && \text{on } \mathcal{F}_h^i, \\ &\text{(ii)} && C_{\mathrm{L}\boldsymbol{u}}, D_{\boldsymbol{u}p} > 0 && \text{on } \mathcal{F}_h^i \cup \partial\Omega, \\ &\text{(iii)} && \nabla \boldsymbol{V}(K) \subset \mathrm{G}(K) && \forall K \in \mathcal{T}_h, \\ &\text{(iv)} && \nabla Q(K) \subset \boldsymbol{V}(K) && \forall K \in \mathcal{T}_h. \end{aligned}$$

Again, we only have to show that, when we set the data $\boldsymbol{f}$ and $\boldsymbol{u}_D$ to zero, the only solution is the trivial one. But in this case, the above energy identity gives that, by (i) and (ii), that $\mathrm{L}_h = \boldsymbol{0}$ on Ω, that $[\![\boldsymbol{u}_h]\!] = [\![p_h]\!] = \boldsymbol{0}$ on $\mathcal{F}_h^i$, and that $\boldsymbol{u}_h = \boldsymbol{0}$ on $\partial\Omega$. As a consequence, we have that $\widehat{\boldsymbol{u}}_h^{\mathcal{L}} = \boldsymbol{u}_h$ on $\mathcal{F}_h^i \cup \partial\Omega$, and the first equation defining the DG method reads

$$-(\nabla \boldsymbol{u}_h, \mathrm{G})_K = 0$$

for all $\mathrm{G} \in \mathrm{G}(K)$. By (iii) we can take $\mathrm{G} := \nabla \boldsymbol{u}_h$ and conclude that $\boldsymbol{u}_h$ is a constant vector on the element K. Since $\boldsymbol{u}_h = \widehat{\boldsymbol{u}}_h$ on the interelement boundaries, $\boldsymbol{u}_h$ is a vector constant on Ω, and since $\boldsymbol{u}_h = \boldsymbol{0}$ on $\partial\Omega$, we get that $\boldsymbol{u}_h = \boldsymbol{0}$ on Ω.

We still need to show that the approximate pressure is zero. Taking into account that the interelement jumps of p_h are zero, the second equation defining the DG method reads

$$(\nabla p_h, \boldsymbol{v})_K = 0,$$

for all $\boldsymbol{v} \in \boldsymbol{V}(K)$. By property (iv), we can take $\boldsymbol{v} := \nabla p_h$ to conclude that p_h is a constant on the element K. Since p_h is continuous on Ω and has average equal to zero, we conclude that p_h is also zero. This completes the proof.

6.2. DG methods allowing for an easy elimination of L_h

If we discretize each of the components of the Laplacian by using DG methods for the Laplacian allowing for an easy elimination of the variable $\boldsymbol{q}_h$, we immediately obtain a DG method for

Encyclopedia of Computational Mechanics. Edited by Erwin Stein, René de Borst and Thomas J.R. Hughes.
 ISBN: 0-470-84699-2

which the velocity gradient L_h can be easily eliminated. As a consequence, we obtain methods expressed in terms of the velocity $\boldsymbol{u}_h$ and the pressure p_h only. Examples of these methods are the very first DG method proposed by Baker et al. (1990, which uses the IP method to approximate the Laplacian, elementwise solenoidal velocities and a continuous approximation of the pressure, the methods proposed by Cockburn et al. (2002 (for arbitrarily -shaped elements) and Schötzau et al. (2003a (for square and cubic elements), which uses the LDG method, and the method proposed by Girault et al. (2005 (for triangular elements), which considers both the IP and the Baumann-Oden methods.

The convergence properties of these methods are as follows. When the velocities contain the piecewise polynomials of degree k and the pressure (and velocity gradient) are piecewise polynomials of degree $k-1$, both the velocity and the pressure converge optimally (in particular, with order $k+1$ and k in L^2-norms) for any $k \geq 1$; for Girault et al. (2005 the estimates hold for $p = 1, 2, 3$. The p-version of the methods is treated in Schötzau et al. (2003a where optimal convergence properties are proven.

6.3. The HDG methods

The DG methods we just considered allow for an easy elimination of the approximation L_h which gives rise to formulations in terms of $\boldsymbol{u}_h$ and p_h. Here, we consider DG methods which allow for the elimination of L_h, $\boldsymbol{u}_h$ and p_h which results in formulations in terms of $\widehat{\boldsymbol{u}}_h$ and the average of the pressure on each element $\overline{p}_h$ only. This new formulation maintains the original saddle- point structure of the problem for $\boldsymbol{u}_h$ and p_h, but has remarkably less globally-coupled degrees of freedom, which provides an efficient implementation of the method. We follow Cockburn and Shi (2014.

6.3.1. Definition. The HDG methods are obtained as a discrete version of the following characterization of the exact solution. On the element $k \in \mathcal{T}_h$, given $\boldsymbol{f}|_K$, the constant $\overline{p}$ and the Dirichlet boundary data $\widehat{\boldsymbol{u}}\,|_{\partial K}$, we take $(\mathrm{L}, \boldsymbol{u}, p)$ to be the solution of the following *local problem*:

$$\mathrm{L} = \nabla \boldsymbol{u}, \quad -\nu \nabla \cdot \mathrm{L} + \nabla p = \boldsymbol{f}, \quad \nabla \cdot \boldsymbol{u} = \frac{1}{|K|} \langle \widehat{\boldsymbol{u}} \cdot \boldsymbol{n}_K, 1 \rangle_{\partial K} \quad \text{in } K,$$

$$\frac{1}{|K|}(p, 1)_K = \overline{p}, \quad \widehat{\boldsymbol{u}} = \boldsymbol{u}_D \quad \text{on } \partial K,$$

Then, the piecewise-constant function $\overline{p}$ and the single-valued velocity $\widehat{\boldsymbol{u}}$ is determined as the solution of the global problem consisting the following transmission, divergence-free and boundary and average conditions:

$$[\![\nu \mathrm{L} - p\mathrm{Id}]\!] = 0 \quad \text{on } \mathcal{F}_h^i, \quad \langle \widehat{\boldsymbol{u}} \cdot \boldsymbol{n}_K, 1 \rangle_{\partial K} = 0 \quad \forall K \in \mathcal{T}_h, \quad \widehat{\boldsymbol{u}} = \widehat{\boldsymbol{u}}_D \quad \text{on } \partial\Omega, \quad (\overline{p}, 1)_\Omega = 0.$$

Here $[\![\nu \mathrm{L} - p\mathrm{Id}]\!] := \nu(\mathrm{L}^+ \boldsymbol{n}^+ - \mathrm{L}^- \boldsymbol{n}^-) - (p^+ \boldsymbol{n}^+ + p^- \boldsymbol{n}^-)$, with the obvious notation.

Let us note that the velocity $\boldsymbol{u}$ solving the local problems is *not* necessarily divergence-free because we do not want to assume that the Dirichlet data $\widehat{\boldsymbol{u}}\,|_{\partial K}$ is such that $\langle \widehat{\boldsymbol{u}} \cdot \boldsymbol{n}, 1 \rangle_K = 0$.

Encyclopedia of Computational Mechanics. Edited by Erwin Stein, René de Borst and Thomas J.R. Hughes.
 ISBN: 0-470-84699-2

We want these local problems to be solvable for any values of $\widehat{\boldsymbol{u}}\,|_{\partial K}$. For this reason, we need to introduce the second equation in the the definition of the global problem.

To obtain the HDG methods, we solve the local problem on each element $K \in \mathcal{T}_h$ by using a DG method. We solve the global problem by imposing the transmission, divergence-free, boundary and beverage conditions weakly. So, for any given arbitrary function $\widehat{\boldsymbol{u}}_h\,|_{\partial K}$ and constant $\overline{p}_h$, we define $(\mathrm{L}_h, \boldsymbol{u}_h, p_h) \in \mathrm{G}(K) \times \boldsymbol{V}(K) \times Q(K)$ as the solution of the local problem for all $(\mathrm{G}, \boldsymbol{v}, q) \in \mathrm{G}(K) \times \boldsymbol{V}(K) \times Q(K)$,

$$\begin{aligned}
(\mathrm{L}_h, \mathrm{G})_K + (\boldsymbol{u}_h, \nabla \cdot \mathrm{G})_K - \langle \widehat{\boldsymbol{u}}_h, \mathrm{G}\boldsymbol{n}\rangle_{\partial K} &= 0,\\
\nu\,(\mathrm{L}_h, \nabla \boldsymbol{v})_K - (p_h, \nabla \cdot \boldsymbol{v})_K - \langle \widehat{\nu \mathrm{L}}_h \boldsymbol{n} - \widehat{p}_h \boldsymbol{n}, \boldsymbol{v}\rangle_{\partial K} &= (\boldsymbol{f}, \boldsymbol{v})_K,\\
-(\boldsymbol{u}_h, \nabla q)_K + \langle \widehat{\boldsymbol{u}}_h \cdot \boldsymbol{n}, q\rangle_{\partial K} &= \langle \widehat{\boldsymbol{u}}_h \cdot \boldsymbol{n}, \overline{q}\rangle_{\partial K},\\
(p_h, 1)_K &= (\overline{p}_h, 1)_K,\\
\widehat{\nu \mathrm{L}}_h \boldsymbol{n} - \widehat{p}_h \boldsymbol{n} := \nu \mathrm{L}_h \boldsymbol{n} - p_h \boldsymbol{n} - \mathrm{S}(\boldsymbol{u}_h - \widehat{\boldsymbol{u}}_h) \quad &\text{on } \partial K.
\end{aligned}$$

We take the function $(\widehat{\boldsymbol{u}}_h, \overline{p}_h)$ in the space $\boldsymbol{M}_h \times Q_h^0$, where,

$$\begin{aligned}
\boldsymbol{M}_h &:= \{\boldsymbol{\mu} \in \boldsymbol{L}^2(\mathcal{F}_h): \quad \boldsymbol{\mu}|_F \in \boldsymbol{M}(F) \qquad \forall\, F \in \mathcal{F}_h\},\\
Q_h^0 &:= \{q \in L^2(\mathcal{T}_h): \quad q|_K \text{ is a constant} \quad \forall\, K \in \mathcal{T}_h\},
\end{aligned}$$

where the *local* space $\boldsymbol{M}(F)$ is a general finite dimensional space, and determine it by requiring that, for all $(\boldsymbol{\mu}, q) \in \boldsymbol{M}_h \times Q_h^0$,

$$\begin{aligned}
\langle -\widehat{\nu \mathrm{L}}_h \boldsymbol{n} + \widehat{p}_h\, \boldsymbol{n}, \boldsymbol{\mu}\rangle_{\partial \mathcal{T}_h \setminus \partial\Omega} &= 0,\\
\langle \widehat{\boldsymbol{u}}_h \cdot \boldsymbol{n}, \overline{q}\rangle_{\partial \mathcal{T}_h} &= 0,\\
\langle \widehat{\boldsymbol{u}}_h, \boldsymbol{\mu}\rangle_{\partial\Omega} &= \langle \boldsymbol{g}, \boldsymbol{\mu}\rangle_{\partial\Omega},\\
(\overline{p}_h, 1)_\Omega &= 0.
\end{aligned}$$

Note, again, that $(\widehat{\boldsymbol{u}}_h, \overline{p}_h)$ is *data* of the local problem but the *unknown* of the global problem. We need to solve the global problem in order to get the actual values of $(\widehat{\boldsymbol{u}}_h, \overline{p}_h)$. However, we first need to solve the local problems to be able to construct the matrix equations of the global problem. We show how to do that next.

6.3.2. The problem for $(\widehat{\boldsymbol{u}}_h, \overline{p}_h)$. We start by introducing notation related to the local problems. On the element $K \in \mathcal{T}_h$, for any $\boldsymbol{\mu} \in \boldsymbol{L}^2(\partial K)$, we define $(\mathrm{L}^{\boldsymbol{\mu}}, \mathbf{U}^{\boldsymbol{\mu}}, \mathsf{P}^{\boldsymbol{\mu}}) \in \mathrm{G}(K) \times \boldsymbol{V}(K) \times Q(K)$ as the solution, for all $(\mathrm{G}, \boldsymbol{v}, q) \in \mathrm{G}(K) \times \boldsymbol{V}(K) \times Q(K)$, of the equations

$$\begin{aligned}
(\mathrm{L}^{\boldsymbol{\mu}}, \mathrm{G})_K + (\mathbf{U}^{\boldsymbol{\mu}}, \nabla \cdot \mathrm{G})_K - \langle \boldsymbol{\mu}, \mathrm{G}\boldsymbol{n}\rangle_{\partial K} &= 0,\\
\nu\,(\mathrm{L}^{\boldsymbol{\mu}}, \nabla \boldsymbol{v})_K - (\mathsf{P}^{\boldsymbol{\mu}}, \nabla \cdot \boldsymbol{v})_K - \langle \widehat{\nu \mathrm{L}}^{\boldsymbol{\mu}} \boldsymbol{n} - \widehat{\mathsf{P}}^{\boldsymbol{\mu}} \boldsymbol{n}, \boldsymbol{v}\rangle_{\partial K} &= 0,\\
-(\mathbf{U}^{\boldsymbol{\mu}}, \nabla q)_K + \langle \boldsymbol{\mu} \cdot \boldsymbol{n}, q\rangle_{\partial K} &= \langle \boldsymbol{\mu} \cdot \boldsymbol{n}, \overline{q}\rangle_{\partial K},\\
(\mathsf{P}^{\boldsymbol{\mu}}, 1)_K &= 0,\\
\widehat{\nu \mathrm{L}}^{\boldsymbol{\mu}} \boldsymbol{n} - \widehat{\mathsf{P}}^{\boldsymbol{\mu}} \boldsymbol{n} := \nu \mathrm{L}^{\boldsymbol{\mu}} \boldsymbol{n} - \mathsf{P}^{\boldsymbol{\mu}} \boldsymbol{n} - \mathrm{S}(\mathbf{U}^{\boldsymbol{\mu}} - \boldsymbol{\mu}) \quad &\text{on } \partial K.
\end{aligned}$$

Encyclopedia of Computational Mechanics. Edited by Erwin Stein, René de Borst and Thomas J.R. Hughes.
 ISBN: 0-470-84699-2

Similarly, for any $\boldsymbol{f} \in \boldsymbol{L}^2(K)$, we define $(\mathrm{L}^{\boldsymbol{f}}, \mathbf{U}^{\boldsymbol{f}}, \mathsf{P}^{\boldsymbol{f}}) \in \mathrm{G}(K) \times \boldsymbol{V}(K) \times Q(K)$ as the solution, for all $(\mathrm{G}, \boldsymbol{v}, q) \in \mathrm{G}(K) \times \boldsymbol{V}(K) \times Q(K)$, the equations

$$\begin{aligned}
(\mathrm{L}^{\boldsymbol{f}}, \mathrm{G})_K + (\mathbf{U}^{\boldsymbol{f}}, \nabla \cdot \mathrm{G})_K &= 0, \\
\nu\,(\mathrm{L}^{\boldsymbol{f}}, \nabla \boldsymbol{v})_K - (\mathsf{P}^{\boldsymbol{f}}, \nabla \cdot \boldsymbol{v})_K - \langle \nu \widehat{\mathrm{L}}^{\boldsymbol{f}} \boldsymbol{n} - \widehat{\mathsf{P}}^{\boldsymbol{f}} \boldsymbol{n}, \boldsymbol{v} \rangle_{\partial K} &= (\boldsymbol{f}, \boldsymbol{v})_K, \\
-(\mathbf{U}^{\boldsymbol{f}}, \nabla q)_K &= 0, \\
(\mathsf{P}^{\boldsymbol{f}}, 1)_K &= 0, \\
\nu \widehat{\mathrm{L}}^{\boldsymbol{f}} \boldsymbol{n} - \widehat{\mathsf{P}}^{\boldsymbol{f}} \boldsymbol{n} := \nu \mathrm{L}^{\boldsymbol{f}} \boldsymbol{n} - \mathsf{P}^{\boldsymbol{f}} \boldsymbol{n} - \mathrm{S}(\mathbf{U}^{\boldsymbol{f}}) &\quad \text{on } \partial K.
\end{aligned}$$

With this notation, we can write that

$$(\mathrm{L}_h, \boldsymbol{u}_h, p_h) = (\mathrm{L}^{\widehat{\boldsymbol{u}}_h}, \mathbf{U}^{\widehat{\boldsymbol{u}}_h}, \mathsf{P}^{\widehat{\boldsymbol{u}}_h}) + (\mathrm{L}^{\boldsymbol{f}}, \mathbf{U}^{\boldsymbol{f}}, \mathsf{P}^{\boldsymbol{f}}) + (0, \boldsymbol{0}, \overline{p}_h),$$

where $(\widehat{\boldsymbol{u}}_h, \overline{p}_h)$ is the solution of the global problem. The next result, by Nguyen et al. (2010b, gives a characterization of this function. Therein, we use the following notation:

$$\boldsymbol{M}_h(\boldsymbol{g}) := \{\boldsymbol{\mu} \in \boldsymbol{M}_h : \ \langle \boldsymbol{\mu}, \boldsymbol{\lambda} \rangle_{\partial\Omega} = \langle \boldsymbol{g}, \boldsymbol{\lambda} \rangle_{\partial\Omega} \ \forall \boldsymbol{\lambda} \in \boldsymbol{M}_h\}.$$

Theorem 5 (Characterization of $(\widehat{\boldsymbol{u}}_h, \overline{p}_h)$) *Assume that*

$$\begin{aligned}
&\text{(i)} \quad \mathrm{S}|_F \text{ is symmetric and uniformly positive definite} && \forall F \in \mathcal{F}_h, \\
&\text{(ii)} \quad \nabla \mathbf{V}(K) \subset \mathrm{G}(K) && \forall K \in \mathcal{T}_h, \\
&\text{(iii)} \quad \nabla Q(K) \subset \mathbf{V}(K) && \forall K \in \mathcal{T}_h.
\end{aligned}$$

The function $(\widehat{\boldsymbol{u}}_h, \overline{p}_h)$ is the element in $\mathbf{M}_h(\mathbf{u}_D) \times Q_h^0$ satisfying

$$\begin{aligned}
a_h(\widehat{\boldsymbol{u}}_h, \boldsymbol{\mu}) + b_h(\boldsymbol{\mu}, \overline{p}_h) &= (\mathbf{f}, \mathbf{u}_h^{\boldsymbol{\mu}})_{\mathcal{T}_h} && \forall \boldsymbol{\mu} \in \mathbf{M}_h(\mathbf{0}), \\
-b_h(\widehat{\boldsymbol{u}}_h, \overline{q}) &= 0 && \forall \overline{q} \in Q_h^0, \\
(\overline{p}_h, 1)_\Omega &= 0,
\end{aligned}$$

where $a_h(\boldsymbol{\lambda}, \boldsymbol{\mu}) := \langle \nu \widehat{\mathrm{L}}_{\mathrm{h}}^{\boldsymbol{\mu}} \mathbf{n} - \widehat{p}_h^{\boldsymbol{\mu}} \mathbf{n}, \boldsymbol{\lambda} \rangle_{\partial \mathcal{T}_h}$ and $b_h(\boldsymbol{\lambda}, \overline{q}) := -\langle \overline{q}, \boldsymbol{\lambda} \cdot \mathbf{n} \rangle_{\partial \mathcal{T}_h}$. Moreover,

$$a_h(\boldsymbol{\lambda}, \boldsymbol{\mu}) \quad = \quad \nu\,(\mathrm{L}_h^{\boldsymbol{\lambda}}, \mathrm{L}_h^{\boldsymbol{\mu}})_{\mathcal{T}_h} + \langle \mathrm{S}(\mathbf{u}_h^{\boldsymbol{\lambda}} - \boldsymbol{\lambda}), (\mathbf{u}_h^{\boldsymbol{\mu}} - \boldsymbol{\mu}) \rangle_{\partial \mathcal{T}_h},$$

for all $\boldsymbol{\lambda}$, $\boldsymbol{\mu}$ in $\boldsymbol{M}_h$, and $a_h(\cdot, \cdot)$ is symmetric and positive definite in $\boldsymbol{M}_h(\mathbf{0}) \times \boldsymbol{M}_h(0)$.

This implies that, as claimed, the **HDG** methods can be easily implemented. Indeed, we see that the only globally coupled degrees of freedom are those of the approximation of the velocity on $\mathcal{F}_h$, $\widehat{\boldsymbol{u}}_h$, and those of the elementwise average of the pressure $\overline{p}_h$. This global problem can be solved by using, for example, the augmented Lagrangian method, see Nguyen et al. (2010b. Once this global problem is solved, the approximate solution $(\mathrm{L}_h, \boldsymbol{u}_h, p_h)$ can be easily obtained in an element-by-element fashion by using the very first identity of this Subsection.

This also implies that we can see $\widehat{\boldsymbol{u}}_h$ as the only minimum of the functional

$$J_h(\boldsymbol{\lambda}) := \frac{1}{2}\, a_h(\boldsymbol{\lambda}, \boldsymbol{\lambda}) - (\boldsymbol{f}, \boldsymbol{u}_h^{\boldsymbol{\lambda}})_{\mathcal{T}_h},$$

Encyclopedia of Computational Mechanics. Edited by Erwin Stein, René de Borst and Thomas J.R. Hughes.
 ISBN: 0-470-84699-2

on the space $\boldsymbol{D} := \{\boldsymbol{\mu} \in \boldsymbol{M}_h(\boldsymbol{g}) : \ b_h(\boldsymbol{\lambda}, \overline{q}) = 0 \ \forall \ \overline{q} \in Q_h\}$. Note that a related method can be obtained by dropping the restriction that $\boldsymbol{\lambda}$ lie on the space $\boldsymbol{D}$, by requiring that the approximate velocities be divergence-free on each element and by penalizing their interelement normal jump. This was originally proposed by Hansbo and Larson (2008 for a DG method defined by means of an IP discretization. This approach was then applied to a DG method proposed in Montlaur et al. (2008 which uses globally divergence-free velocities. The resulting method turned out to be identical to the DG method proposed by Hansbo and Larson (2008.

6.3.3. The numerical traces. Let us give an idea of the explicit form of the numerical traces of the HDG methods in the simple case in which the stabilization tensor is just a constant time the identity, that is, $\mathrm{S} := \tau\,\mathrm{Id}$ where τ is taken to be constant on each face. Then, when the local spaces are taken in such a way that the transmission condition implies

$$[\![-\nu\widehat{\mathrm{L}}_h\boldsymbol{n} + \widehat{p}_h\boldsymbol{n}]\!] = \boldsymbol{0} \quad \text{on } \mathcal{F}_h^i,$$

a simple computation gives us that the numerical traces *must* given by the following formulas:

$$\begin{aligned}
\widehat{\boldsymbol{u}}_h &= \frac{\tau^+ {\boldsymbol{u}_h}^+ + \tau^- {\boldsymbol{u}_h}^-}{\tau^+ + \tau^-} + \frac{1}{\tau^+ + \tau^-}[\![-\nu\mathrm{L}_h + p_h\mathrm{Id}]\!], \\
-\nu\widehat{\mathrm{L}}_h + \widehat{p}_h\mathrm{Id} &= \frac{\tau^-}{\tau^+ + \tau^-}(-\nu\mathrm{L}_h^+ + p_h^+\mathrm{Id}) \\
&\quad + \frac{\tau^+}{\tau^+ + \tau^-}(-\nu\mathrm{L}_h^- + p_h^-\mathrm{Id}) + \frac{\tau^+\tau^-}{\tau^+ + \tau^-}[\![\boldsymbol{u}_h]\!].
\end{aligned}$$

Note that for this HDG method, we have that $\widehat{\boldsymbol{u}}_h^{\mathrm{L}} = \widehat{\boldsymbol{u}}_h^p = \widehat{\boldsymbol{u}}_h$ and so, it is impossible to relate it to any of the DG methods previously considered. We can, however, compare the stabilization term which in this case is

$$\begin{aligned}
\Theta_h &= \sum_{K\in\mathcal{T}_h} \langle((\nu\mathrm{L}_h - p_h\mathrm{Id}) - (\nu\widehat{\mathrm{L}}_h - \widehat{p}_h\mathrm{Id}))\boldsymbol{n}_K, \boldsymbol{u}_h - \widehat{\boldsymbol{u}}_h\rangle_{\partial K} \\
&= \sum_{K\in\mathcal{T}_h} \langle\tau(\boldsymbol{u}_h - \widehat{\boldsymbol{u}}_h), \boldsymbol{u}_h - \widehat{\boldsymbol{u}}_h\rangle_{\partial K} \\
&= \langle\frac{1}{\tau^+ + \tau^-}[\![\nu\mathrm{L}_h - p_h\mathrm{Id}]\!], [\![\nu\mathrm{L}_h - p_h\mathrm{Id}]\!]\rangle_{\mathcal{F}_h^i} \\
&\quad + \langle\frac{\tau^+\tau^-}{\tau^+ + \tau^-}[\![\boldsymbol{u}_h]\!], [\![\boldsymbol{u}_h]\!]\rangle_{\mathcal{F}_h^i} + \langle\tau(\boldsymbol{u}_h - \boldsymbol{u}_D), (\boldsymbol{u}_h - \boldsymbol{u}_D)\rangle_{\partial\Omega}.
\end{aligned}$$

We thus see that the stabilization of the HDG methods is through the interelement jumps of $\boldsymbol{u}_h$ and those of the normal component of $\nu\mathrm{L}_h - p_h\mathrm{Id}$.

6.3.4. Convergence properties. Consider meshes $\mathcal{T}_h$ is a regular-shaped elements polygonal or polyhedral element K. For the HDG methods with the local spaces

$$\mathrm{G}(K) = \mathrm{P}_k(K), \ \ \boldsymbol{V}(K) = \boldsymbol{\mathcal{P}}_k(K), \ \ Q(K) = \mathcal{P}_k(K), \ \ \boldsymbol{M}(F) = \boldsymbol{\mathcal{P}}_k(F).$$

and the stabilization function $\mathrm{S} = \tau\,\mathrm{Id}$, it was proven in Cockburn and Shi (2014 that, when τ is a positive constant, the order of convergence for the velocity is $k+1$ but those for the pressure

Encyclopedia of Computational Mechanics. Edited by Erwin Stein, René de Borst and Thomas J.R. Hughes.
 ISBN: 0-470-84699-2

and the velocity gradient are only $k+1/2$ (The same orders hold if we take $\mathrm{G}(K) = \nabla \boldsymbol{\mathcal{P}}_k(K)$). Whenever $\tau = 1/h$, then the order of convergence for the velocity is $k+1$ but those for the pressure and the velocity gradient are only k. The same orders hold if we take $\mathrm{G}(K) = \mathrm{P}_{k-1}(K)$ and $Q(K) = \mathcal{P}_{k-1}(K)$. In this case, the orders are optimal.

6.3.5. Superconvergent **HDG** *methods.* It is possible to devise superconvergent **HDG** methods for the Stokes flow in terms superconvergent **HDG** methods for the model diffusion problem previously considered. Suppose that the local spaces of the latter methods are $\boldsymbol{V}^{\mathrm{D}}(K)$, $W^{\mathrm{D}}(K)$ and $M^{\mathrm{D}}(F)$, and that their stabilization function is τ^{D}. We construct a superconvergent **HDG** method as follows.

Denote by $\mathrm{G}_i(K)$ the space of all the i-th rows of functions in $\mathrm{G}(K)$, and by $\boldsymbol{V}_i(K)$ and $\boldsymbol{M}_i(F)$ the space of the i-th component of functions in $\boldsymbol{V}(K)$ and $\boldsymbol{M}(F)$, respectively, for $i = 1, \ldots, d$. Then, we take the local spaces as

$$\mathrm{G}_i(K) := \boldsymbol{V}^{\mathrm{D}}(K), \quad \boldsymbol{V}_i(K) := W^{\mathrm{D}}(K), \quad \boldsymbol{M}_i(F) := M^{\mathrm{D}}(F), \tag{8a}$$

for $i = 1, \ldots, d$, and the stabilization function as

$$\mathrm{S} := \tau^{\mathrm{D}} \, \mathrm{Id}. \tag{8b}$$

The choice of the space for the pressure $Q(K)$ has to be done in such a way that

$$\sum_{j=1}^{d} \partial_j W^{\mathrm{D}}(K) \subset Q(K) \subset \cap_{j=1}^{d} \{ v_j : \boldsymbol{v} \in \boldsymbol{V}^{\mathrm{D}}(K) : v_i = 0 \text{ for } i \neq j \}. \tag{8c}$$

Examples of such methods are displayed in Table 11, taken from Cockburn et al. (2012a. We display the orders of convergence for mixed methods ($\tau^{\mathrm{D}} = 0$) and **HDG** methods ($\tau^{\mathrm{D}} = 1$) using different elements K. We only show the space for the pressure $Q(K)$; the the other spaces are explicitly given in Cockburn et al. (2012a. The new approximation of the velocity $\boldsymbol{u}_h^*$ on the element $K \in \mathcal{T}_h$ is defined, see Gastaldi and Nochetto (1989; Stenberg (1988; Stenberg (1991, as the element of finite dimensional space $\boldsymbol{V}^*(K)$ such that

$$(\nabla \boldsymbol{u}_h^*, \nabla \boldsymbol{v})_K = (\mathrm{L}_h, \nabla \boldsymbol{v})_K \quad \forall \boldsymbol{v} \in \boldsymbol{V}^*(K), \tag{9a}$$

$$(\boldsymbol{u}_h^*, \boldsymbol{v})_K = (\boldsymbol{u}_h, \boldsymbol{v})_K \qquad \forall \in \boldsymbol{\mathcal{P}}_0(K). \tag{9b}$$

In the examples in Table 11, it is enough to take $\boldsymbol{V}_h^*(K) \supset \boldsymbol{\mathcal{P}}_{k+1}(K)$ for all elements $K \in \mathcal{T}_h$.

The application of the theory of M-decompositions to devise superconvergent **HDG** and mixed methods has been developed in Cockburn et al. (2016a. Examples of other methods are the staggered DG method obtained by Kim et al. (2013, which is related to the SFH method, as pointed out by Chung et al. (2016, and the method proposed by Oikawa (2016, which is related to the reduced-order HDG method analyzed in Oikawa (2015.

Encyclopedia of Computational Mechanics. Edited by Erwin Stein, René de Borst and Thomas J.R. Hughes.
 ISBN: 0-470-84699-2

Table 11. Order of convergence for superconvergent **HDG** methods ($k \geq 1$)

	$Q(K)$	$\|\mathrm{L} - \mathrm{L}_h\|_{L^2(\Omega)}$	$\|p - p_h\|_{L^2(\Omega)}$	$\|\boldsymbol{u} - \boldsymbol{u}_h^\star\|_{L^2(\Omega)}$
K simplex and $\boldsymbol{M}(F) = \boldsymbol{P}_k(F)$				
$\mathbf{BDFM}_{k+1}$	$\mathcal{P}_k(K)$	$k+1$	$k+1$	$k+2$
$\mathbf{RT}_k$	$\mathcal{P}_k(K)$	$k+1$	$k+1$	$k+2$
$\mathbf{HDG}_k$	$\mathcal{P}_k(K)$	$k+1$	$k+1$	$k+2$
$\mathbf{BDM}_k$ $k\geq 2$	$\mathcal{P}_k(K)$	$k+1$	$k+1$	$k+2$
K square or cube and $\boldsymbol{M}(F) = \boldsymbol{P}_k(F)$				
$\mathbf{BDFM}_{[k+1]}$	$\mathcal{P}_k(K)$	$k+1$	$k+1$	$k+2$
$\mathbf{HDG}^P_{[k]}$	$\mathcal{P}_k(K)$	$k+1$	$k+1$	$k+2$
$\mathbf{BDM}_{[k]}$ $k\geq 2$	$\mathcal{P}_k(K)$	$k+1$	$k+1$	$k+2$
K square or cube and $\boldsymbol{M}(F) = \boldsymbol{Q}_k(F)$				
$\mathbf{RT}_{[k]}$	$\mathcal{Q}_k(K)$	$k+1$	$k+1$	$k+2$
$\mathbf{TNT}_{[k]}$	$\mathcal{Q}_k(K)$	$k+1$	$k+1$	$k+2$
$\mathbf{HDG}^Q_{[k]}$	$\mathcal{Q}_k(K)$	$k+1$	$k+1$	$k+2$

6.4. Obtaining divergence-free approximate velocities

6.4.1. Using $\mathbf{H}(\mathrm{div},\Omega)$*-conforming velocity spaces.* A very simple way to obtain divergence-free approximate velocities, see Cockburn et al. (2005; Cockburn et al. (2007, is to pick the velocity space in such a way that

$$\begin{aligned} &\text{(i)} \quad \nabla \cdot \boldsymbol{V}(K) \subset Q(K) \qquad \forall\, K \in \mathcal{T}_h, \\ &\text{(ii)} \quad \boldsymbol{V}(K) \subset \boldsymbol{H}(\mathrm{div},\Omega), \end{aligned}$$

and set

$$\widehat{\boldsymbol{u}}_h \cdot \boldsymbol{n}_K := \boldsymbol{u}_h \cdot \boldsymbol{n}_K \quad \text{ on } \partial K \quad \forall\, K \in \mathcal{T}_h.$$

Indeed, in the case, the third equation defining the DG method reads, after a simple integration by parts,

$$(\nabla \cdot \boldsymbol{u}_h, q)_K = 0$$

for all $q \in Q(K)$. By property (i) and the choice of the normal component of the numerical trace, this implies that we can take $q := \nabla \cdot \boldsymbol{u}_h$ to conclude that $\nabla \cdot \boldsymbol{u}_h = 0$ on the element K. By property (ii), this implies that $\boldsymbol{u}_h$ is a divergence-free function in $\boldsymbol{H}(\mathrm{div},\Omega)$.

In Cockburn and Sayas (2014, a new approach was proposed to devising HDG methods with $\mathbf{H}(\mathrm{div})$-conforming velocity spaces which are also superconvergent. It consists in considering the superconvergent $\mathbf{HDG}_k$ method in Table 11 with the following stabilization function

$$\mathrm{S} := \nu\, \tau_n\, \boldsymbol{n} \otimes \boldsymbol{n} + \nu\, \tau_t\, (\mathrm{Id} - \boldsymbol{n} \otimes \boldsymbol{n}),$$

Encyclopedia of Computational Mechanics. Edited by Erwin Stein, René de Borst and Thomas J.R. Hughes.
 ISBN: 0-470-84699-2

where $\boldsymbol{n}$ is the normal to the faces on $\partial\mathcal{T}_h$, and let τ_n go to infinity. In Cockburn and Sayas (2014, it was proven that, when τ_n goes to infinity, we obtain a well defined method with the very same convergence and superconvegence properties of the original method $\mathbf{HDG}_k$.

6.4.2. Divergence-free velocities by local postprocessing. An alternative to the previous approach is to postprocess the approximation to obtain the wanted $\boldsymbol{H}(\mathrm{div},\Omega)$-conforming, divergence-free approximate velocity; see Bastian and Rivière (2003; Cockburn et al. (2005; A. Ern and Vohralík (2007. For example, let us assume that all the elements K are tetrahedra. Then, on the tetrahedron $K\in\mathcal{T}_h$, the postprocessed velocity $\mathbf{u}_h^*$ is defined as the element of $\boldsymbol{\mathcal{P}}_k(K)$ such that

$$\langle(\mathbf{u}_h^*-\widehat{\boldsymbol{u}}_h)\cdot\boldsymbol{n},\mu\rangle_F=0\quad\forall\,\mu\in\mathcal{P}_{k-1}(F),$$

for all faces F of K, and such that

$$\begin{aligned}(\mathbf{u}_h^*-\boldsymbol{u}_h,\nabla w)_K&=0\quad\forall\,w\in\mathcal{P}_{k-1}(K),\\(\nabla\times\mathbf{u}_h^*-\mathbf{w}_h,(\nabla\times\boldsymbol{v})\,\mathrm{B}_K)_K&=0\quad\forall\,\boldsymbol{v}\in\boldsymbol{\mathcal{S}}_{k-1}(K)\end{aligned}$$

where B_K is the so-called *symmetric bubble matrix* introduced in Cockburn et al. (2010b, namely,

$$\mathrm{B}_K:=\sum_{\ell=0}^{3}\lambda_{\ell-3}\lambda_{\ell-2}\lambda_{\ell-1}\nabla\lambda_\ell\otimes\nabla\lambda_\ell,$$

where λ_i are the barycentric coordinates associated with the tetrahedron K, the subindices being counted modulo 4. Finally, $\boldsymbol{\mathcal{S}}_{k-1}(K):=\sum_{\ell=1}^{k-1}\boldsymbol{S}_\ell(K)$ where $\boldsymbol{S}_\ell$ is the space of vector-valued homogeneous polynomials $\boldsymbol{v}$ of degree ℓ such that $\boldsymbol{v}\cdot\boldsymbol{x}=0$, see Nédélec (1980; Nédélec (1986.

The fact that $\mathbf{u}_h^*$ is well defined follows from the projection of the so-called BDM method. The fact that $\mathbf{u}_h^*$ lies in $\boldsymbol{H}(\mathrm{div},\Omega)$ is a consequence of the first equation defining the postprocessing and from the fact that $\widehat{\boldsymbol{u}}_h$ is single valued. Finally, the fact that the divergence of $\mathbf{u}_h^*$ is zero follows from the third equation defining the approximation. Indeed, we have, for all $Q\in Q(K)$,

$$\begin{aligned}(\nabla\cdot\mathbf{u}_h^*,q)_K&=-(\mathbf{u}_h^*,\nabla q)_K+\langle\mathbf{u}_h^*\cdot\boldsymbol{n}_K,q\rangle_{\partial K}\\&=-(\boldsymbol{u}_h,\nabla q)_K+\langle\widehat{\boldsymbol{u}}_h\cdot\boldsymbol{n}_K,q\rangle_{\partial K}\\&=0.\end{aligned}$$

It is not difficult to show that this new approximation to the velocity has the same convergence properties than the original approximation, that is,

$$\|\boldsymbol{u}-\mathbf{u}_h^*\|_{L^2(\Omega)}\le C\,h^{k+1},$$

when the exact solution is smooth enough and whenever $k\ge1$.

6.4.3. Divergence-free superconvergent velocities by local postprocessing. The following postprocessing was introduced in Cockburn et al. (2011 and, in three-space dimensions, is

Encyclopedia of Computational Mechanics. Edited by Erwin Stein, René de Borst and Thomas J.R. Hughes.
 ISBN: 0-470-84699-2

defined as follows. On the tetrahedron $K \in \mathcal{T}_h$, $\mathbf{u}_h^*$ is defined as the element of $\boldsymbol{\mathcal{P}}_{k+1}(K)$ such that

$$\langle (\mathbf{u}_h^* - \widehat{\boldsymbol{u}}_h) \cdot \boldsymbol{n}, \mu \rangle_F = 0 \quad \forall\, \mu \in \mathcal{P}_k(F), \tag{10a}$$

$$\langle (\boldsymbol{n} \times \nabla)(\mathbf{u}_h^* \cdot \boldsymbol{n}) - \boldsymbol{n} \times (\{\mathrm{L}_h^t\}\boldsymbol{n}), (\boldsymbol{n} \times \nabla)\mu \rangle_F = 0 \quad \forall\, \mu \in \mathcal{P}_{k+1}(F)^{\perp}, \tag{10b}$$

for all faces F of K, and such that

$$(\mathbf{u}_h^* - \boldsymbol{u}_h, \nabla w)_K = 0 \quad \forall\, w \in \mathcal{P}_k(K), \tag{10c}$$

$$(\nabla \times \mathbf{u}_h^* - \mathbf{w}_h, (\nabla \times \boldsymbol{v})\, \mathrm{B}_K)_K = 0 \quad \forall\, \boldsymbol{v} \in \boldsymbol{\mathcal{S}}_k(K). \tag{10d}$$

Here

$$\mathcal{P}_{k+1}(F)^{\perp} := \{\mu \in \mathcal{P}_{k+1}(F) \,:\, \langle \mu, \widetilde{\mu} \rangle_F = 0, \quad \forall \widetilde{\mu} \in \mathcal{P}_k(F)\},$$

the operator $\mathbf{n} \times \nabla$ is the tangential gradient and the function $\{\mathrm{L}_h^t\}$ is the single-valued function on $\mathcal{E}_h$ equal to $((\mathrm{L}_h^t)^+ + (\mathrm{L}_h^t)^-)/2$ on the set $\mathcal{E}_h \setminus \partial\Omega$ and equal to L_h^t on $\partial\Omega$. Moreover,

$$\mathbf{w}_h := (\mathrm{L}_{32\,h} - \mathrm{L}_{23\,h}, \mathrm{L}_{13\,h} - \mathrm{L}_{31\,h}, \mathrm{L}_{21\,h} - \mathrm{L}_{12\,h})$$

is the approximation to the vorticity. This elementwise post-processing has many properties we gather in the following result.

The fact that $\mathbf{u}_h^*$ is well defined and that it is a divergence-free function in $\boldsymbol{H}(\mathrm{div}, \Omega)$ can be proven exactly as in the previous case. In Cockburn et al. (2011, it has been shown that we also have

$$\|\boldsymbol{u} - \mathbf{u}_h^*\|_{L^2(\Omega)} \leq C\, h^{k+2},$$

when the exact solution is smooth enough and whenever $k \geq 1$.

6.4.4. Using $\mathbf{H}(\mathrm{div}, \Omega)$*-conforming divergence-free velocity spaces.* It is very well known that the construction of finite dimensional spaces of divergence-free velocities functions is, in practice, impossible due to the many inter-element continuity constraints that need to be imposed; see Thomasset (1981; Hecht (1981; Scott and Vogelius (1985. This difficulty can completely be bypassed by a simple technique called *hybridization*. Roughly speaking, it consists two steps. In the first step, we remove the continuity constraints of the interelement normal component of the space of velocities. In this way, the new space of velocities is completely discontinuous across elements. In the second step, we restore the above interelement constraints, but only for the approximation of the velocity. In this manner, only locally divergence-free approximations need to be constructed. The technique was introduced in Carrero et al. (2006 for DG methods and then in Cockburn and Gopalakrishnan (2005a; Cockburn and Gopalakrishnan (2005b for a classical mixed method. See also the reviews Cockburn and Gopalakrishnan (2005c; Cockburn (2009. This hybridization technique coincides with the way in which the HDG methods are devised. Thus, HDG methods using divergence-free, globally divergence-free velocities are very easy to define.

6.5. Extensions

Although we have used a velocity gradient-velocity-pressure formulation of the Stokes system, we could have used others using, for example, the symmetric gradient of the velocity or the

Encyclopedia of Computational Mechanics. Edited by Erwin Stein, René de Borst and Thomas J.R. Hughes.
 ISBN: 0-470-84699-2

vorticity instead of the velocity gradient. Numerical experiments carried out in Nguyen et al. (2010a for the HDG method show that the formulation using the velocity gradient is superior to that of the symmetric gradient which in turn is better than that of the vorticity; see also Cockburn and Cui (2012a; Cockburn and Cui (2012b. The use of the velocity gradient formulation does not allow in a natural way the imposition of the normal stress as a boundary condition. This problem has been partially addressed in Nguyen et al. (2011, but although the optimal convergence of all the variables was retained, the superconvergence of the velocity is lost.

In defining the HDG methods, we have used as data of the local problems the velocity at the boundary and the average on the pressure in the element. However, this is certainly not the only way to define the local problems. For example, an **HDG** method based on the vorticty formulation was studied in Cockburn and Gopalakrishnan (2009. The very same method can be obtained in four different ways according to what are the data of the local problems. Each of these ways can be thought as a different way of implementing the method.

7. Convection-dominated Problems

In this section, we consider the application of the DG method to various problems in fluid dynamics in which convection plays a dominant role. We start with the convection-diffusion and the shallow water equations. We then consider the equations of incompressible and compressible fluid flow. To obtain the DG methods, we simply have to combine the DG discretization techniques for the equations for the corresponding purely hyperbolic problems with those of the purely elliptic equations. Since the discretizations are straightforward, we only discuss important features of the discretization not previously considered.

7.1. Convection-diffusion problems

In this section, we consider the LDG methods for the following convection-diffusion model problem

$$\begin{aligned} u_t + \nabla \cdot (\boldsymbol{f}(u) - a(u)\nabla u) &= 0 \quad \text{in } \Omega \times (0,T) \\ u(x,0) &= u_0(x) \quad \forall x \in \Omega \end{aligned}$$

To define a DG method, we first notice that, since the matrix $a(u)$ is assumed to be symmetric and semipositive definite, there exists a symmetric matrix $b(u)$ such that $a = b^2$. This allows us to introduce the auxiliary variable $\boldsymbol{q} = b\,\nabla u$, and rewrite the model problem as follows:

$$\begin{gathered} u_t + \nabla \cdot f(u) - \nabla \cdot (b(u)\boldsymbol{q}) = 0 \quad \text{in } \Omega \times (0,T) \\ q_i = \nabla \cdot \boldsymbol{g}_i(u) \quad \text{in } \Omega \times (0,T), \quad 1 \le i \le N \\ u(x,0) = u_0(x) \quad \forall\, x \in \Omega \end{gathered}$$

where q_i is the $i-$th component of the vector $\boldsymbol{q}$, and $\boldsymbol{g}_i(u)$ is the vector whose jth component is $\int^u b_{ji}(s)\mathtt{d}s$. A DG method is now obtained in a most straightforward way. For details, see

Encyclopedia of Computational Mechanics. Edited by Erwin Stein, René de Borst and Thomas J.R. Hughes.
 ISBN: 0-470-84699-2

Cockburn and Shu (1998a and Cockburn and Dawson (2000.

Let us give a computational result of the application of the LDG method to the two-dimensional flow and transport in shallow water from the paper by Aizinger and Dawson (2003; see also Dawson and Proft (2002; Dawson and Proft (2003; Dawson and Proft (2004. The system of shallow water equations can be written as

$$\boldsymbol{c}_t + \nabla \cdot (\boldsymbol{A} + (D\nabla)\boldsymbol{c}) = \boldsymbol{h}(\boldsymbol{c})$$

where $\boldsymbol{c}^t = (\xi, u, v)$; here, ξ is the deflection of the air-water interface from the mean sea level, and (u, v) is the depth-averaged horizontal velocity. For details about the remaining terms, see Aizinger and Dawson (2003. What is relevant for our purposes is that the above is a nonlinear convection-diffusion-reaction equation which can be easily discretized by the LDG method. In Figure 33, we see a mesh (top) of 14 269 triangles, highly graded towards the coast, and the function ξ (bottom) computed for a high inflow of $35\,000\,\mathrm{m}^3\,\mathrm{s}^{-1}$ for the Mississippi River; an open sea boundary condition is assumed. In comparison with the no-inflow situation (not shown here), the elevation increases about half a foot near the lower Louisiana coast.

A posteriori error estimates have been obtained, for example, by Baccouch and Adjerid (2015. Error estimates of LDG methods using implicit-explicit time-marching schemes was carried out by Wang et al. (2015; Wang et al. (2016.

The definition of HDG methods for steady-state convection-diffusion problems is straightforward. For details, see Cockburn et al. (2009a and Nguyen et al. (2009a, where linear convection was considered, and Nguyen et al. (2009b, where nonlinear convection was treated. When the diffusion dominates, the convergence properties of the methods are those of the purely diffusive case whereas when the convection dominates. In particular, the superconvergence of scalar variable can be recovered. When convection dominates, the method behaves like the original DG method as shown by Fu et al. (2015. See also Egger and Schöberl (2010, where a mixed method is used to approximate the second-order elliptic term. An space-time HDG method for the advection-diffusion equation on moving and deforming meshes was proposed by Rhebergen and Cockburn (2013.

7.2. Oseen flow

Next, let us consider the Oseen equations of incompressible fluid flow, namely,

$$\begin{aligned} -\nu\Delta\boldsymbol{u} + (\mathbf{w}\cdot\nabla)\boldsymbol{u} + \gamma\,\boldsymbol{u} + \nabla p &= \boldsymbol{f} \quad \text{in } \Omega \\ \nabla\cdot\boldsymbol{u} &= 0 \quad \text{in } \Omega \\ \boldsymbol{u} &= \boldsymbol{g} \quad \text{on } \Gamma \end{aligned}$$

where $\boldsymbol{u}$ is the velocity, p the pressure, $\boldsymbol{f} \in L^2(\Omega)^2$ a prescribed external body force, $\nu > 0$ the kinematic viscosity, $\mathbf{w}$ a convective velocity field and γ a given scalar function. As usual, we take Ω to be a bounded domain of $\mathbb{R}^2$ with boundary $\Gamma = \partial\Omega$, and the Dirichlet datum

Encyclopedia of Computational Mechanics. Edited by Erwin Stein, René de Borst and Thomas J.R. Hughes.
 ISBN: 0-470-84699-2

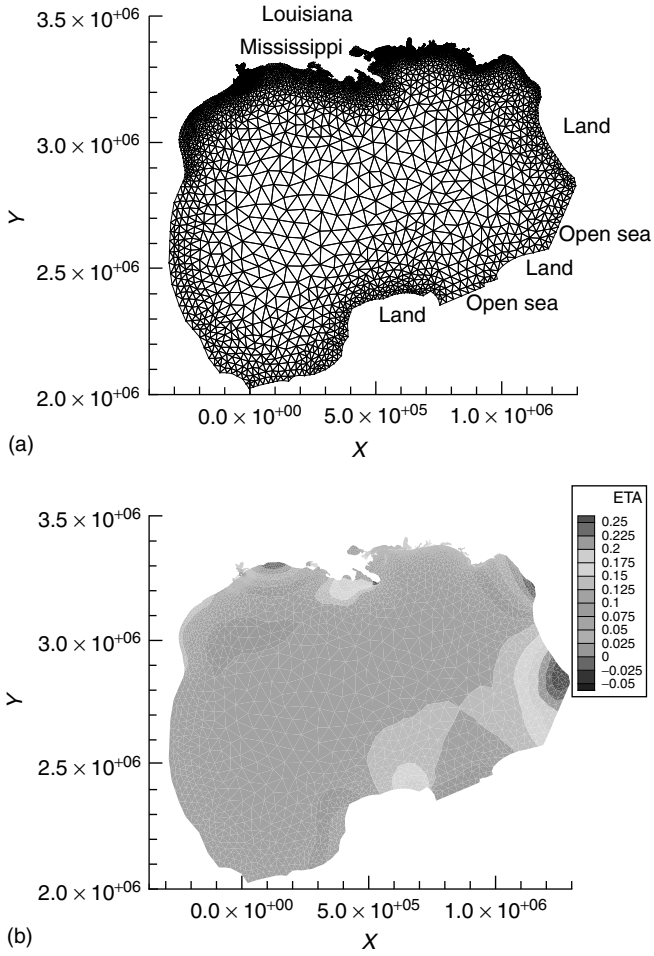

Figure 33. Gulf of Mexico mesh (a) and surface elevation for high inflow of the Mississippi river (b). (From Aizinger V and Dawson CN. *A Discontinuous Galerkin Method for Two-Dimensional Flow and Transport in Shallow Water*. Technical Report 03-16, TICAM, 2003.)

$\boldsymbol{g} \in H^{1/2}(\Gamma)^2$ to satisfy the compatibility condition $\int_\Gamma \boldsymbol{g} \cdot \boldsymbol{n} \mathrm{d}s = 0$, where $\boldsymbol{n}$ denotes the unit outward normal vector to Γ. We also assume that

$$\gamma(\boldsymbol{x}) - \tfrac{1}{2}\nabla \cdot \mathbf{w}(\boldsymbol{x}) =: \gamma_0(\boldsymbol{x}) \geq 0, \quad \boldsymbol{x} \in \Omega \tag{11}$$

This condition guarantees the existence and uniqueness of a solution $(\boldsymbol{u}, p) \in H^1_g(\Omega)^2 \times L^2_0(\Omega)$ where $H^1_g(\Omega)^2 := \{\boldsymbol{u} \in H^1(\Omega)^2 : \boldsymbol{u}|_\Gamma = \boldsymbol{g}\}$ and $L^2_0(\Omega) := \{p \in L^2(\Omega) : \int_\Omega p \mathrm{d}x = 0\}$.

In Figure 34, we display the norms of the error in the velocity and the pressure for the LDG method as a function of the mesh size for several Reynolds numbers for the so-called Kovasznay flow. Bi-quadratic approximations on squares are used. The norms are scaled with

Encyclopedia of Computational Mechanics. Edited by Erwin Stein, René de Borst and Thomas J.R. Hughes.
 ISBN: 0-470-84699-2

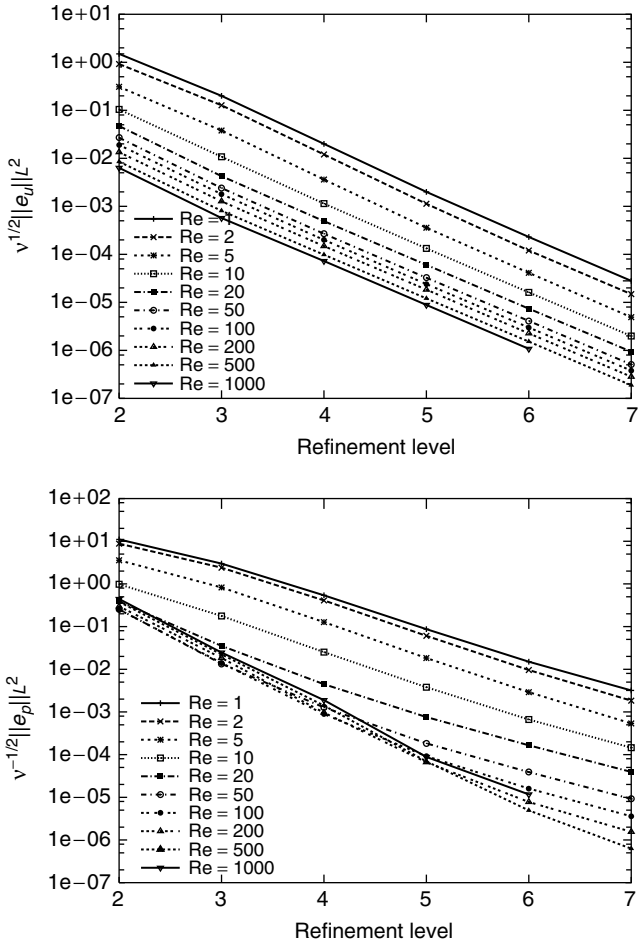

Figure 34. Scaled L^2-errors in $\boldsymbol{u}$ and p with bilinear approximations for different Reynolds numbers. (From Cockburn B, Kanschat G and Schötzau D. Local discontinuous Galerkin methods for the Oseen equations. *Math. Comput.* 2004; **73**:569-593.)

the appropriate powers of ν so as the make all the quantities dimensionally equivalent - see Cockburn et al. (2004 for details. We can see that the convergence of the above errors is not altered as the Reynolds number varies from 1 to 1000 which confirms the expected robustness of the LDG method with respect to an increase in the strength of the convection.

Encyclopedia of Computational Mechanics. Edited by Erwin Stein, René de Borst and Thomas J.R. Hughes.

7.3. The Navier-Stokes of equations incompressible flow

Here, we consider DG methods for the stationary incompressible Navier-Stokes equations

$$\begin{aligned} \mathrm{L} - \nabla \mathbf{u} &= 0 && \text{in } \Omega, \\ -\nu \nabla \cdot \mathrm{L} + \nabla \cdot (\mathbf{u} \otimes \mathbf{u}) + \nabla p &= \mathbf{f} && \text{in } \Omega, \\ \nabla \cdot \mathbf{u} &= 0 && \text{in } \Omega, \\ (p, 1)_\Omega &= 0, \\ \mathbf{u} &= \mathbf{u}_D && \text{on } \partial\Omega, \end{aligned}$$

where $\langle \mathbf{u}_D \cdot \boldsymbol{n}, 1 \rangle_{\partial\Omega} = 0$. Since the only difference with the Oseen equations is the nonlinear convective term, we restrict our discussion to the DG discretization of such a term. The emphasis will be placed on how to obtain (provable) $\boldsymbol{H}^1$-bounded DG methods which are also locally conservative.

7.3.1. $\mathbf{H}^1$*-boundedness, local conservativity and incompressibility.* Témam (1966; Témam (1968, see also Témam (1979, proposed a way to discretize the nonlinear convective term of the Navier-Stokes equations, $\nabla \cdot (\mathbf{u} \otimes \mathbf{u})$. It consists in *replacing* the convective nonlinear term by the term

$$\nabla \cdot (\mathbf{u} \otimes \mathbf{u}) - \frac{1}{2} (\nabla \cdot \mathbf{u})\, \mathbf{u}.$$

This approach became the approach of choice in the finite element literature because it allowed to obtain the $\boldsymbol{H}^1$-boundedness of the approximate velocity without requiring that it be exactly divergence free. The first DG method for the Navier-Stokes equations proposed by Karakashian and Jureidini (1998, which also uses divergence-free polynomial approximations of the velocity inside each element, and the method proposed by Girault et al. (2005 use this classic approach. The only drawback is that, unlike all other DG methods, these methods cannot achieve local conservativity because the above nonlinear term does not have divergence form.

As pointed out by Cockburn et al. (2005, this difficulty can be overcome by simply *replacing* the pressure p by the new unknown $P := p - \frac{1}{2}|\mathbf{u}|^2$. Indeed, in this case the nonlinear term, namely,

$$\nabla \cdot (\mathbf{u} \otimes \mathbf{u}) + \frac{1}{2} \nabla |\mathbf{u}|^2$$

is in divergence form. Hence, locally conservative (and $\boldsymbol{H}^1$-bounded) DG methods can be obtained. The drawback is, however, that the new unknown P does not have a clear physical interpretation.

Yet another possibility to achieve $\boldsymbol{H}^1$-boundedness and local conservativity is to rewrite the Navier-Stokes equations as the Oseen problem

$$\begin{aligned} -\nu \Delta \mathbf{u} + (\mathbf{w} \cdot \nabla)\, \mathbf{u} + \nabla p &= \mathbf{f} && \text{in } \Omega, \\ \nabla \cdot \mathbf{u} &= 0 && \text{in } \Omega, \\ \mathbf{u} &= \mathbf{0} && \text{on } \Gamma, \end{aligned}$$

Encyclopedia of Computational Mechanics. Edited by Erwin Stein, René de Borst and Thomas J.R. Hughes.
 ISBN: 0-470-84699-2

where $\mathbf{w} = \mathbf{u}$. It is known that, for $\boldsymbol{f}$ small enough, the sequence sequence $\{\mathbf{u}^n\}_{n\in\mathbb{N}}$, where $\mathbf{u}^{n+1}$ is the solution of the above Oseen problem with $\mathbf{w} = \mathbf{u}^n$. The limit is thus a solution of the Navier-Stokes equations. Thus, at the discrete level, the idea is to use an approximation for $\mathbf{u}$ and another for $\mathbf{w}$ which should be *globally* divergence free. This can be achieved by an elementwise postprocessing as pointed out in the previous section. The resulting method is both $\boldsymbol{H}^1$-bounded and local conservative.

7.3.2. Examples. DG methods for the Navier-Stokes can be obtained by combining a DG method for the Stokes system with an approximation of the nonlinear convective terms. The corresponding convergence properties are usually identical. Recall that to define a DG method for the Stokes system, it is enough to choose a DG method for a scalar second-order elliptic problem (to discretize the terms associated to the viscosity) and to choose to weakly or strongly impose the divergence-free condition. Let us give some examples:

• The DG method by Karakashian and Jureidini (1998; Karakashian and Katsaounis (2000 extend the IP method DG method by Baker et al. (1990 using locally divergence-free velocities. It approximates the nonlinear terms by using Témam's approach. Similarly, the main DG method proposed by Girault et al. (2005 extends the IP method and also approximates the nonlinear terms by using Témam's approach.

• The method by Crivellini et al. (2013 is an extension of the DG method by Bassi et al. (2006.

• The hybrid method by Montlaur et al. (2010 extends the hybrid method by Montlaur et al. (2008; since it uses exactly divergence-free velocities, it can discretize directly the nonlinear term $\nabla \cdot (\mathbf{u} \otimes \mathbf{u})$.

• The LDG methods by Cockburn et al. (2005; Cockburn et al. (2007; Cockburn et al. (2009d extend the LDG methods by Cockburn et al. (2002 and use the last of the above-mentioned approaches to discretize the nonlinearity. Similarly, the LDG method by Schötzau et al. (2003a extends the LDG method in Schötzau et al. (2003b.

• The so-called Galerkin interface stabilisation (GIS) method Labeur and Wells (2007; Labeur and Wells (2012 does not quite fit the general form of the HDG methods considered here. It is is, in part, an extension of the multiscale DG method by Bochev et al. (2006; Hughes et al. (2006; Buffa et al. (2006. It approximates the nonlinear convective term by directly discretizing the term

$$\nabla \cdot (\mathbf{u} \otimes \mathbf{u}) - (1 - \chi)(\nabla \cdot \mathbf{u})\, \mathbf{u},$$

where $\chi \in [0, 1]$. Interestingly enough, the method is actually $\boldsymbol{H}^1$-bounded even though its approximate velocities are not exactly divergence free. If the trace spaces are continuous, the numerical traces of the method are no longer single-valued, as is typical of the multiscale DG method.

• The superconvergent HDG method by Nguyen et al. (2010c; Nguyen et al. (2011 extends

Encyclopedia of Computational Mechanics. Edited by Erwin Stein, René de Borst and Thomas J.R. Hughes.
 ISBN: 0-470-84699-2

the superconvergent HDG method for Stokes by Nguyen et al. (2010b also by using last of the above-mentioned approaches to discretize the nonlinearity. (An HDG method was proposed and analyzed by Cesmelioglu et al. (2013.) Space-time HDG methods were considered in Rhebergen and Cockburn (2012; Rhebergen et al. (2013.

• The HDG method by Lehrenfeld and Schöberl (2015 extends the method using the Lehrenfeld-Schöberl stabilization function introduced by Lehrenfeld (2010; since it uses exactly divergence-free velocities, it can discretize directly the nonlinear term $\nabla \cdot (\mathbf{u} \otimes \mathbf{u})$.

• The staggered DG method by Cheung et al. (2015 extends the corresponding method for the Stokes system by Kim et al. (2013. It employs an exactly divergence-free approximation of the velocity but its discretization of the nonlinear convection does not quite fit our general framework.

7.4. The compressible Navier-Stokes equations of fluid flow

To end this section, we consider the compressible Navier-Stokes equations:

$$\begin{aligned} \varrho_t + (\varrho\, v_j)_{,j} &= 0 \\ (\varrho\, v_i)_t + (\varrho\, v_i\, v_j - \sigma_{ij})_{,j} &= f_i \\ (\varrho\, e)_t + (\varrho\, e\, v_j - \sigma_{ij}\, v_i + q_i)_{,j} &= f_i\, v_i \end{aligned}$$

where ϱ is the density, v the velocity, e the internal energy, and f the external body forces. The viscous stress σ and the heat flux q are given by

$$\begin{aligned} \sigma_{ij} &= (-p + \lambda\, v_{i,i})\, \delta_{ij} + \mu\, (v_{i,j} + v_{j,i}) \\ q_i &= -\kappa\, T_{,i} \end{aligned}$$

where p is the pressure and T the temperature.

To obtain a DG method, we first rewrite the equations as

$$\begin{aligned} \boldsymbol{q} - \nabla \boldsymbol{u} &= 0 \qquad \text{in } \Omega \times (0,T), \\ \partial_t \boldsymbol{u} + \nabla \cdot (\boldsymbol{F}(\boldsymbol{u}) + \boldsymbol{G}(\boldsymbol{u}, \boldsymbol{q})) &= 0 \qquad \text{in } \Omega \times (0,T), \end{aligned}$$

where $\boldsymbol{G}(\boldsymbol{u}, \boldsymbol{q})$ are the viscous fluxes. We then can use a space-time, or a semidiscrete DG discretization of these equations by properly choosing the convective fluxes and the viscous fluxes as sketched in the previous sections. A suitable time-marching scheme has then to be applied to the semidiscretization. For example, see the high-order accurate implicit Runge-Kutta methods in Montlaur et al. (2011.

7.4.1. Examples of DG methods. There are many DG methods for the compressible Navier-Stokes equations. Let us mention a few to give an idea.

The first DG method for the compressible Navier-Stokes equations was proposed by Bassi and Rebay (1997a. Based on the work by Bassi and Rebay (1997a and by Cockburn and

Encyclopedia of Computational Mechanics. Edited by Erwin Stein, René de Borst and Thomas J.R. Hughes.
 ISBN: 0-470-84699-2

Shu (1998a, a DG method for the compressible Navier-Stokes equations was proposed by Lomtev and Karniadakis (1999. A DG method based on the IP discretization of the second-order operators was proposed by Hartmann and Houston (2002b. A space-Time Discontinuous Galerkin method for the compressible Navier-Stokes were proposed by Klaij et al. (2006. The compact discontinuous Galerkin method Peraire and Persson (2008 has also been applied to compressible viscous flows Persson and Peraire (2008 and turbulent flows Nguyen et al. (2007. More recently, an HDG methods was developed by Peraire et al. (2010. Its EDG version was explored in Nguyen et al. (2015. A hybrid mixed method for the compressible Navier-Stokes equations was proposed by Schütz and May (2013. Adjoint-based error estimation and mesh adaptation using HDG methods were explored by Woopen et al. (2014. A high-order discontinuous Galerkin discretization with multiwavelet-based grid adaptation for compressible flows was explored by Gerhard et al. (2015.

For time-marching methods for DG methods for compressible flow, see Nigro et al. (2014a; Nigro et al. (2014b; Bassi et al. (2015. For implicit high-order DG methods DNS and implicit LES of turbulent flows see Bassi et al. (2016.

Domain decomposition preconditioners have been explored by Giani and Houston (2014. And p-multigrid discontinuous Galerkin solver in Ghidoni et al. (2014.

7.4.2. Some numerical examples. We present some numerical experiments obtained by using the LDG method developed by Lomtev and Karniadakis (1999. We present some numerical results for the compressible Navier-Stokes equations, In Figure 35, we show a steady state calculation of the laminar Mach 0.8 flow around a NACA 0012 airfoil with Reynolds number 73. No limiter was applied.

Another example is a time-dependent computation of the flow around a cylinder in two space dimensions. The Reynolds number is 10 000 and the Mach number 0.2. In Figure 36, we see the detail of a mesh of 680 triangles (with curved sides fitting the cylinder) and polynomials whose degree could vary from element to element; the maximum degree was 5. Note how the method is able to capture the shear layer instability observed experimentally.

We end by presenting the application of the HDG method by Peraire et al. (2010 to the Reynolds-averaged Navier-Stokes equations, see Spalart and Allmaras (1994, in Figure 7.4.2. We also show its application to the Euler equations in Figure 7.4.2.

8. Concluding remarks and bibliographic notes

Most of the material in this article has been taken from the monograph by Cockburn (1999, from the reviews by Cockburn and Shu (2001; Cockburn (2003; Cockburn and Shi (2014 and from the short essay by Cockburn (2015. The references do not pretend to be exhaustive.

Encyclopedia of Computational Mechanics. Edited by Erwin Stein, René de Borst and Thomas J.R. Hughes.
 ISBN: 0-470-84699-2

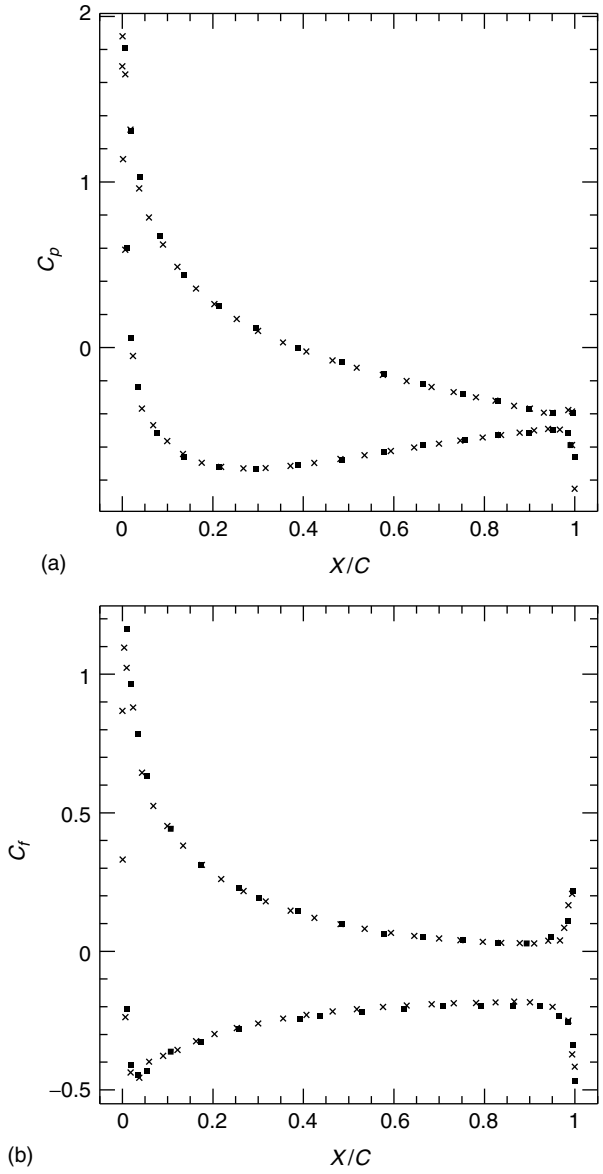

Figure 35. Pressure (a) and drag (b) coefficient distributions. The squares were obtained by using polynomials of degree 3 by Bassi F and Rebay S. A high-order accurate discontinuous finite element method for the numerical solution of the compressible Navier-Stokes equations. *J. Comput. Phys.* 1997a; **131**:267-279; and the crosses by using polynomials of degree 6 by Lomtev I and Karniadakis GE. A discontinuous Galerkin method for the Navier-Stokes equations. *Int. J. Numer. Methods Fluids* 1999; **29**:587-603.

Encyclopedia of Computational Mechanics. Edited by Erwin Stein, René de Borst and Thomas J.R. Hughes.
 ISBN: 0-470-84699-2

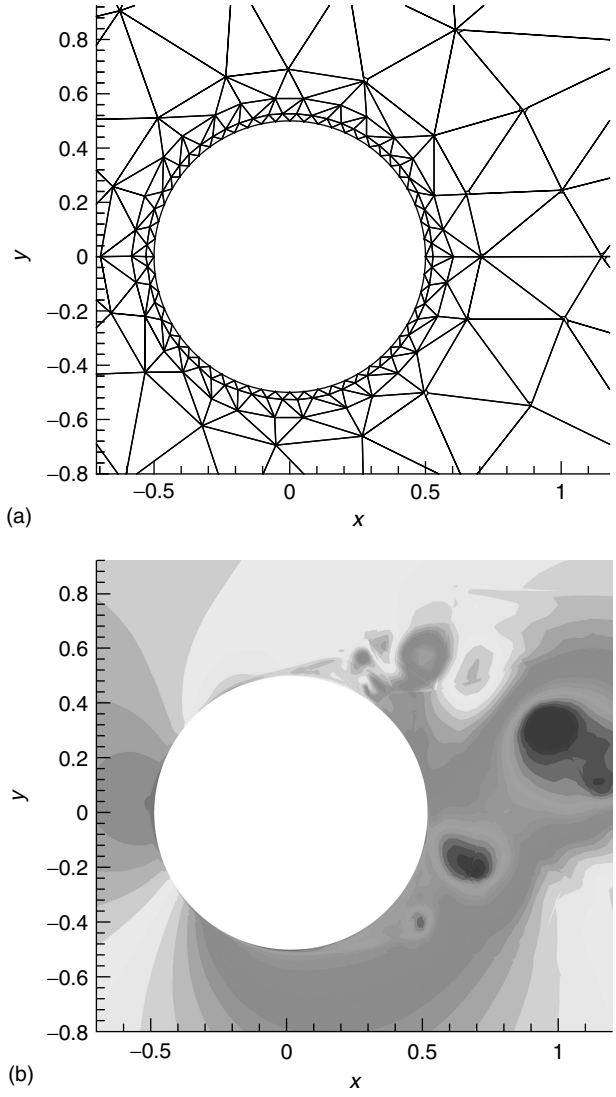

Figure 36. Flow around a cylinder with Reynolds number 10 000 and Mach number 0.2. Detail of the mesh (a) and density (b) around the cylinder. (From Lomtev I and Karniadakis GE. A discontinuous Galerkin method for the Navier-Stokes equations. *Int. J. Numer. Methods Fluids* 1999; **29**:587-603.)

Encyclopedia of Computational Mechanics. Edited by Erwin Stein, René de Borst and Thomas J.R. Hughes.
 ISBN: 0-470-84699-2

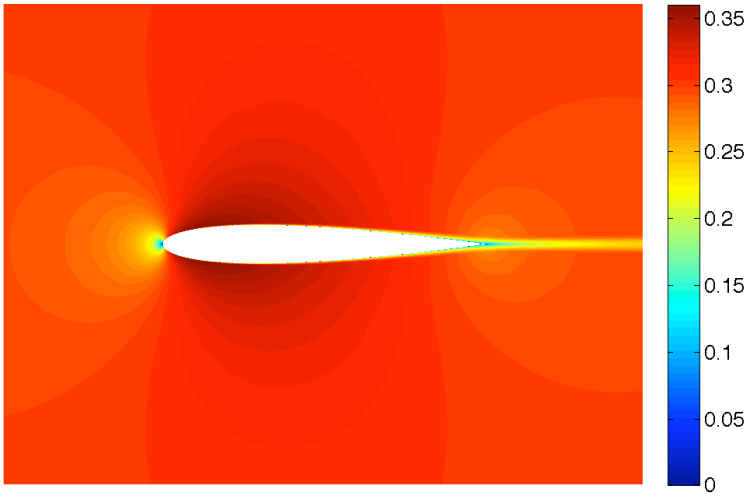

Figure 37. Reynolds-averaged Navier-Stokes equations over the NACA 0012 airfoil at Mach number 0.3, Reynolds number 1.85 millions, and 0 angle of attack. Mach number contour plot provided by the HDG method with $k = 4$. Courtesy of Ngoc-Cuong Nguyen.

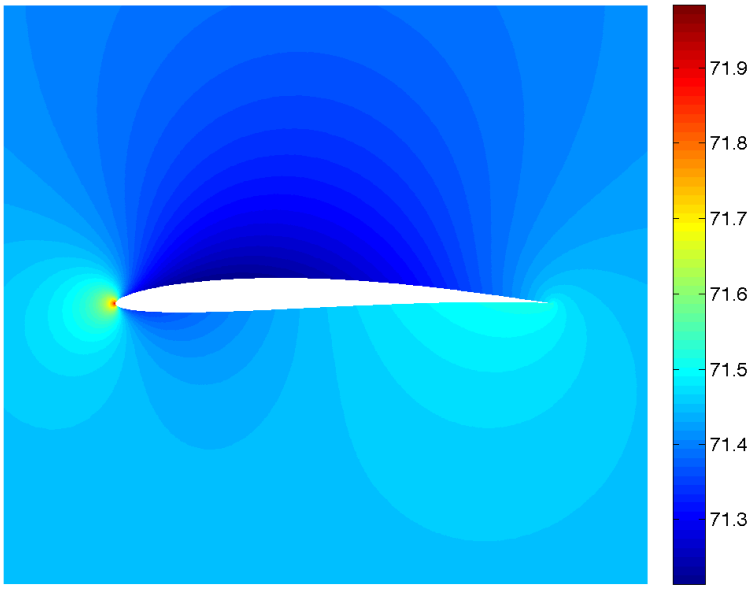

Figure 38. Euler equations over the Trefftz airfoil at Mach number 0.2 and 0 angle of attack. Pressure contour plot provided by the EDG method with $k = 4$. Courtesy of Ngoc-Cuong Nguyen.

Encyclopedia of Computational Mechanics. Edited by Erwin Stein, René de Borst and Thomas J.R. Hughes.
 ISBN: 0-470-84699-2

For a history of the development of DG methods up to 1999, see Cockburn et al. (2000. For a theory of DG methods for Friedrichs' systems, see Ern and Guermond (2006a; Ern and Guermond (2006b; Ern and Guermond (2008; see also a systematic way of picking the corresponding numerical traces by Bui-Thanh (2015. See also the reviews by Cheng and Shu (2013; Shu (2014 and the monograph by Shu (2009. For books on DG methods, see Di-Pietro and Ern (2012, Hesthaven and Warburton (2008, Kanschat (2008, Li (2006, and Rivière (2008.

9. Related Chapters

(*See also* Finite Element Methods, Finite Volume Methods: Foundation and Analysis; Multiscale and Stabilized Methods)

Acknowledgments

The author would like to thank Thomas Hughes for the kind invitation to write this paper. Concerning the first edition, the author would like to thank the many colleagues that provided most of the figures in this paper: Francesco Bassi, Paul Castillo, Nicolas Chauvegeon, Clint Dawson, Paul Houston, Igor Lomtev, Guido Kanschat, George Karniadakis, Manoj Prasad, Stefano Rebay, Chi-Wang Shu, Jaap van der Vegt and Harmen van der Ven. Thanks are also due to Paul Houston for a careful reading of the paper. Finally, the author would like to thank Clint Dawson, Guido Kanschat, Paul Houston, Dominik Schötzau and Harmen van der Ven for useful feedback on the first version of the manuscript. Concerning the second edition, the author would like to thank Ngoc-Cuong Nguyen, Jiguang Shen, Chi-Wang Shu and Xiongxiang Zhang for providing new figures, and to Mauricio Flores, Ilaria Perugia and Jennifer Ryan for providing bibliographic material.

REFERENCES

S. Adjerid and M. Baccouch (2012). A superconvergent local discontinuous Galerkin method for elliptic problems. *J. Sci. Comput.*, 52(1):113–152.

S. Adjerid and T.C. Massey (2002). A posteriori discontinuous finite element error estimation for two-dimensional hyperbolic problems. *Comput. Methods Appl. Mech. Engrg.*, 191:5877–5897.

S. Adjerid and I. Mechai (2014). A superconvergent discontinuous Galerkin method for hyperbolic problems on tetrahedral meshes. *J. Sci. Comput.*, 58(1):203–248.

Encyclopedia of Computational Mechanics. Edited by Erwin Stein, René de Borst and Thomas J.R. Hughes.
 ISBN: 0-470-84699-2

S. Adjerid and T. Weinhart (2011). Discontinuous Galerkin error estimation for linear symmetrizable hyperbolic systems. *Math. Comp.*, 80(275):1335–1367.

S. Adjerid and T. Weinhart (2014). Asymptotically exact discontinuous Galerkin error estimates for linear symmetric hyperbolic systems. *Appl. Numer. Math.*, 76:101–131.

M. Ainsworth (2004). Dispersive and dissipative behaviour of high order discontinuous Galerkin finite element methods. *J. Comput. Phys.*, 198(1):106–130.

M. Ainsworth (2007). A posteriori error estimation for discontinuous Galerkin finite element approximation. *SIAM J. Numer. Anal.*, 44:1777–1798.

M. Ainsworth and R. Rankin (2010). Fully computable error bounds for discontinuous Galerkin finite element approximations on meshes with an arbitrary number of levels of hanging nodes. *SIAM J. Numer. Anal.*, 46:4112–4141.

V. Aizinger and C.N. Dawson (2003). A Discontinuous Galerkin Method for two-dimensional flow and transport in shallow water. Technical Report 03-16, TICAM.

V. Aizinger, C.N. Dawson, B. Cockburn and P. Castillo (2000). Local discontinuous Galerkin method for contaminant transport. *Advances in Water Resources*, 24:73–87.

P. Alotto, A. Bertoni, I. Perugia and D. Schötzau (2001). Discontinuous Finite Element Methods for the Simulation of Rotating Electrical Machines. *COMPEL*, 20:448–462.

P. F. Antonietta, S. Giani and P. Houston (2014). Domain decomposition preconditioners for discontinuous Galerkin methods for elliptic problems on complicated domains. *J. Sci. Comput.*, 60(1):203–227.

D. N. Arnold (1982). An interior penalty finite element method with discontinuous elements. *SIAM J. Numer. Anal.*, 19:742–760.

D. N. Arnold and F. Brezzi (1985). Mixed and nonconforming finite element methods: implementation, postprocessing and error estimates. *RAIRO Modél. Math. Anal. Numér.*, 19:7–32.

D. N. Arnold, F. Brezzi, B. Cockburn and L. D. Marini (2002). Unified analysis of discontinuous Galerkin methods for elliptic problems. *SIAM J. Numer. Anal.*, 39:1749–1779.

H.L. Atkins and C.-W. Shu (1998). Quadrature-free implementation of discontinuous Galerkin methods for hyperbolic equations. *AIAA Journal*, 36.

I. Babuška and M. Zlámal (1973). Nonconforming elements in the finite element method with penalty. *SIAM J. Numer. Anal.*, 10:863–875.

M. Baccouch and S. Adjerid (2015). A posteriori local discontinuous Galerkin error estimation for two-dimensional convection-diffusion problems. *J. Sci. Comput.*, 62(2):399–430.

G. A. Baker (1977). Finite element methods for elliptic equations using nonconforming elements. *Math. Comp.*, 31:45–59.

G. A. Baker, W.N. Jureidini and O. A. Karakashian (1990). Piecewise solenoidal vector fields and the Stokes problem. *SIAM J. Numer. Anal.*, 27:1466–1485.

G. E. Barter and D. L. Darmofal (2010). Shock capturing with PDE-based artificial viscosity for DGFEM. I. Formulation. *J. Comput. Phys.*, 229(5):1810–1827.

Encyclopedia of Computational Mechanics. Edited by Erwin Stein, René de Borst and Thomas J.R. Hughes.
 ISBN: 0-470-84699-2

T. Barth (2000). Simplified DG methods for systems of conservation laws with convex extension. In Cockburn, B., Karniadakis, G., and Shu, C.-W., editors, *Discontinuous Galerkin Methods. Theory, Computation and Applications*, volume 11 of *Lect. Notes Comput. Sci. Engrg.*, pages 63–75, Berlin. Springer Verlag.

F. Bassi, L. Botti, A. Colombo, A. Crivellini, A. Ghidoni and F. Massa (2016). On the development of an implicit high-order Discontinuous Galerkin method for DNS and implicit LES of turbulent flows. *Eur. J. Mech. B Fluids*, 55(part 2):367–379.

F. Bassi, L. Botti and A. Colombo, A. Ghidoni and F. Massa (2015). Linearly implicit Rosenbrock-type Runge-Kutta schemes applied to the discontinuous Galerkin solution of compressible and incompressible unsteady flows. *Comput. & Fluids*, 118:305–320.

F. Bassi, A. Crivellini, D. A. Di-Pietro and S. Rebay (2006). An artificial compressibility flux for the discontinuous Galerkin solution of the incompressible Navier-Stokes equation. *J. Comput. Phys.*, 218:794–815.

F. Bassi and S. Rebay (1997a). A high-order accurate discontinuous finite element method for the numerical solution of the compressible Navier-Stokes equations. *J. Comput. Phys.*, 131:267–279.

F. Bassi and S. Rebay (1997b). High-order accurate discontinuous finite element solution of the 2D Euler equations. *J. Comput. Phys.*, 138:251–285.

F. Bassi, S. Rebay, G. Mariotti, S. Pedinotti and M. Savini (1997). A High-Order Accurate Discontinuous Finite Element Method for Inviscid and Viscous Turbomachinery Flows. In Decuypere, R. and Dibelius, G., editors, *2nd European Conference on Turbomachinery Fluid Dynamics and Thermodynamics*, pages 99–108, Antwerpen, Belgium. Technologisch Instituut.

P. Bastian and B. Rivière (2003). Superconvergence and $H(\mathrm{div})$ projection for discontinuous Galerkin methods. *Internat. J. Numer. Methods Fluids*, 42:1043–1057.

C. E. Baumann and J. T. Oden (1999). A discontinuous *hp*-finite element method for convection-diffusion problems. *Comput. Methods Appl. Mech. Engrg.*, 175:311–341.

R. Becker, P. Hansbo and M. G. Larson (2003). Energy norm a posteriori error estimation for discontinuous Galerkin methods. *Comput. Methods Appl. Mech. Engrg.*, 192:723–733.

K.S. Bey (1994). *An hp-adaptive discontinuous Galerkin method for hyperbolic conservation laws.* PhD thesis, The University of Texas at Austin.

K.S. Bey and J. T. Oden (1996). *hp*-version discontinuous Galerkin methods for hyperbolic conservation laws. *Comput. Methods Appl. Mech. Engrg.*, 133:259–286.

R. Biswas, K.D. Devine and J.E. Flaherty (1994). Parallel, adaptive finite element methods for conservation laws. *Appl. Numer. Math.*, 14:255–283.

P. B. Bochev, J. T. R. Hughes and G. Scovazzi (2006). A multiscale discontinuous Galerkin method. In I. Lirkov, S. M. and Waśniewski, J., editors, *Large-scale scientific computing*, volume 3743 of *Lecture Notes in Comput. Sci.*, pages 84–93. Springer-Verlag Berlin Heidelberg.

A. Bonito and R. H. Nochetto (2010). Quasi-optimal convergence rate of an adaptive discontinuous Galerkin method. *SIAM J. Numer. Anal.*, 48(2):734–771.

Encyclopedia of Computational Mechanics. Edited by Erwin Stein, René de Borst and Thomas J.R. Hughes.
 ISBN: 0-470-84699-2

J. H. Bramble and A. H. Schatz (1977). Higher order local accuracy by averaging in the finite element method. *Math. Comp.*, 31:94–111.

F. Brezzi, B. Cockburn, L. D. Marini and E. Süli (2006). Stabilization mechanisms in discontinuous Galerkin finite element methods. *Comput. Methods Appl. Mech. Engrg.*, 195:3293–3310. C. Dawson, Ed.

F. Brezzi, J. Douglas, Jr. and L. D. Marini (1985). Two families of mixed finite elements for second order elliptic problems. *Numer. Math.*, 47:217–235.

F. Brezzi, G. Manzini, L. D. Marini, P. Pietra and A. Russo (1999). Discontinuous finite elements for diffusion problems. In *in Atti Convegno in onore di F. Brioschi (Milan 1997)*, pages 197–217. Istituto Lombardo, Accademia di Scienze e Lettere.

F. Brezzi, G. Manzini, L. D. Marini, P. Pietra and A. Russo (2000). Discontinuous Galerkin Approximations for elliptic Problems. *Numer. Methods Partial Differential Equations.*, 16:365–378.

A. Buffa, T. J. R. Hughes and G. Sangalli (2006). Analysis of a multiscale discontinuous Galerkin method for convection-diffusion problems. *SIAM J. Numer. Anal.*, 44:1420–1440 (electronic).

T. Bui-Thanh (2015). From Godunov to a unified hybridized discontinuous Galerkin framework for partial differential equations. *J. Comput. Phys.*, 295:114–146.

A. Burbeau, P. Sagaut and Ch.-H. Bruneau (2001). A problem-independent limiter for high-order Runge-Kutta discontinuous Galerkin methods. *J. Comput. Phys.*, 169:111–150.

R. Bustinza, G.N. Gatica and B. Cockburn (2005). An a posteriori error estimate for the local discontinuous Galerkin method applied to linear and nonlinear diffusion problems. *J. Sci. Comput.*, 22/23:147–185.

A. Cangiani, E. H. Georgoulis and P. Houston (2014). *hp*-version discontinuous Galerkin methods on polygonal and polyhedral meshes. *Math. Models Methods Appl. Sci.*, 24(10):2009–2041.

J. Carrero, B. Cockburn and D. Schötzau (2006). Hybridized, globally divergence-free LDG methods. Part I: The Stokes problem. *Math. Comp.*, 75:533–563.

C. Carstensen, T. Gudi and M. Jensen (2009). A unifying theory of a posteriori error control for discontinuous Galerkin FEM. *Numer. Math.*, 112:363–379.

E. Casoni, J. Peraire and A. Huerta (2013). One-dimensional shock-capturing for high-order discontinuous Galerkin methods. *Internat. J. Numer. Methods Fluids*, 71(6):737–755.

P. Castillo (2002). Performance of discontinuous Galerkin methods for elliptic PDE's. *SIAM J. Sci. Comput.*, 24:524–547.

P. Castillo (2005). An a posteriori error estimate for the local discontinuous Galerkin method. *J. Sci. Comput.*, 22/23:187–204.

P. Castillo, B. Cockburn, I. Perugia and D. Schötzau (2000). An a priori error analysis of the local discontinuous Galerkin method for elliptic problems. *SIAM J. Numer. Anal.*, 38:1676–1706.

P. E. Castillo (2010). Stencil reduction algorithms for the local discontinuous Galerkin method. *Internat. J. Numer. Methods Engrg.*, 81(12):1475–1491.

Encyclopedia of Computational Mechanics. Edited by Erwin Stein, René de Borst and Thomas J.R. Hughes.
 ISBN: 0-470-84699-2

P. E. Castillo and F. A. Sequeira (2013). Computational aspects of the local discontinuous Galerkin method on unstructured grids in three dimensions. *Math. Comput. Modelling*, 57(9-10):2279–2288.

F. Celiker and B. Cockburn (2007). Superconvergence of the numerical traces of discontinuous Galerkin and hybridized mixed methods for convection-diffusion problems in one space dimension. *Math. Comp.*, 76:67–96.

A. Cesmelioglu, B. Cockburn, N.-C. Nguyen and J. Peraire (2013). Analysis of HDG methods for Oseen equations. *J. Sci. Comput.*, 55(2):392–431.

B. Chabaud and B. Cockburn (2012). Uniform-in-time superconvergence of HDG methods for the heat equation. *Math. Comp.*, 81:107–129.

Y. Chen and B. Cockburn (2012). Analysis of variable-degree HDG methods for Convection-Diffusion equations. Part I: General nonconforming meshes. *IMA J. Num. Anal.*, 32:1267–1293.

Y. Chen and B. Cockburn (2014). Analysis of variable-degree HDG methods for Convection-Diffusion equations. Part II: Semimatching nonconforming meshes. *Math. Comp.*, 83:87–111.

Z. Chen and H. Chen (2004). Pointwise error estimates of discontinuous Galerkin methods with penalty for second-order elliptic problems. *SIAM J. Numer. Anal.*, 42(3):1146–1166 (electronic).

J. Cheng and C.-W. Shu (2013). Recent developments on the Lagrangian and remapping methods for compressible fluid flows. In *Numerical methods for hyperbolic equations: theory and applications*, pages 9–19. CRC Press/Balkema, Leiden.

S. W. Cheung, E. T. Chung, H. H. Kim and Y. Qian (2015). Staggered discontinuous Galerkin methods for the incompressible Navier-Stokes equations. *J. Comput. Phys.*, 302:251–266.

E. T. Chung, B. Cockburn and G. Fu (2014). The staggered DG method is the limit of a hybridizable DG method. *SIAM J. Numer. Anal.*, 52:915–932.

E. T. Chung, B. Cockburn and G. Fu (2016). The staggered DG method is the limit of a hybridizable DG method. Part II: The Stokes flow. *J. Sci. Comput.*, 66(2):870–887.

E. T. Chung and B. Engquist (2009). Optimal discontinuous Galerkin methods for the acoustic wave equation in higher dimensions. *SIAM J. Numer. Anal.*, 47(5):3820–3848.

S. Cochez-Dhondt and S. Nicaise (2008). Equilibrated error estimators for discontinuous Galerkin methods. *Numer. Methods Partial Differential Equations.*, 24:1236–1252.

B. Cockburn (1999). Discontinuous Galerkin Methods for Convection-Dominated Problems. In Barth, T. and Deconink, H., editors, *High-Order Methods for Computational Physics*, volume 9 of *Lect. Notes Comput. Sci. Engrg.*, pages 69–224. Springer Verlag, Berlin.

B. Cockburn (2001). Devising discontinuous Galerkin methods for non-linear hyperbolic conservation laws. *Journal of Computational and Applied Mathematics*, 128:187–204.

B. Cockburn (2003). Discontinuous Galerkin Methods. *ZAMM Z. Angew. Math. Mech.*, 83:731–754.

B. Cockburn (2009). Two new techniques for generating exactly incompressible approximate velocities. In Deconinck, H. and Dick, E., editors, *Computational Fluid Dynamics 2006.*

Encyclopedia of Computational Mechanics. Edited by Erwin Stein, René de Borst and Thomas J.R. Hughes.
 ISBN: 0-470-84699-2

Proceedings of the Fourth International Conference in Fluid Dynamics, ICCDF4, Ghent, Belgium, 10-14 July 2006, pages 1–11. Springer Verlag.

B. Cockburn (2015). Static condensation, hybridization, and the devising of the HDG methods. In G.R. Barrenechea, F. Brezzi, A. C. and Georgulis, E., editors, *Building Bridges: Connections and Challenges in Modern Approaches to Numerical Partial Differential Equations*, volume 114 of *Lect. Notes Comput. Sci. Engrg.*, pages 1–45. Springer Verlag, Berlin. LMS Durham Symposia funded by the London Mathematical Society. Durham, U.K., on July 8–16, 2014.

B. Cockburn and J. Cui (2012a). An analysis of HDG methods for the vorticity-velocity-pressure formulation of the Stokes problem in three dimensions. *Math. Comp.*, 81:1355–1368.

B. Cockburn and J. Cui (2012b). Divergence-Free HDG Methods for the Vorticity-Velocity Formulation of the Stokes Problem. *J. Sci. Comput.*, 52:256–270.

B. Cockburn and C. Dawson (2000). Some extensions of the local discontinuous Galerkin method for convection-diffusion equations in multidimensions. In Whiteman, J., editor, *The Proceedings of the Conference on the Mathematics of Finite Elements and Applications: MAFELAP X*, pages 225–238. Elsevier.

B. Cockburn and C. Dawson (2002). Approximation of the velocity by coupling discontinuous Galerkin and mixed finite element methods for flow problems. *Comput. Geosci. (Special issue: Locally Conservative Numerical Methods for Flow in Porous Media)*, 6:502–522.

B. Cockburn, D. A. Di-Pietro and A. Ern (2015). Bridging the Hybrid High-Order and Hybridizable Discontinuous Galerkin Methods. *ESAIM Math. Model. Numer. Anal.* to appear.

B. Cockburn and B. Dong (2007). An analysis of the minimal dissipation local discontinuous Galerkin method for convection-diffusion problems. *J. Sci. Comput.*, 32:233–262.

B. Cockburn and B. Dong and J. Guzmán (2008a). Optimal convergence of the original DG method for the transport-reaction equation on special meshes. *SIAM J. Numer. Anal.*, 46:1250–1265.

B. Cockburn and B. Dong and J. Guzmán (2008b). A superconvergent LDG-hybridizable Galerkin method for second-order elliptic problems. *Math. Comp.*, 77:1887–1916.

B. Cockburn, B. Dong, J. Guzmán and J. Qian (2010a). Optimal convergence of the original DG method on special meshes for variable convective velocity. *SIAM J. Numer. Anal.*, 48(1):133–146.

B. Cockburn, B. Dong, J. Guzmán, M. Restelli and R. Sacco (2009a). Superconvergent and optimally convergent LDG-hybridizable discontinuous Galerkin methods for convection-diffusion-reaction problems. *SIAM J. Sci. Comput.*, 31:3827–3846.

B. Cockburn, O. Dubois, J. Gopalakrishnan and S. Tan (2014). Multigrid for an HDG method. *IMA J. Numer. Anal.*, 34(4):1386–1425.

B. Cockburn and G. Fu (2016a). Superconvergence by M-decompositions. Part II: Construction of two-dimensional finite elements. *Modél. Math. Anal. Numér.* To appear.

B. Cockburn and G. Fu (2016b). Superconvergence by M-decompositions. Part III: Construction of three-dimensional finite elements. *Modél. Math. Anal. Numér.* To appear.

Encyclopedia of Computational Mechanics. Edited by Erwin Stein, René de Borst and Thomas J.R. Hughes.
 ISBN: 0-470-84699-2

B. Cockburn, G. Fu and W. Qiu (2016a). A note on the devising of superconvergent HDG methods for Stokes flow by M-decompositions. *IMA J. Num. Anal.* To appear.

B. Cockburn, G. Fu and F.-J. Sayas (2016b). Superconvergence by M-decompositions. Part I: General theory for HDG methods for diffusion. *Math. Comp.* to appear.

B. Cockburn and J. Gopalakrishnan (2005a). Incompressible finite elements via hybridization. Part I: The Stokes system in two space dimensions. *SIAM J. Numer. Anal.*, 43:1627–1650.

B. Cockburn and J. Gopalakrishnan (2005b). Incompressible finite elements via hybridization. Part II: The Stokes system in three space dimensions. *SIAM J. Numer. Anal.*, 43:1651–1672.

B. Cockburn and J. Gopalakrishnan (2005c). New hybridization techniques. *GAMM Mitt. Ges. Angew. Math. Mech.*, 2:154–183.

B. Cockburn and J. Gopalakrishnan (2009). The derivation of hybridizable discontinuous Galerkin methods for Stokes flow. *SIAM J. Numer. Anal.*, 47:1092–1125.

B. Cockburn, J. Gopalakrishnan and J. Guzmán (2010b). A new elasticity element made for enforcing weak stress symmetry. *Math. Comp.*, 79:1331–1349.

B. Cockburn, J. Gopalakrishnan and R. Lazarov (2009b). Unified Hybridization of discontinuous Galerkin, mixed and continuous Galerkin methods for second order elliptic problems. *SIAM J. Numer. Anal.*, 47:1319–1365.

B. Cockburn, J. Gopalakrishnan, F. Li, N.-C. Nguyen and J. Peraire (2010c). Hybridization and postprocessing techniques for mixed eigenfunctions. *SIAM J. Numer. Anal.*, 48:857–881.

B. Cockburn, J. Gopalakrishnan, N. C. Nguyen, J. Peraire and F.-J. Sayas (2011). Analysis of an HDG method for Stokes flow. *Math. Comp.*, 80:723–760.

B. Cockburn, J. Gopalakrishnan and F.-J. Sayas (2010d). A projection-based error analysis of HDG methods. *Math. Comp.*, 79:1351–1367.

B. Cockburn and P.-A. Gremaud (1996). Error estimates for finite element methods for nonlinear conservation laws. *SIAM J. Numer. Anal.*, 33:522–554.

B. Cockburn and J. Guzmán (2008). Error estimates for the Runge-Kutta discontinuous Galerkin method for the transport equation with discontinuous initial data. *SIAM J. Numer. Anal.*, 46:1364–1398.

B. Cockburn, J. Guzmán, S.-C. Soon and H.K. Stolarski (2009c). An analysis of the embedded discontinuous Galerkin method for second-order elliptic problems. *SIAM J. Numer. Anal.*, 47:2686–2707.

B. Cockburn, S. Hou and C.-W. Shu (1990). TVB Runge-Kutta Local Projection Discontinuous Galerkin Finite Element Method for Conservation Laws IV: The Multidimensional Case. *Math. Comp.*, 54:545–581.

B. Cockburn, G. Kanschat, I. Perugia and D. Schötzau (2001). Superconvergence of the local discontinuous Galerkin method for elliptic problems on Cartesian grids. *SIAM J. Numer. Anal.*, 39:264–285.

B. Cockburn, G. Kanschat and D. Schötzau (2004). Local discontinuous Galerkin methods for the Oseen equations. *Math. Comp.*, 73:569–593.

Encyclopedia of Computational Mechanics. Edited by Erwin Stein, René de Borst and Thomas J.R. Hughes.
 ISBN: 0-470-84699-2

B. Cockburn, G. Kanschat and D. Schötzau (2005). A locally conservative LDG method for the incompressible Navier-Stokes equations. *Math. Comp.*, 74:1067–1095.

B. Cockburn, G. Kanschat and D. Schötzau (2007). A note on discontinuous Galerkin divergence-free solutions of the Navier-Stokes equations. *J. Sci. Comput.*, 31:61–73.

B. Cockburn, G. Kanschat and D. Schötzau (2009d). An equal-order DG method for the incompressible Navier-Stokes equations. *J. Sci. Comput.*, 40:141–187.

B. Cockburn, G. Kanschat, D. Schötzau and C. Schwab (2002). Local discontinuous Galerkin methods for the Stokes system. *SIAM J. Numer. Anal.*, 40:319–343.

B. Cockburn, G.E. Karniadakis and C.-W. Shu (2000). The development of discontinuous Galerkin methods. In Cockburn, B., Karniadakis, G., and Shu, C.-W., editors, *Discontinuous Galerkin Methods. Theory, Computation and Applications*, volume 11 of *Lect. Notes Comput. Sci. Engrg.*, pages 3–50, Berlin. Springer Verlag.

B. Cockburn, M. Luskin, C.-W. Shu and E. Süli (2003). Enhanced accuracy by post-processing for finite element methods for hyperbolic equations. *Math. Comp.*, 72:577–606 (electronic).

B. Cockburn and R. H. Nochetto and W. Zhang (2016c). Contraction property of adaptive hybridizable discontinuous Galerkin methods. *Math. Comp.*, 85(299):1113–1141.

B. Cockburn and W. Qiu (2014). Commuting diagrams for the TNT elements on cubes. *Math. Comp.*, 83:603–633.

B. Cockburn, W. Qiu and K. Shi (2012a). Conditions for superconvergence of HDG methods for second-order eliptic problems. *Math. Comp.*, 81:1327–1353.

B. Cockburn, W. Qui and K. Shi (2012b). Conditions for superconvergence of HDG methods on curvilinear elements for second-order eliptic problems. *SIAM J. Numer. Anal.*, 50:1417–1432.

B. Cockburn and F.-J. Sayas (2014). Divergence–conforming HDG methods for Stokes flow. *Math. Comp.*, 83:1571–1598.

B. Cockburn, F.-J. Sayas and M. Solano (2012c). Coupling at a distance HDG and BEM. *SIAM J. Sci. Comput.*, 34:A28–A47.

B. Cockburn and Shen, Jiguang (2016). A Hybridizable Discontinuous Galerkin Method for the p-Laplacian. *SIAM J. Sci. Comput.*, 38(1):A545–A566.

B. Cockburn and K. Shi (2014). Devising HDG methods for Stokes flow: An overview. *Computers & Fluids*, 98:221–229.

B. Cockburn and C.-W. Shu (1998a). The local Discontinuous Galerkin Method for time-dependent convection-diffusion systems. *SIAM J. Numer. Anal.*, 35:2440–2463.

B. Cockburn and C.-W. Shu (1998b). The Runge-Kutta Discontinuous Galerkin Finite Element Method for Conservation Laws V: Multidimensional Systems. *J. Comput. Phys.*, 141:199–224.

B. Cockburn and C.-W. Shu (2001). Runge-Kutta Discontinuous Galerkin Methods for convection-dominated problems. *J. Sci. Comput.*, 16:173–261.

B. Cockburn and W. Zhang (2012). A posteriori error estimates for HDG methods. *J. Sci. Comput.*, 51(3):582–607.

Encyclopedia of Computational Mechanics. Edited by Erwin Stein, René de Borst and Thomas J.R. Hughes.
 ISBN: 0-470-84699-2

B. Cockburn and W. Zhang (2013). A posteriori error analysis for hybridizable discontinuous Galerkin methods for second order elliptic problems. *SIAM J. Numer. Anal.*, 51:676–693.

E. Creusé and S. Nicaise (2010). A posteriori error estimator based on gradient recovery by averaging for discontinuous Galerkin methods. *J. Comput. Appl. Math.*, 234:2903–2915.

A. Crivellini, V. D'Alessandro and F. Bassi (2013). Assessment of a high-order discontinuous Galerkin method for incompressible three-dimensional Navier-Stokes equations: benchmark results for the flow past a sphere up to Re = 500. *Comput. & Fluids*, 86:442–458.

S. Curtis, R. M. Kirby, J. K. Ryan and C.-W. Shu (2007/08). Postprocessing for the discontinuous Galerkin method over nonuniform meshes. *SIAM J. Sci. Comput.*, 30(1):272–289.

C. Dawson and J. Proft (2002). Discontinuous and coupled continuous/discontinuous Galerkin methods for the shallow water equations. *Comput. Methods Appl. Mech. Engrg.*, 191(41-42):4721–4746.

C. Dawson and J. Proft (2003). Discontinuous/continuous Galerkin methods for coupling the primitive and wave continuity equations of shallow water. *Comput. Methods Appl. Mech. Engrg.*, 192(47-48):5123–5145.

C. Dawson and J. Proft (2004). Coupled discontinuous and continuous Galerkin finite element methods for the depth-integrated shallow water equations. *Comput. Methods Appl. Mech. Engrg.*, 193(3-5):289–318.

K.D. Devine and J.E. Flaherty (1996). Parallel adaptive *hp*-refinement techniques for conservation laws. *Appl. Numer. Math.*, 20:367–386.

K.D. Devine, J.E. Flaherty, R.M. Loy and S.R. Wheat (1995). Parallel partitioning strategies for the adaptive solution of conservation laws. In Babuška, I., Flaherty, J., Henshaw, W., Hopcroft, J., Oliger, J., and Tezduyar, T., editors, *Modeling, mesh generation, and adaptive numerical methods for partial differential equations*, volume 75 of *The IMA Volumes in Mathematics and its Applications*, pages 215–242, New York, New York. Sringer-Verlag.

D. A. Di-Pietro and A. Ern (2012). *Mathematical aspects of discontinuous Galerkin methods*, volume 69 of *Mathématiques & Applications (Berlin) [Mathematics & Applications]*. Springer, Heidelberg.

D. A. Di-Pietro and A. Ern (2015). A hybrid high-order locking-free method for linear elasticity on general meshes. *Comput. Meth. Appl. Mech. Engrg.*, 283:1–21.

M. Dubiner (1991). Spectral Methods on Triangles and Other Domains. *J. Sci. Comp.*, 6:345–390.

Y. Efendiev, R. Lazarov and K. Shi (2015). A multiscale HDG method for second order elliptic equations. Part I. Polynomial and homogenization-based multiscale spaces. *SIAM J. Numer. Anal.*, 53(1):342–369.

H. Egger and J. Schöberl (2010). A hybrid mixed discontinuous Galerkin finite-element method for convection-diffusion problems. *IMA J. Numer. Anal.*, 30(4):1206–1234.

A. Ern and J. L. Guermond (2006a). Discontinuous Galerkin Methods for Friedrichs' Systems. I. General theory. *SIAM J. Numer. Anal.*, 44:753–778.

Encyclopedia of Computational Mechanics. Edited by Erwin Stein, René de Borst and Thomas J.R. Hughes.
 ISBN: 0-470-84699-2

A. Ern and J.-L. Guermond (2006b). Discontinuous Galerkin methods for Friedrichs' systems. II. Second-order elliptic PDEs. *SIAM J. Numer. Anal.*, 44(6):2363–2388.

A. Ern and J.-L. Guermond (2008). Discontinuous Galerkin methods for Friedrichs' systems. III. Multifield theories with partial coercivity. *SIAM J. Numer. Anal.*, 46(2):776–804.

A. Ern, S. Nicaise and M. Vohralík (2007). An accurate **H**(div) flux reconstruction for discontinuous Galerkin approximations of elliptic problems. *C. R. Math. Acad. Sci. Paris*, 345:709–712.

R.S. Falk and G.R. Richter (1999). Explicit finite element methods for symmetric hyperbolic equations. *SIAM J. Numer. Anal.*, 36:935–952.

X. Feng and O. A. Karakashian (2001). Two-level non-overlapping Schwarz methods for a discontinuous Galerkin method. *SIAM J. Numer. Anal.*, 39:1343–1365 (electronic).

J.E. Flaherty, R.M. Loy, C. Özturan, M.S. Shephard, B.K. Szymanski, J.D. Teresco and L.H. Ziantz (1998). Parallel Structures and Dynamic Load Balancing for Adaptive Finite Element Computation. *Appl. Numer. Math.*, 26:241–265.

J.E. Flaherty, R.M. Loy, M.S. Shephard, M.L. Simone, B.K. Szymanski , J.D. Teresco and L.H. Ziantz (1999). Distributed Octree Data Structures and Local Refinement Method for the Parallel Solution of Three-Dimensional Conservation Laws. In Bern, M., Flaherty, J., and Luskin, M., editors, *Grid Generation and Adaptive Algorithms*, volume 113 of *The IMA Volumes in Mathematics and its Applications*, pages 113–134, Minneapolis. Institute for Mathematics and its Applications, Springer.

J.E. Flaherty, R.M. Loy, M.S. Shephard, B.K. Szymanski, J.D. Teresco and L.H. Ziantz (1997). Adaptive local refinement with octree load-balancing for the parallel solution of three-dimensional conservation laws. *J. Parallel and Dist. Comput.*, 47:139–152.

J.E. Flaherty, R. Loy, M.S. Shephard and J. Teresco (2000). Software for the parallel adaptive solution of conservation laws by a discontinuous Galerkin method. In Cockburn, B., Karniadakis, G., and Shu, C.-W., editors, *Discontinuous Galerkin Methods. Theory, Computation and Applications*, volume 11 of *Lect. Notes Comput. Sci. Engrg.*, pages 113–123, Berlin. Springer Verlag.

B. M. Fraejis de Veubeke (1977). Displacement and equilibrium models in the finite element method. In Zienkiewicz, O. and Holister, G., editors, *Stress Analysis*, pages 145–197. Wiley, New York.

K.O. Friedrichs (1958). Symmetric positive linear differential equations. *Comm. Pure and Appl. Math.*, 11:333–418.

G. Fu, W. Qiu and W. Zhang (2015). An analysis of HDG methods for convection-dominated diffusion problems. *ESAIM Math. Model. Numer. Anal.*, 49(1):225–256.

L. Gastaldi and R. H. Nochetto (1989). Sharp maximum norm error estimates for general mixed finite element approximations to second order elliptic equations. *RAIRO Modél. Math. Anal. Numér.*, 23:103–128.

N. Gerhard, F. Iacono, G. May, S. Müller and R. Schäfer (2015). A high-order discontinuous Galerkin discretization with multiwavelet-based grid adaptation for compressible flows. *J. Sci. Comput.*, 62(1):25–52.

Encyclopedia of Computational Mechanics. Edited by Erwin Stein, René de Borst and Thomas J.R. Hughes.
 ISBN: 0-470-84699-2

A. Ghidoni, A. Colombo, F. Bassi and S. Rebay (2014). Efficient p-multigrid discontinuous Galerkin solver for complex viscous flows on stretched grids. *Internat. J. Numer. Methods Fluids*, 75(2):134–154.

S. Giani and P. Houston (2014). Domain decomposition preconditioners for discontinuous Galerkin discretizations of compressible fluid flows. *Numer. Math. Theory Methods Appl.*, 7(2):123–148.

J. Giesselmann, Ch. Makridakis and T. Pryer (2015). A posteriori analysis of discontinuous Galerkin schemes for systems of hyperbolic conservation laws. *SIAM J. Numer. Anal.*, 53(3):1280–1303.

V. Girault, B. Rivière and M. F. Wheeler (2005). A discontinuous Galerkin method with non-overlapping domain decomposition for the Stokes and Navier-Stokes problems. *Math. Comp.*, 74:53–84.

J. Gopalakrishnan and G. Kanschat (2003a). Application of unified DG analysis to preconditioning DG methods. In Bathe, K., editor, *Proceedings of the Second M.I.T. Conference on Computational Fluid and Solid Mechanics, Cambridge, MA, USA*, pages 1943–1945. Elsevier.

J. Gopalakrishnan and G. Kanschat (2003b). A multilevel discontinuous Galerkin method. *Numer. Math.*, 95:527–550.

J. Gopalakrishnan, F. Li, N.-C. Nguyen and J. Peraire (2015). Spectral approximations by the HDG method. *Math. Comp.*, 84:1037–1059.

S. Gottlieb and C.-W. Shu (1998). Total variation diminishing Runge-Kutta schemes. *Math. Comp.*, 67:73–85.

S. Gottlieb, C.-W. Shu and E. Tadmor (2000). Strong stability preserving high order time discretization methods. *SIAM Rev.*, 43:89–112.

R. J. Guyan (1965). Reduction of Stiffness and Mass Matrices. *J. Am. Inst. Aron. and Astro.*, 3:380.

S. Güzey, B. Cockburn and H.K. Stolarski (2007). The embedded discontinuous Galerkin methods: Application to linear shells problems. *Internat. J. Numer. Methods Engrg.*, 70:757–790.

J. Guzmán (2006). Pointwise error estimates for discontinuous Galerkin methods with lifting operators for elliptic problems. *Math. Comp.*, 75(255):1067–1085 (electronic).

J. Guzmán and B. Rivière (2009). Sub-optimal convergence of non-symmetric discontinuous Galerkin methods for odd polynomial approximations. *J. Sci. Comput.*, 40(1-3):273–280.

P. Hansbo and M.G. Larson (2008). Piecewise divergence-free discontinuous Galerkin methods for Stokes flow. *Comm. Numer. Methods Engrg.*, 24:355–366.

K. Harriman, P. Houston, B. Senior and E. Süli (2003). hp-version discontinuous Galerkin methods with interior penalty for partial differential equations with nonnegative characteristic form. In Shu, C.-W., Tang, T., and Cheng, S.-Y., editors, *Recent advances in scientific computing and partial differential equations (Hong Kong, 2002)*, volume 330 of *Contemp. Math.*, pages 89–119. Amer. Math. Soc., Providence, RI.

Encyclopedia of Computational Mechanics. Edited by Erwin Stein, René de Borst and Thomas J.R. Hughes.
 ISBN: 0-470-84699-2

R. Hartmann and P. Houston (2002a). Adaptive discontinuous Galerkin finite element methods for nonlinear hyperbolic conservation laws. *SIAM J. Sci. Comput.*, 24:979–1004 (electronic).

R. Hartmann and P. Houston (2002b). Adaptive discontinuous Galerkin finite element methods for the compressible Euler equations. *J. Comput. Phys.*, 183:508–532.

F. Hecht (1981). Construction d'une base P_1 non conforme à divergence nulle. *RAIRO Modél. Math. Anal. Numér.*, 15:119–150.

J. S. Hesthaven and T. Warburton (2002). Nodal high-order methods on unstructured grids. I. Time-domain solution of Maxwell's equations. *J. Comput. Phys.*, 181:186–221.

J. S. Hesthaven and T. Warburton (2008). *Nodal discontinuous Galerkin methods*, volume 54 of *Texts in Applied Mathematics*. Springer, New York. Algorithms, analysis, and applications.

R. H. W. Hoppe , G. Kanschat and T. Warburton (2008). Convergence analysis of an adaptive interior penalty discontinuous Galerkin method. *SIAM J. Numer. Anal.*, 47(1).

P. Houston, D. Schötzau and T. P. Wihler (2007). Energy norm a posteriori error estimation of *hp*-adaptive discontinuous Galerkin methods for elliptic problems. *Math. Models Methods Appl. Sci.*, 17:33–62.

P. Houston, C. Schwab and E. Süli (2000). Stabilized *hp*-finite element methods for hyperbolic problems. *SIAM J. Numer. Anal.*, 37:1618–1643.

P. Houston, C. Schwab and E. Süli (2001). *hp*-adaptive discontinuous Galerkin finite element methods for hyperbolic problems. *SIAM J. Sci. Comput.*, 23:1226–1252.

P. Houston, B. Senior and E. Süli (2002). *hp*-discontinuous Galerkin finite element methods for hyperbolic problems: error analysis and adaptivity. *Internat. J. Numer. Methods Fluids*, 40:153–169. ICFD Conference on Numerical Methods for Fluid Dynamics (Oxford, 2001).

P. Houston and E. Süli (2001). *hp*-adaptive discontinuous Galerkin finite element methods for first-order hyperbolic problems. *SIAM J. Sci. Comput.*, 23:1226–1252 (electronic).

X. Y. Hu, N. A. Adams and C.-W. Shu (2013). Positivity-preserving method for high-order conservative schemes solving compressible Euler equations. *J. Comput. Phys.*, 242:169–180.

F. Q. Hu and H. L. Atkins (2002). Eigensolution analysis of the discontinuous Galerkin method with nonuniform grids. I. One space dimension. *J. Comput. Phys.*, 182(2):516–545.

A. Huerta, A. Angeloski, X. Roca and J. Peraire (2013). Efficiency of high-order elements for continuous and discontinuous Galerkin methods. *Internat. J. Numer. Methods Engrg.*, 96(9):529–560.

A. Huerta, E. Casoni and J. Peraire (2012). A simple shock-capturing technique for high-order discontinuous Galerkin methods. *Internat. J. Numer. Methods Fluids*, 69(10):1614–1632.

J. T. R. Hughes, G. Scovazzi, P. B. Bochev and A. Buffa (2006). A multiscale discontinuous Galerkin method with the computational structure of a continuous Galerkin method. *Comput. Methods Appl. Mech. Engrg.*, 195:2761–2787.

Encyclopedia of Computational Mechanics. Edited by Erwin Stein, René de Borst and Thomas J.R. Hughes.
 ISBN: 0-470-84699-2

J. Jaffré, C. Johnson and A. Szepessy (1995). Convergence of the discontinuous Galerkin finite element method for hyperbolic conservation laws. *Mathematical Models & Methods in Applied Sciences*, 5:367–386.

L. Ji, P. van Slingerland, J. K. Ryan and K. Vuik (2014). Superconvergent error estimates for position-dependent smoothness-increasing accuracy-conserving (SIAC) post-processing of discontinuous Galerkin solutions. *Math. Comp.*, 83(289):2239–2262.

L. Ji, Y. Xu and J. K. Ryan (2012). Accuracy-enhancement of discontinuous Galerkin solutions for convection-diffusion equations in multiple-dimensions. *Math. Comp.*, 81(280):1929–1950.

L. Ji, Y. Xu and J. K. Ryan (2013). Negative-order norm estimates for nonlinear hyperbolic conservation laws. *J. Sci. Comput.*, 54(2-3):531–548.

G.-S. Jiang and C.-W. Shu (1994). On a cell entropy inequality for discontinuous Galerkin methods. *Math. Comp.*, 62:531–538.

C. Johnson, U. Nävert and J. Pitkäranta (1984). Finite element methods for linear hyperbolic problems. *Comput. Methods Appl. Mech. Engrg.*, 45:285–312.

C. Johnson and J. Pitkäranta (1986). An analysis of the discontinuous Galerkin method for a scalar hyperbolic equation. *Math. Comp.*, 46:1–26.

M. Juntunen and R. Stenberg (2008). On a mixed discontinuous Galerkin method. *Electron. Trans. Numer. Anal.*, 32:17–32.

G. Kanschat (2003). Preconditioning Methods for local discontinuous Galerkin Discretizations. *SIAM J. Sci. Comp.*, 25:815–831.

G. Kanschat (2008). *Discontinuous Galerkin methods for viscous incompressible flows*. Teubner, Deutscher Universits-Verlag, GWV Fachverlage GmbH, Wiesbaden.

G. Kanschat and R. Rannacher (2002). Local error analysis of the interior penalty discontinuous Galerkin method for second order elliptic problems. *J. Numer. Math.*, 10(4):249–274.

O. A. Karakashian and W.N. Jureidini (1998). A nonconforming finite element method for the stationary Navier-Stokes equations. *SIAM J. Numer. Anal.*, 35:93–120.

O. A. Karakashian and T. Katsaounis (2000). A discontinuous Galerkin method for the incompressible Navier-Stokes equations. In Cockburn, B., Karniadakis, G., and Shu, C.-W., editors, *Discontinuous Galerkin Methods. Theory, Computation and Applications*, volume 11 of *Lect. Notes Comput. Sci. Engrg.*, pages 157–166, Berlin. Springer Verlag.

O. A. Karakashian and F. Pascal (2003). A posteriori error estimates for a discontinuous Galerkin approximation of a second order elliptic problems. *SIAM J. Numer. Anal.*, 41:2374–2399.

O. A. Karakashian and F. Pascal (2007). Convergence of adaptive discontinuous Galerkin approximations of second-order elliptic problems. *SIAM J. Numer. Anal.*, 45(2):641–665 (electronic).

G.E. Karniadakis and S.J. Sherwin (1999). *Spectral/hp Element Methods in CFD*. Oxford University Press.

Encyclopedia of Computational Mechanics. Edited by Erwin Stein, René de Borst and Thomas J.R. Hughes.
 ISBN: 0-470-84699-2

D.S. Kershaw, M.K. Prasad, M.J. Shaw and J.L. Milovich (1998). 3D unstructured mesh ALE hydrodynamics with the upwind discontinuous Galerkin method. *Comput. Methods Appl. Mech. Engrg.*, 158:81–116.

H. H. Kim, E. T. Chung and C. S. Lee (2013). A staggered discontinuous Galerkin method for the Stokes system. *SIAM J. Numer. Anal.*, 51(6):3327–3350.

R.M. Kirby, S.J. Sherwin and B. Cockburn (2012). To HDG or to CG: A comparative study. *J. Sci. Comput.*, 51(1):183–212.

C.M. Klaij, J. J. W. van der Vegt and H. van der Ven (2006). Space-Time Discontinuous Galerkin method for the compressible Navier-Stokes equations. *J. Comput. Phys.*, 217:589–611.

L. Krivodonova (2007). Limiters for high-order discontinuous Galerkin methods. *J. Comput. Phys.*, 226(1):879–896.

L. Krivodonova and R. Qin (2013a). An analysis of the spectrum of the discontinuous Galerkin method. *Appl. Numer. Math.*, 64:1–18.

L. Krivodonova and R. Qin (2013b). An analysis of the spectrum of the discontinuous Galerkin method II: Nonuniform grids. *Appl. Numer. Math.*, 71:41–62.

R. J. Labeur and G. N. Wells (2007). A Galerkin interface stabilisation method for the advection-diffusion and incompressible Navier-Stokes equations. *Comput. Methods Appl. Mech. Engrg.*, 196(49-52):4985–5000.

R. J. Labeur and G. N. Wells (2012). Energy stable and momentum conserving hybrid finite element method for the incompressible Navier-Stokes equations. *SIAM J. Sci. Comput.*, 34(2):A889–A913.

C. Lasser and A. Toselli (2000). An overlapping domain decomposition preconditioner for a class of discontinuous Galerkin approximations of advection-diffusion problems. Technical Report 2000-12, Seminar für Angewandte Mathematik, ETH Zürich.

C. Lehrenfeld (2010). *Hybrid discontinuous Galerkin methods for solving incompressible flow problems*. PhD thesis, Diplomigenieur Rheinisch-Westfalishen Technischen Hochchule Aachen.

C. Lehrenfeld and J. Schöberl (2015). High order exactly divergence-free hybrid discontinuous Galerkin methods for unsteady incompressible flows. *ASC Report No. 27*.

P. Lesaint and P. A. Raviart (1974). On a finite element method for solving the neutron transport equation. In de Boor, C., editor, *Mathematical aspects of finite elements in partial differential equations*, pages 89–145. Academic Press.

B. Q. Li (2006). *Discontinuous finite elements in fluid dynamics and heat transfer*. Computational Fluid and Solid Mechanics. Springer-Verlag London, Ltd., London.

X. Li, J. K. Ryan, R. M. Kirby and C. Vuik (2016). Smoothness-increasing accuracy-conserving (SIAC) filters for derivative approximations of discontinuous Galerkin (DG) solutions over nonuniform meshes and near boundaries. *J. Comput. Appl. Math.*, 294:275–296.

H. Liu and J. Yan (2010). The direct discontinuous Galerkin (DDG) method for diffusion with interface corrections. *Commun. Comput. Phys.*, 8(3):541–564.

Encyclopedia of Computational Mechanics. Edited by Erwin Stein, René de Borst and Thomas J.R. Hughes.
 ISBN: 0-470-84699-2

I. Lomtev and G.E. Karniadakis (1999). A discontinuous Galerkin method for the Navier-Stokes equations. *Int. J. Numer. Meth. Fluids*, 29:587–603.

C. Lovadina and L. D. Marini (2009). A-posteriori error estimates for discontinuous Galerkin approximations of second order elliptic problems. *J. Sci. Comput.*, 40(1-3):340–359.

R.B. Lowrie (1996). *Compact higher-order numerical methods for hyperbolic conservation laws.* PhD thesis, University of Michigan.

R. B. Lowrie, P. L. Roe and B. van Leer (1995). A Space-Time Discontinuous Galerkin Method for the Time-Accurate Numerical Solution of Hyperbolic Conservation Laws. In *Proceedings of the 12th AIAA Computational Fluid Dynamics Conference*. Paper 95-1658.

R. B. Lowrie, P. L. Roe and B. van Leer (1998). Space-Time Methods for Hyperbolic Conservation Laws. In *Barriers and Challenges in Computational Fluid Dynamics*, volume 6 of *ICASE/LaRC Interdisciplinary Series in Science and Engineering*, pages 79–98. Kluwer.

J. Luo, C.-W. Shu and Q. Zhang (2015). *A priori* error estimates to smooth solutions of the third order Runge-Kutta discontinuous Galerkin method for symmetrizable systems of conservation laws. *ESAIM Math. Model. Numer. Anal.*, 49(4):991–1018.

X. Meng, C.-W. Shu and B. Wu (2016). Optimal error estimates for discontinuous Galerkin methods based on upwind-biased fluxes for linear hyperbolic equations. *Math. Comp.*, 85(299):1225–1261.

H. Mirzaee, L. Ji, J. K. Ryan and R. M. Kirby (2011). Smoothness-increasing accuracy-conserving (SIAC) postprocessing for discontinuous Galerkin solutions over structured triangular meshes. *SIAM J. Numer. Anal.*, 49(5):1899–1920.

H. Mirzaee, J. King, J. K. Ryan and R. M. Kirby (2013). Smoothness-increasing accuracy-conserving filters for discontinuous Galerkin solutions over unstructured triangular meshes. *SIAM J. Sci. Comput.*, 35(1):A212–A230.

H. Mirzaee, J. K. Ryan and R. M. Kirby (2014). Smoothness-increasing accuracy-conserving (SIAC) filters for discontinuous Galerkin solutions: application to structured tetrahedral meshes. *J. Sci. Comput.*, 58(3):690–704.

A. Montlaur, S. Fernández-Méndez and A. Huerta (2008). Discontinuous Galerkin methods for the Stokes equations using divergence-free approximations. *Internat. J. Numer. Methods Fluids*, 57(9):1071–1092.

A. Montlaur, S. Fernández-Méndez and A. Huerta (2011). Higher-order implicit Runge-Kutta methods for unsteady incompressible flows. *Rev. Internac. Métod. Numér. Cálc. Diseñ. Ingr.*, 27(1):77–91.

A. Montlaur, S. Fernández-Méndez, J. Peraire and A. Huerta (2010). Discontinuous Galerkin methods for the Navier-Stokes equations using solenoidal approximations. *Internat. J. Numer. Methods Fluids*, 64(5):549–564.

J.-C. Nédélec (1980). Mixed finite elements in $\mathbf{R}^3$. *Numer. Math.*, 35:315–341.

J.-C. Nédélec (1986). A new family of mixed finite elements in $\mathbf{R}^3$. *Numer. Math.*, 50:57–81.

N. C. Nguyen, J. Peraire and B. Cockburn (2009a). An implicit high-order hybridizable discontinuous Galerkin method for linear convection-diffusion equations. *J. Comput. Phys.*, 228:3232–3254.

Encyclopedia of Computational Mechanics. Edited by Erwin Stein, René de Borst and Thomas J.R. Hughes.
 ISBN: 0-470-84699-2

N. C. Nguyen, J. Peraire and B. Cockburn (2009b). An implicit high-order hybridizable discontinuous Galerkin method for nonlinear convection-diffusion equations. *J. Comput. Phys.*, 228:8841–8855.

N. C. Nguyen, J. Peraire and B. Cockburn (2010a). A comparison of HDG methods for Stokes flow. *J. Sci. Comput.*, 45:215–237.

N. C. Nguyen, J. Peraire and B. Cockburn (2010b). A hybridizable discontinuous Galerkin method for Stokes flow. *Comput. Methods Appl. Mech. Engrg.*, 199:582–597.

N. C. Nguyen, J. Peraire and B. Cockburn (2010c). A Hybridizable Discontinuous Galerkin Method for the Incompressible Navier-Stokes Equations (AIAA Paper 2010-362). In *Proceedings of the 48th AIAA Aerospace Sciences Meeting, Exhibit*, Orlando, Florida.

N. C. Nguyen, J. Peraire and B. Cockburn (2011). An implicit high-order hybridizable discontinuous Galerkin method for the incompressible Navier-Stokes equations. *J. Comput. Phys.*, 230:1147–1170.

N. C. Nguyen, J. Peraire and B. Cockburn (2015). A class of embedded discontinuous Galerkin methods for computational fluid dynamics. *J. Comput. Phys.*, 302:674–692.

N. C. Nguyen, P.-O. Persson and J. Peraire (2007). RANS solutions using high order discontinuous Galerkin methods. In *45th. AAIA Aerospace Sciences Meeting and Exhibit, Reno, Nevada,*.

A. Nigro, C. De Bartolo, F. Bassi and A. Ghidoni (2014a). Up to sixth-order accurate A-stable implicit schemes applied to the discontinuous Galerkin discretized Navier-Stokes equations. *J. Comput. Phys.*, 276:136–162.

A. Nigro, A. Ghidoni, S. Rebay and F. Bassi (2014b). Modified extended BDF scheme for the discontinuous Galerkin solution of unsteady compressible flows. *Internat. J. Numer. Methods Fluids*, 76(9):549–574.

M. Ohlberger (2009). A review of a posteriori error control and adaptivity for approximations of non-linear conservation laws. *Internat. J. Numer. Methods Fluids*, 59(3):333–354.

I. Oikawa (2015). A hybridized discontinuous Galerkin method with reduced stabilization. *J. Sci. Comput.*, 65:327–340.

I. Oikawa (2016). Analysis of a Reduced-Order HDG Method for the Stokes Equations. *J. Sci. Comput.*, 67(2):475–492.

S. Osher (1984). Convergence of Generalized MUSCL Schemes. *SIAM J. Numer. Anal.*, 22:947–961.

P. E. Castillo, Paul and E. S. Velázquez (2008). A numerical study of a semi-algebraic multilevel preconditioner for the local discontinuous Galerkin method. *Internat. J. Numer. Methods Engrg.*, 74(2):255–268.

J. Peraire, N. C. Nguyen and B. Cockburn (2010). A Hybridizable Discontinuous Galerkin Method for the compressible Euler and Navier-Stokes Equations (AIAA Paper 2010-363). In *Proceedings of the 48th AIAA Aerospace Sciences Meeting and Exhibit*, Orlando, Florida.

J. Peraire and P.-O. Persson (2008). The compact discontinuous Galerkin (CDG) method for elliptic problems. *SIAM J. Sci. Comput.*, 30(4):1806–1824.

Encyclopedia of Computational Mechanics. Edited by Erwin Stein, René de Borst and Thomas J.R. Hughes.
 ISBN: 0-470-84699-2

P.-O. Persson and J. Peraire (2008). Newton-GMRES preconditioning for discontinuous Galerkin discretizations of the Navier-Stokes equations. *SIAM J. Sci. Comput.*, 30(6):2709–2733.

I. Perugia and D. Schötzau (2001). On the coupling of local discontinuous Galerkin and conforming finite element methods. *J. Sci. Comput.*, 16:411–433.

T. Peterson (1991). A note on the convergence of the Discontinuous Galerkin method for a scalar hyperbolic equation. *SIAM J. Numer. Anal.*, 28:133–140.

T. Qin, C.-W. Shu and Y. Yang (2016). Bound-preserving discontinuous Galerkin methods for relativistic hydrodynamics. *J. Comput. Phys.*, 315:323–347.

J. Qiu and C.-W. Shu (2005). A comparison of troubled-cell indicators for Runge-Kutta discontinuous Galerkin methods using weighted essentially nonoscillatory limiters. *SIAM J. Sci. Comput.*, 27(3):995–1013.

R. Lazarov, S. Repin and S. K. Tomar (2009). Functional a posteriori error estimates for discontinuous Galerkin approximations of elliptic problems. *Numer. Methods Partial Differential Equations.*, 25:952–971.

P. A. Raviart and J. M. Thomas (1977). A mixed finite element method for second order elliptic problems. In Galligani, I. and Magenes, E., editors, *Mathematical Aspects of Finite Element Method, Lecture Notes in Math. 606*, pages 292–315. Springer-Verlag, New York.

W.H. Reed and T.R. Hill (1973). Triangular mesh methods for the neutron transport equation. Technical Report LA-UR-73-479, Los Alamos Scientific Laboratory.

S. Rhebergen and B. Cockburn (2012). A space-time hybridizable discontinuous Galerkin method for incompressible flows on deforming domains. *J. Comput. Phys.*, 231(11):4185–4204.

S. Rhebergen and B. Cockburn (2013). Space-time hybridizable discontinuous Galerkin method for the advection-diffusion equation on moving and deforming meshes. In *The Courant-Friedrichs-Lewy (CFL) condition*, pages 45–63. Birkhäuser/Springer, New York.

S. Rhebergen and B. Cockburn and van der Vegt, Jaap J. W. (2013). A space-time discontinuous Galerkin method for the incompressible Navier-Stokes equations. *J. Comput. Phys.*, 233:339–358.

G.R. Richter (1988). An optimal-order error estimate for the Discontinuous Galerkin method. *Math. Comp.*, 50:75–88.

G. R. Richter (2008). On the order of convergence of the discontinuous Galerkin method for hyperbolic equations. *Math. Comp.*, 77:1871–1885.

B. Rivière (2008). *Discontinuous Galerkin methods for solving elliptic and parabolic equations*, volume 35 of *Frontiers in Applied Mathematics*. Society for Industrial and Applied Mathematics (SIAM), Philadelphia, PA. Theory and implementation.

B. Rivière and M. F. Wheeler (2003). A posteriori error estimates for a discontinuous Galerkin method applied to elliptic problems. Log number: R74. *Comput. Math. Appl.*, 46(1):141–163. *p*-FEM2000: *p* and *hp* finite element methods—mathematics and engineering practice (St. Louis, MO).

Encyclopedia of Computational Mechanics. Edited by Erwin Stein, René de Borst and Thomas J.R. Hughes.
 ISBN: 0-470-84699-2

B. Rivière, M. F. Wheeler and V. Girault (1999). Improved energy estimates for interior penalty, constrained and discontinuous Galerkin methods for elliptic problems. Part I. *Comp. Geosci.*, 3:337–360.

J. Ryan and C.-W. Shu (2003). On a one-sided post-processing technique for the discontinuous Galerkin methods. *Methods and Applications of Analysis*, 10:295–307.

J. K. Ryan and B. Cockburn (2009). Local derivative post-processing for the discontinuous Galerkin method. *J. Comput. Phys.*, 228(23):8642–8664.

J. K. Ryan, X. Li, R. M. Kirby and K. Vuik (2015). One-sided position-dependent smoothness-increasing accuracy-conserving (SIAC) filtering over uniform and non-uniform meshes. *J. Sci. Comput.*, 64(3):773–817.

R. Sanders (1983). On convergence of monotone finite difference schemes with variable spacing differencing. *Math. Comp.*, 40:91–106.

D. Schötzau, C. Schwab and A. Toselli (2003a). hp-DGFEM for incompressible flows. *SIAM J. Numer. Anal.*, 40:2171–2194.

D. Schötzau, C. Schwab and A. Toselli (2003b). Stabilized *hp*-DGFEM for incompressible flow. *Math. Models Methods Appl. Sci.*, 13:1413–1436.

J. Schütz and G. May (2013). A hybrid mixed method for the compressible Navier-Stokes equations. *J. Comput. Phys.*, 240:58–75.

L. R. Scott and M. Vogelius (1985). Norm estimates for a maximal right inverse of the divergence operator in spaces of piecewise polynomials. *RAIRO Modél. Math. Anal. Numér.*, 19:111–143.

S.J. Sherwin (2000). Dispersion analysis of the continuous and discontinuous Galerkin formulations. In Cockburn, B., Karniadakis, G., and Shu, C.-W., editors, *Discontinuous Galerkin Methods. Theory, Computation and Applications*, volume 11 of *Lect. Notes Comput. Sci. Engrg.*, pages 425–431, Berlin. Springer Verlag.

A.I. Shestakov, J.L. Milovich and M.K. Prasad (2001). Combining cell- and point-centered methods in 3D, unstructured-grid hydrodynamics codes. *J. Comput. Phys.*, 170:81–111.

A.I. Shestakov, M.K. Prasad, J.L. Milovich, N.A. Gentile, J.F. Painter and G. Furnish (2000). The radition-hydrodynamic ICF3D code. *Comput. Methods Appl. Mech. Engrg.*, 187:181–.

C.-W. Shu (1988). TVD time discretizations. *SIAM J. Sci. Stat. Comput.*, 9:1073–1084.

C.-W. Shu (2009). Discontinuous Galerkin methods: general approach and stability. In *Numerical solutions of partial differential equations*, Adv. Courses Math. CRM Barcelona, pages 149–201. Birkhäuser, Basel.

C.-W. Shu (2014). Discontinuous Galerkin method for time-dependent problems: survey and recent developments. In *Recent developments in discontinuous Galerkin finite element methods for partial differential equations*, volume 157 of *IMA Vol. Math. Appl.*, pages 25–62. Springer, Cham.

C.-W. Shu and S. Osher (1988). Efficient implementation of essentially non-oscillatory shock-capturing methods. *J. Comput. Phys.*, 77:439–471.

Encyclopedia of Computational Mechanics. Edited by Erwin Stein, René de Borst and Thomas J.R. Hughes.
 ISBN: 0-470-84699-2

C.-W. Shu and Q. Zhang (2004). Error estimates to smooth solutions of Runge-Kutta discontinuous Galerkin methods for scalar conservation laws. *SIAM J. Numer. Anal.*, 42:641–666.

P. R. Spalart and S. R. Allmaras (1994). A one-equation turbulence model for aerodynamic flows. *La Recherche Aerospatiale*, 1:5–21.

R. Stenberg (1988). A Family of Mixed Finite Elements for the Elasticity Problem. *Numer. Math.*, 53:513–538.

R. Stenberg (1991). Postprocessing schemes for some mixed finite elements. *RAIRO Modél. Math. Anal. Numér.*, 25:151–167.

E. Süli and P. Houston (2002). Adaptive Finite Element Approximation of Hyperbolic Problems. In Barth, T. and Deconink, H., editors, *Error Estimation and Adaptive Discretization Methods in Computational Fluid Dynamics*, volume 25 of *Lect. Notes Comput. Sci. Engrg.*, pages 269–344. Springer Verlag, Berlin.

R. Témam (1966). Sur l'approximation des solutions des équations de Navier-Stokes. *C. R. Acad. Sci. Paris Sér. A*, 216:219–221.

R. Témam (1968). Une méthode d'approximation de la solutions des équations de Navier-Stokes. *Bull. Soc. Math. France*, 98:115–152.

R. Témam (1979). *Navier-Stokes equations*, volume 2 of *Studies in Mathematics and its Applications*. North-Holland Publishing Co., Amsterdam-New York, revised edition. Theory and numerical analysis, With an appendix by F. Thomasset.

F. Thomasset (1981). *Implementation of finite element methods for Navier-Stokes equations*. Springer Series in Computational Physics. Springer Verlag, New York.

V. Thomée (1977). High order local approximations to derivatives in the finite element method. *Math. Comp.*, 31:652–660.

J. J. W. van der Vegt and H. van der Ven (2002a). Slip flow boundary conditions in discontinuous Galerkin discretizations of the Euler equations of gas dynamics. In *Fifth World Congress on Computational Mechanics, July 7-12, Vienna, Austria*.

J. J. W. van der Vegt and H. van der Ven (2002b). Space-Time Discontinuous Galerkin Finite Element Method with Dynamic Grid Motion for Inviscid Compressible Flows: I. General Formulation. *J. Comput. Phys.*, 182:546–585.

H. van der Ven and J. J. W. van der Vegt (2002). Space-Time Discontinuous Galerkin Finite Element Method with Dynamic Grid Motion for Inviscid Compressible Flows: II. Efficient flux quadrature. *Comput. Methods Appl. Mech. Engrg.*, 191:4747–4780.

B. van Leer (1974). Towards the ultimate conservation difference scheme, II. *J. Comput. Phys.*, 14:361–376.

B. van Leer (1979). Towards the ultimate conservation difference scheme, V. *J. Comput. Phys.*, 32:1–136.

P. van Slingerland, J. K. Ryan and C. Vuik (2011). Position-dependent smoothness-increasing accuracy-conserving (SIAC) filtering for improving discontinuous Galerkin solutions. *SIAM J. Sci. Comput.*, 33(2):802–825.

Encyclopedia of Computational Mechanics. Edited by Erwin Stein, René de Borst and Thomas J.R. Hughes.
 ISBN: 0-470-84699-2

F. Vilar, C.-W. Shu and P.-H. Maire (2016a). Positivity-preserving cell-centered Lagrangian schemes for multi-material compressible flows: From first-order to high-orders. Part I: The one-dimensional case. *J. Comput. Phys.*, 312:385–415.

F. Vilar, C.-W. Shu and P.-H. Maire (2016b). Positivity-preserving cell-centered Lagrangian schemes for multi-material compressible flows: From first-order to high-orders. Part II: The two-dimensional case. *J. Comput. Phys.*, 312:416–442.

D. Walfisch, J. K. Ryan, R. M. Kirby and R. Haimes (2009). One-sided smoothness-increasing accuracy-conserving filtering for enhanced streamline integration through discontinuous fields. *J. Sci. Comput.*, 38(2):164–184.

H. Wang, C.-W. Shu and Q. Zhang (2015). Stability and error estimates of local discontinuous Galerkin methods with implicit-explicit time-marching for advection-diffusion problems. *SIAM J. Numer. Anal.*, 53(1):206–227.

H. Wang, C.-W. Shu and Q. Zhang (2016). Stability analysis and error estimates of local discontinuous Galerkin methods with implicit-explicit time-marching for nonlinear convection-diffusion problems. *Appl. Math. Comput.*, 272(part 2):237–258.

W. Wang, J. Guzmán and C.-W. Shu (2011). The multiscale discontinuous Galerkin method for solving a class of second order elliptic problems with rough coefficients. *Int. J. Numer. Anal. Model.*, 8(1):28–47.

T.C. Warburton (1998). *Spectral/hp methods on polymorphic multi-domains: Algorithms and Applications*. PhD thesis, Brown University.

M. Wierse (1997). A new theoretically motivated higher order upwind scheme on unstructured grids of simplices. *Adv. Comput. Math.*, 7:303–335.

P. Woodward and P. Colella (1984). The numerical simulation of two-dimensional fluid flow with strong shocks. *J. Comput. Phys.*, 54:115–173.

M. Woopen, G. May and J. Schütz (2014). Adjoint-based error estimation and mesh adaptation for hybridized discontinuous Galerkin methods. *Internat. J. Numer. Methods Fluids*, 76(11):811–834.

L. Yin, A. Acharya, N. Sobh, R.B.Haber and D.A.Tortorelli (2000). A space-time discontinuous Galerkin method for elastodynamic analysis. In Cockburn, B., Karniadakis, G., and Shu, C.-W., editors, *Discontinuous Galerkin Methods. Theory, Computation and Applications*, volume 11 of *Lect. Notes Comput. Sci. Engrg.*, pages 459–464, Berlin. Springer Verlag.

Q. Zhang and C.-W. Shu (2006). Error estimates to smooth solutions of Runge-Kutta discontinuous Galerkin method for symmetrizable systems of conservation laws. *SIAM J. Numer. Anal.*, 44(4):1703–1720 (electronic).

Q. Zhang and C.-W. Shu (2010a). Stability analysis and a priori error estimates of the third order explicit Runge-Kutta discontinuous Galerkin method for scalar conservation laws. *SIAM J. Numer. Anal.*, 48.

Q. Zhang and C.-W. Shu (2014). Error estimates for the third order explicit Runge-Kutta discontinuous Galerkin method for a linear hyperbolic equation in one-dimension with discontinuous initial data. *Numer. Math.*, 126(4):703–740.

X. Zhang and C.-W. Shu (2010b). On maximum-principle-satisfying high order schemes for scalar conservation laws. *J. Comput. Phys.*, 229(9):3091–3120.

Encyclopedia of Computational Mechanics. Edited by Erwin Stein, René de Borst and Thomas J.R. Hughes.
 ISBN: 0-470-84699-2

X. Zhang and C.-W. Shu (2010c). On positivity-preserving high order discontinuous Galerkin schemes for compressible Euler equations on rectangular meshes. *J. Comput. Phys.*, 229(23):8918–8934.

X. Zhang and C.-W. Shu (2011). Positivity-preserving high order discontinuous Galerkin schemes for compressible Euler equations with source terms. *J. Comput. Phys.*, 230(4):1238–1248.

X. Zhang, Y. Xia and C.-W. Shu (2012). Maximum-principle-satisfying and positivity-preserving high order discontinuous Galerkin schemes for conservation laws on triangular meshes. *J. Sci. Comput.*, 50.

Y. Zhang, X. Zhang and C.-W. Shu (2013). Maximum-principle-satisfying second order discontinuous Galerkin schemes for convection-diffusion equations on triangular meshes. *J. Comput. Phys.*, 234:295–316.

J. Zhu, X. Zhong, C.-W. Shu and J. Qiu (2013). Runge-Kutta discontinuous Galerkin method using a new type of WENO limiters on unstructured meshes. *J. Comput. Phys.*, 248:200–220.

Encyclopedia of Computational Mechanics. Edited by Erwin Stein, René de Borst and Thomas J.R. Hughes.